Rheology and Hydraulics of Drilling Fluids

1 Scope

1.1 Objective

The objective of this recommended practice (RP) is to provide a basic understanding of and guidance about drilling fluid rheology and hydraulics to assist with drilling wells of various complexities, including high-temperature/high-pressure (HTHP), extended-reach drilling (ERD), and highly directional wells.

Office and wellsite engineers are the target audience for this document. This standard has been designed such that office and wellsite engineers can implement complex topics and equation sets into a standard spreadsheet program to conduct hydraulic analyses. Given that the equations used herein are constrained by this spreadsheet limitation, more advanced numerical solutions containing multiple subroutines and macros are not offered. This limitation does not suggest that only the results given by the spreadsheet methods are valid engineering solutions but are a basic determination of them as their order of magnitude.

1.2 Rheology and Hydraulics

Rheology is the study of the deformation and flow of matter. For this document, rheology is the study of the flow characteristics of drilling fluids and how these characteristics affect movement of the fluids. The discussion of rheology in this document is limited to single-phase liquid flow.

Rheological properties directly affect flow characteristics and hydraulic behavior. Properties shall be controlled for drilling fluids to perform their various functions. Certain properties are measured at the wellsite for monitoring and treatment and in the laboratory for development of new additives and systems, formulation for specific applications, and diagnosis of special problems.

Measurement of rheological properties also makes possible mathematical descriptions of circulating fluid flow important for the following hydraulics-related determinations:

- calculating frictional pressure losses in pipes and annuli,
- determining equivalent circulating density (ECD) of the drilling fluid under downhole conditions,
- determining flow regimes,
- estimating hole-cleaning efficiency,
- estimating swab/surge pressures, and
- optimizing the drilling fluid circulating system to improve drilling efficiency.

The concepts of viscosity, shear stress, and shear rate are important in understanding the flow characteristics of fluids. Specific measurements are made on fluids to determine rheological parameters under a variety of conditions. From this information, the circulating system can be designed and evaluated to accomplish desired objectives.

Drilling fluid hydraulics involves hydrostatic pressures, frictional pressure losses, carrying capacity, swab/surge pressures, and equivalent static and circulating densities, among others. Mathematical models relating shear stress to shear rate and formulas for estimating drilling fluid hydraulics are included. Calculation methods used herein consider the effects of temperature and pressure on drilling fluid rheology and density.

1.3 Units

The U.S. customary (USC) unit system is used in the document . However, any consistent system of units may be used where so indicated, as in the development of equations in Section 4. The term “pressure” means “gauge pressure” unless otherwise noted.

NOTE The term “consistent units” refers to a set of units that does not require an extra conversion factor to complete a calculation. In consistent International System of units (SI unit), time is expressed in seconds (s), length in meters (m), mass in kilograms (kg), force in newtons (N), temperature in degrees Celsius (°C), and absolute temperature in kelvins (K). In USC units , time is expressed in seconds (s), length in feet (ft), mass in pound mass (lbm), force in pound force (lbf), temperature in degrees Fahrenheit (°F), and absolute temperature in degrees Rankine (°R).

Symbols are defined in 3.3 with the units used in the document. Factors for converting USC units to SI units or SI units to USC units are provided Table 1.

1.4 Calculation Examples

Annexes A through F contain example calculations to illustrate how equations contained within the document can be used to model a sample well. Step-by-step procedures are not included for every case; however, final results serve as benchmarks to replicate given cases. Annexes cover following subjects:

- Annex A: Worked Example parameters.
- Annex B: Downhole-properties example.
- Annex C: Pressure-loss example.
- Annex D: Swab/surge-pressures example.
- Annex E: Hole-cleaning example.
- Annex F: Hydraulics-optimization example.

2 Normative References

The following referenced documents are indispensable for the application of this document. For dated references, only the edition cited applies. For undated references, the latest edition of the referenced document (including any amendments) applies.

API Recommended Practice 13B-1, *Field Testing Water-based Drilling Fluids*

API Recommended Practice 13B-2, *Field Testing Nonaqueous-based Drilling Fluids*

3 Terms, Definitions, Acronyms, Abbreviations, and Symbols

3.1 Terms and Definitions

3.1.1
hydraulic diameter, d_{hyd}
The hydraulic diameter allows for non-circular flows such annular flows to define a pipe equivalent diameter to perform fluid dynamic calculation taking in account frictions on all surfaces. Hydraulic diameter is defined as the ratio of 4 times the cross-sectional area over the wetted perimeter. It is derived from the hydraulic radius, the ratio of the cross-sectional area to the wetted perimeter (see 7.4.4).

3.1.2
Newtonian fluid
A fluid with a constant viscosity independently of the shear rate applied when flowing. The relationship shear rate vs shear stress is linear

3.1.3
Non-Newtonian fluid
Non-Newtonian fluids don't follow the linear Newton law of viscosity. In non-Newtonian fluid the viscosity changes under shear stress vs shear rate and is not constant.

3.1.4
Reynolds number
Reynolds
In fluid dynamics, the Reynolds number is a dimensionless value that helps to predict fluid flow patterns, i.e. if the fluid is flowing in laminar or turbulent

3.1.5
Rheogram
A graphical representation of the rheological properties of a fluid , i.e. a graph of shear stress versus shear rate.

3.1.6
shear rate, γ
Rate of deformation of the liquid during flow (see 4.3).

NOTE Symbol γ is used in the document, shear rate can be also represented by the symbol $\dot{\gamma}$.

3.1.7
shear stress, τ
Force tending to cause deformation of a material (then a liquid flowing) by slippage along planes parallel to the imposed stress (see 4.3).

3.2 Acronyms and Abbreviations

For the purpose of this document , the following acronyms and abbreviations are used.

BOP	blow out preventer
ERD	extended-reach drilling
H-B	Herschel–Bulkley

HTHP	high-temperature high-pressure
ID	internal diameter
LCM	lost circulation material
LOT	leak-off test
MD	measured depth
MPD	managed pressure drilling
MWD	measurement while drilling
NADF	nonaqueous drilling fluid
OD	outside diameter
PIT	pressure integrity test
PDC	polycrystalline diamond compact (cutter)
PDM	positive-displacement motor
POI	point of interest
PVT	pressure, volume and temperature
RPM	revolutions per minute
RWD	ream while drilling
R#B#	viscometer rotor (#) and bob (#) combination
SPP	system parasitic pressure
TD	total depth
TVD	true vertical depth

NOTE Few symbols considered as abbreviations in this document are defined under 3.3. Examples include ECD for equivalent circulating density, ESD for equivalent static density, HHP for hydraulic horsepower, etc…

3.3 Symbols

For the purpose of this document symbols given in Table 1 should apply. This list is not exhaustive.

Table 1—Symbols, Definitions, and Units

Symbol	Definition	U.S. Customary Units	Conversion Factor [a]	SI Units (base or derived)
A	Surface area	$in.^2$	645.16	mm^2
a	Blasius form of friction-factor equation numerator	—	—	—
a_1	Density correction coefficient for pressure	lbm/gal	119.83	kg/m^3
a_2	Density correction coefficient for temperature	(lbm/gal)/°F	215.69	$(kg/m^3)/°C$
a_{ds}	Drill string (pipe) acceleration	ft/s^2	0.3048	m/s^2
B_a	Well geometry correction factor	—	—	—
B_x	Viscometer geometry correction factor	—	—	—
b	Exponent in Blasius form of friction-factor equation	—	—	—
b_1	Density correction coefficient for pressure	$(lbm/gal)/(lbf/in.^2)$	0.017379	$(kg/m^3)/Pa$
b_2	Density correction coefficient for temperature	$[(lbm/gal)/(lbf/in.^2)]/°F$	0.031283	$[(kg/m^3)/Pa]/°C$
C_d	Jet nozzle discharge coefficient	—	—	—
C_{dt}	Proportionality constant for downhole tool pressure loss	—	—	—
C_g	Drilling fluid clinging factor on pipe for surge/swab operations	—	—	—
C_{sc}	Proportionality constant for surface-connection pressure loss	—	—	—
CCI	Carrying capacity index	—	—	—
c_a	In-situ cuttings volume concentration	decimal fraction	—	decimal fraction
c_1	Density correction coefficient for pressure	$(lbm/gal)/(lbf/in.^2)^2$	2.5206E-06	$(kg/m^3)/Pa^2$
c_2	Density correction coefficient for temperature	$[(lbm/gal)/(lbf/in.^2)^2]/°F$	4.5370E-06	$[(kg/m^3)/Pa^2]/°C$
D_{td}	Total depth (measured)	ft	0.3048	m
D_{tvd}	True vertical depth	ft	0.3048	m
D_w	Water depth	ft	0.3048	m
d	Diameter	in.	25.4	mm
d_b	Bit diameter	in.	25.4	mm
d_c	Cuttings diameter	in.	25.4	mm
d_h	Hole diameter or casing ID (inside diameter)	in.	25.4	mm
d_{hyd}	Hydraulic diameter	in.	25.4	mm
d_i	Pipe internal diameter (ID)	in.	25.4	mm
d_n	Bit nozzle diameter	$^1/_{32}$ in.	0.79375	mm
d_{ni}	Diameter of bit nozzle i	$^1/_{32}$ in.	0.79375	mm
d_p	Pipe outside diameter (OD)	in.	25.4	mm

Symbol	Definition	U.S. Customary Units	Conversion Factor [a]	SI Units (base or derived)
ECD	Equivalent circulating density	lbm/gal	119.8264	kg/m^3
ECD_a	Equivalent circulating density in annulus	lbm/gal	119.8264	kg/m^3
ECD_{ac}	Equivalent circulating density including cuttings in annulus	lbm/gal	119.8264	kg/m^3
EDD	Equivalent dynamic density	lbm/gal	119.8264	kg/m^3
EMW	Equivalent mud weight	lbm/gal	119.8264	kg/m^3
ESD	Equivalent static density	lbm/gal	119.8264	kg/m^3
ESD_{D+L}	Equivalent static density at depth $D + L$	lbm/gal	119.8264	kg/m^3
ESD_{tvd}	Equivalent static density at true vertical depth	lbm/gal	119.8264	kg/m^3
ESD_a	Equivalent static density in annulus	lbm/gal	119.8264	kg/m^3
ESD_{ac}	Equivalent static density including cuttings in annulus	lbm/gal	119.8264	kg/m^3
ESD_p	Equivalent static density in pipe (drill string)	lbm/gal	119.8264	kg/m^3
ESD_{td}	Equivalent static density at total depth	lbm/gal	119.8264	kg/m^3
e	Eccentricity (annular)	decimal fraction	—	decimal fraction
F	Force	lbf	4.448222	N
F_j	Jet impact force	lbf	4.448222	N
f	Fanning friction factor	—	—	—
f_a	Ratio of annular flow rate to total displaced flow rate in open pipe mode (swab and surge)	—	—	—
f_{int}	Intermediate fanning factor, transitional and turbulent flow	—	—	—
f_{lam}	Friction factor, laminar flow	—	—	—
f_{trans}	Friction factor, transitional flow	—	—	—
f_{turb}	Friction factor, turbulent flow	—	—	—
G_f	Geometry factor	—	—	—
G_p	Geometry shear rate correction factor (power law)	—	—	—
HHP_p	Hydraulic horsepower at the bit	hp	0.746043	kW
HHP_{max}	Maximum hydraulic horsepower	hp	0.746043	kW
HPO	Hydraulic pump-off force	1000 lbf	4.448222	kN
HSI	hydraulic horsepower per square inch	hp/in.^{2}	1.15637	W/mm^2
h	Distance between two parallel plates or layers	in.	25.4	mm
h_c	Cutting thickness	in.	25.4	mm
IF	Jet impact force	lbf	4.448222	N
K_x	System parasitic pressure loss coefficient	(lbf/in.^{2})/(gal/min)^u	6.894757	kPa/(3.78541 L/min)^u
k	Consistency factor (Herschel–Bulkley)	lbf•s^n/100 ft^2	478.803	mPa•s^n
k_1	Power law viscosity at 1 s^{-1}	cP	1.0	mPa•s

Symbol	Definition	U.S. Customary Units	Conversion Factor [a]	SI Units (base or derived)
k_P	Power law and high shear rate consistency factor	lbf•s^{n_P}/100 ft^2	478.803	mPa•s^{n_P}
k_{Pa}	Low shear rate consistency factor (power law)	lbf•s$^{n_{Pa}}$/100 ft^2	478.803	mPa•s$^{n_{Pa}}$
L	Length of drill string (pipe) or annular segment	ft	0.3048	m
$LSYP$	Low shear rate yield point	lbf/100 ft^2	0.4788026	Pa
N_{Re}	Reynolds number	—	—	—
$N_{Re,crit}$	Critical Reynolds number	—	—	—
N_{ReG}	Generalized Reynolds number	—	—	—
n	Flow behavior index (Herschel–Bulkley)	—	—	—
n_P	Power law flow behavior index (high shear rate behavior index)	—	—	—
n_{Pa}	Low shear rate flow behavior index (power law)	—	—	—
P	Pressure	lbf/in.^{2}	6.894757	kPa
$P_{Ref\text{-}dt}$	Reference pressure loss used for empirical downhole tools pressure loss	lbf/in.^{2}	6.894757	kPa
P_a	Annular pressure loss	lbf/in.^{2}	6.894757	kPa
$P_{a\text{-}ec}$	Eccentric annular pressure loss	lbf/in.^{2}	6.894757	kPa
$P_{a\text{-}min}$	Minimum annular pressure loss to break drilling fluid gel	lbf/in.^{2}	6.894757	kPa
P_b	Bit pressure loss	lbf/in.^{2}	6.894757	kPa
P_{bh}	Bottomhole pressure	lbf/in.^{2}	6.894757	kPa
$P_{b\text{-}opt}$	Optimum pressure loss through the bit	lbf/in.^{2}	6.894757	kPa
P_c	Casing pressure, back pressure on annulus	lbf/in.^{2}	6.894757	kPa
P_{cs}	Shut-in casing pressure	lbf/in.^{2}	6.894757	kPa
P_{cl}	Choke line pressure loss	lbf/in.^{2}	6.894757	kPa
P_{dca}	Downhole circulating annular pressure	lbf/in.^{2}	6.894757	kPa
P_{ds}	Drill string pressure loss	lbf/in.^{2}	6.894757	kPa
$P_{ds\text{-}min}$	Minimum drill string pressure loss to break drilling fluid gel	lbf/in.^{2}	6.894757	kPa
P_{dt}	Downhole tools + motors pressure loss	lbf/in.^{2}	6.894757	kPa
P_f	Formation pressure	lbf/in.^{2}	6.894757	kPa
P_{ha}	Annular hydrostatic pressure	lbf/in.^{2}	6.894757	kPa
P_{hac}	Annular hydrostatic pressure including cuttings	lbf/in.^{2}	6.894757	kPa
P_{hd}	Drill string hydrostatic pressure	lbf/in.^{2}	6.894757	kPa
P_{max}	Maximum pump (standpipe) pressure	lbf/in.^{2}	6.894757	kPa
P_p	Pump (standpipe) pressure	lbf/in.^{2}	6.894757	kPa
P_{sc}	Surface-connections pressure loss	lbf/in.^{2}	6.894757	kPa

Symbol	Definition	U.S. Customary Units	Conversion Factor [a]	SI Units (base or derived)
P_{ss}	Inertial surge pressure, closed-pipe mode	lbf/in.^{2}	6.894757	kPa
$P_{ss,av}$	Average inertial surge pressure, open-pipe mode	lbf/in.^{2}	6.894757	kPa
P_x	System parasitic pressure loss	lbf/in.^{2}	6.894757	kPa
Q	Flow rate	gal/min	3.785412	l/min
Q_{Ref}	Reference flow rat used for empirical downhole tools pressure loss	gal/min	3.785412	l/min
Q_{crit}	Critical flow rate (laminar to transitional flow)	gal/min	3.785412	l/min
$Q_{crit\text{-}opt}$	Critical flow rate for optimized hydraulics	gal/min	3.785412	l/min
Q_{opt}	Optimum flow rate	gal/min	3.785412	l/min
R	Ratio of H-B yield stress/Bingham yield point (τ_y / Y_P)	decimal fraction	—	decimal fraction
R_3	Viscometer reading at 3 r/min [b]	°	—	°
		lbf/100 ft^2	0.4788026	Pa
R_6	Viscometer reading at 6 r/min [b]	°	—	°
		lbf/100 ft^2	0.4788026	Pa
R_{30}	Viscometer reading at 30 r/min [b]	°	—	°
		lbf/100 ft^2	0.4788026	Pa
R_{60}	Viscometer reading at 30 r/min [b]	°	—	°
		lbf/100 ft^2	0.4788026	Pa
R_{100}	Viscometer reading at 100 r/min [b]	°	—	°
		lbf/100 ft^2	0.4788026	Pa
R_{200}	Viscometer reading at 200 r/min [b]	°	—	°
		lbf/100 ft^2	0.4788026	Pa
R_{300}	Viscometer reading at 300 r/min [b]	°	—	°
		lbf/100 ft^2	0.4788026	Pa
R_{600}	Viscometer reading at 600 r/min [b]	°	—	°
		lbf/100 ft^2	0.4788026	Pa
R_{lam}	Eccentric annulus laminar pressure ratio	decimal fraction	—	decimal fraction
R_t	Cuttings transport ratio	decimal fraction	—	decimal fraction
R_{turb}	Eccentric annulus turbulent pressure ratio	decimal fraction	—	decimal fraction
RF	Rheology factor	—	—	—
ROP	Rate of penetration	ft/h	0.3048	m/h
T	Temperature	°F	(°F – 32)/1.8	°C
T_{bhc}	Bottomhole circulating temperature	°F	(°F – 32)/1.8	°C
T_{bhs}	Bottomhole static temperature	°F	(°F – 32)/1.8	°C
T_{fl}	Flowline temperature	°F	(°F – 32)/1.8	°C
T_{ml}	Temperature at the mudline	°F	(°F – 32)/1.8	°C
T_0	Surface temperature at 50-ft depth	°F	(°F – 32)/1.8	°C

Symbol	Definition	U.S. Customary Units	Conversion Factor [a]	SI Units (base or derived)
TFA	Total flow area	in.^{2}	645.16	mm^2
TI	Transport index	—	—	—
u	Slope of logarithmic system parasitic pressure loss	—	—	—
V	Flow velocity (average)	ft/min	0.3048	m/min
V_{a}	Fluid velocity in annulus (average)	ft/min	0.3048	m/min
V_{crit}	Critical velocity	ft/min	0.3048	m/min
V_{critB}	Critical velocity (Bingham plastic fluids)	ft/min	0.3048	m/min
V_{critP}	Critical velocity (power law fluids)	ft/min	0.3048	m/min
V_{ds}	Drill string (pipe) velocity for surge/swab	ft/min	0.3048	m/min
$V_{\mathrm{a\text{-}circ,eff}}$	Effective annular fluid velocity when circulating (open-pipe, pump on mode) including pipe movement	ft/min	0.3048	m/min
$V_{\mathrm{a,eff}}$	Effective annular fluid velocity due to pipe movement (closed-pipe, pump-off mode)	ft/min	0.3048	m/min
$V_{\mathrm{a\text{-}open,eff}}$	Effective fluid velocity for open-pipe, pump-off mode in annulus	ft/min	0.3048	m/min
$V_{\mathrm{ds\text{-}open,eff}}$	Effective fluid velocity for open-pipe , pump-off mode in drill string (pipe)	ft/min	0.3048	m/min
V_{j}	Jet (nozzle) velocity	ft/s	0.3048	m/s
V_{p}	Fluid velocity inside pipe (average)	ft/min	0.3048	m/min
V_{s}	Cuttings slip velocity	ft/min	0.3048	m/min
V_{u}	Cuttings net upward velocity	ft/min	0.3048	m/min
Vol_i	Volume of a wellbore cell i (local)	bbl	0.1589873	m^3
$Vol_{\%}$	Volume percent	%	—	%
Vol_{wb}	Volume of wellbore	bbl	0.1589873	m^3
$w_{\mathrm{CaCl_2}}$	Aqueous phase mass fraction of calcium chloride	wt%	—	wt%
x	Viscometer diameter ratio (rotor/bob)	—	—	—
Y_{P}	Yield point (Bingham)	lbf/100 ft^2	0.4788026	Pa
α	Geometry factor	—	—	—
β	Intermediate parameter for critical velocity calculation	—	—	—
$\beta_{10\mathrm{m}}$	10-min gel strength [b]	°	—	°
		lbf/100 ft^2	0.4788026	Pa
$\beta_{10\mathrm{s}}$	10-s gel strength [b]	°	—	°
		lbf/100 ft^2	0.4788026	Pa
$\beta_{30\mathrm{m}}$	30-min gel strength [b]	°	—	°
		lbf/100 ft^2	0.4788026	Pa

Symbol	Definition	U.S. Customary Units	Conversion Factor [a]	SI Units (base or derived)
γ	Shear rate	s^{-1}	—	s^{-1}
γ_b	Cuttings (particle) shear rate for N_{Re} = 100	s^{-1}	—	s^{-1}
γ_c	Cuttings shear rate	s^{-1}	—	s^{-1}
γ_i	Iterative shear rate used in curve-fit method	s^{-1}	—	s^{-1}
γ_s	Cuttings (particle) shear rate	s^{-1}	—	s^{-1}
γ_w	Shear rate at the wall	s^{-1}	—	s^{-1}
γ_{wa}	Shear rate at the annulus wall	s^{-1}	—	s^{-1}
γ_{wp}	Shear rate at the pipe wall	s^{-1}	—	s^{-1}
Δ	Change in value when preceding a variable	—	—	—
η_{PV}	Plastic viscosity (Bingham)	cP	1.0	mPa•s
μ	Viscosity	cP	1.0	mPa•s
φ_{base}	Volume fraction of base fluid of the whole drilling fluid	decimal fraction	—	decimal fraction
φ_{brine}	Volume fraction of brine of the whole drilling fluid	decimal fraction	—	decimal fraction
$\varphi_{CaCl_2,brine}$	Volume fraction of salt in a $CaCl_2$ brine	decimal fraction	—	decimal fraction
φ_{ds}	Volume fraction of dried retort solids	decimal fraction	—	decimal fraction
φ_{salt}	Volume fraction of salt (soluble)	decimal fraction	—	decimal fraction
φ_{solids}	Volume fraction of solids (suspended solids) of the whole-drilling fluid	decimal fraction	—	decimal fraction
φ_{total}	Volume fraction of all components	decimal fraction	—	decimal fraction
φ_{water}	Volume fraction of water	decimal fraction	—	decimal fraction
ρ	Fluid density	lbm/gal	119.8264	kg/m^3
$\rho_{(P\text{-}T)}$	Fluid density at pressure P and temperature T	lbm/gal	119.8264	kg/m^3
$\rho_{Ref\text{-}dt}$	Reference drilling fluid density used for empirical downhole tools pressure loss	lbm/gal	119.8264	kg/m^3
ρ_a	Fluid density in annulus (local)	lbm/gal	119.8264	kg/m^3
ρ_b	Fluid density through bit nozzles	lbm/gal	119.8264	kg/m^3
ρ_{base}	Base fluid density	lbm/gal	119.8264	kg/m^3
$\rho_{base(P\text{-}T)}$	Base fluid density at pressure P and temperature T	lbm/gal	119.8264	kg/m^3
ρ_{brine}	Brine density	lbm/gal	119.8264	kg/m^3
$\rho_{brine(P\text{-}T)}$	Brine density at pressure P, temperature T	lbm/gal	119.8264	kg/m^3
ρ_c	Cutting (particle) relative density (specific gravity)	—	—	—
ρ_i	Drilling fluid density (local)	lbm/gal	119.8264	kg/m^3

Symbol	Definition	U.S. Customary Units	Conversion Factor [a]	SI Units (base or derived)
ρ_p	Drilling fluid density in drill string (local)	lbm/gal	119.8264	kg/m^3
ρ_s	Drilling fluid density at surface	lbm/gal	119.8264	kg/m^3
ρ_{solids}	Solids density (suspended solids)	lbm/gal	119.8264	kg/m^3
ρ_{total}	Whole-drilling fluid density	lbm/gal	119.8264	kg/m^3
ρ_{water}	Water density	lbm/gal	119.8264	kg/m^3
τ	Shear stress	lbf/100 ft^2	0.4788026	Pa
τ_c	Shear stress due to particle (cuttings) slip	lbf/100 ft^2	0.4788026	Pa
τ_i	Iterative shear stress in curve-fit method	lbf/100 ft^2	0.4788026	Pa
τ_v	Shear stress at the wall (viscometer flow equation)	°	—	°
τ_w	Shear stress at the wall	lbf/100 ft^2	0.4788026	Pa
τ_y	Yield stress (Herschel–Bulkley)	lbf/100 ft^2	0.4788026	Pa
ψ_g	Geothermal gradient	°F/100 ft	1.8223	°C/100 m
ψ_{gw}	Geothermal gradient adjusted for water depth	°F/100 ft	1.8223	°C/100 m

[a] Conversion Factor is a divider to convert data expressed in SI base or derived units into a value expressed in USC units. It is a multiplier to convert data expressed in USC units into a value expressed in SI base or derived values.

[b] Measurement done in degrees which are approximative equal to lbf/100 ft² with an error of about 6%. Conversion from degrees to lbf/100ft^2 requires multiplying the value by 1.067.

4 Fluid Flow Fundamentals and Rheological Models

4.1 Flow Fundamentals

The behavior of a fluid depends on the flow regime, which in turn directly affects the ability of that fluid to perform its basic functions. Flow can be laminar or turbulent, depending on the fluid velocity, density, viscosity, and size and shape of the flow channel. Between laminar and turbulent flow, the fluid can pass through a transition region where movement of the fluid exhibits both laminar and turbulent characteristics. If the flow occurs in an annulus, as in a drilling situation, the rotation of the inner surface (the drill pipe) can create turbulent instabilities at any flow rate.

In axial laminar flow, the fluid moves parallel to the walls of the flow channel in smooth lines. Flow tends to be laminar when the fluid is moving slowly and/or when the fluid is viscous. In laminar flow, the pressure required to move the fluid increases with increasing velocity and viscosity.

In turbulent flow, the fluid moves in an irregular chaotic manner with oblique swirling and eddying as it moves along the flow channel, even though the bulk of the fluid moves forward. These velocity fluctuations can arise spontaneously. Wall roughness and rapid changes in flow direction can increase the amount of turbulence. Flow tends to be turbulent at higher velocities and/or when the fluid exhibits low viscosity. In turbulent flow, the pressure required to move the fluid increases linearly with density and approximately with the square of the velocity (independent of viscosity). This means more pump pressure is required to move fluid in turbulent flow than in laminar flow. Similarly annular pressure losses and resulting equivalent circulating densities (ECD) will be higher in turbulent flow than in laminar flow.

The transition from axial laminar to turbulent flow is controlled by the relative contributions of viscous and inertial forces in the flow. Viscous forces dominate in laminar flow; inertial forces are more important in turbulent flow. For Newtonian fluids (see 3.1.2), viscous forces vary linearly with the flow rate, while inertial forces vary as the square of the flow rate.

The ratio of inertial forces to viscous forces is the *Reynolds number*, N_{Re}. This value is the main criteria used to determine laminar or turbulent flow. Dimensionless Reynolds number shall be calculated by Equation (1).

$$N_{\mathrm{Re}} = \frac{\rho\, V\, d}{\mu} \tag{1}$$

where in consistent units (see 1.3):

ρ is the fluid density;

V is the average flow velocity;

d is the diameter of the flow channel;

μ is the fluid viscosity.

The transition from laminar to transitional flow occurs at the *critical velocity*. For typical drilling fluids, this normally occurs over a range of conditions corresponding to Reynolds numbers between 2000 and 4000 (see Section 7 for further details).

Secondary flows known as *Taylor vortices* can form in an annulus with a rotating drill string at high revolutions per minute (RPM) due to centrifugal and shear instabilities. This condition can substantially increase annular pressure loss. Additionally, when present, turbulence-like motion may occur even in the absence of axial flow. Flow instabilities like Taylor vortices make pressure loss predictions difficult and are outside the scope of this document.

4.2 Viscosity

Viscosity (μ) is the resistance of fluid to change in shape, or movement of neighboring portions relative to one another, and is defined as the ratio of shear stress to shear rate as shown in Equation (2). The traditional units of viscosity are dyne-s/cm^2, which is termed poise (symbol P). The SI unit of viscosity is the pascal-second (Pa•s). Since one poise and one Pa•s represents a relatively high viscosity for most fluids, the derived units normally used are centipoise (cP) and millipascal-second (mPa•s), which are numerically equivalent (1 cP = 1 mPa•s).

$$\mu = \frac{\tau}{\gamma} \tag{2}$$

where in consistent units (see 1.3):

μ is the fluid viscosity;

τ is the shear stress;

γ is the shear rate.

The viscosity of most drilling fluids decreases with increasing shear rate. Viscosity vs shear rate relationships can be determined and plotted from shear stress measurements made at several shear rates. Viscosity is also a function of the temperature and pressure of the fluid. The term *effective viscosity* is used to describe the viscosity either measured or calculated at the shear rate corresponding to existing flow conditions in the wellbore or drill pipe. This special term is used to differentiate the viscosity as discussed in this section from other viscosity terms.

To be meaningful, viscosity measurements should specify the shear rate, temperature, and pressure (if other than atmospheric).

4.3 Shear Stress

4.3.1 Definition

Shear stress is the force per unit area required to sustain fluid flow. In the parallel-plate example illustrated in Figure 1, a force, F, of 10^{-5} N is applied to each cm^2 of the top plate A to keep it moving. Thus, the shear stress is 10^{-5} N/cm^2 or 0.1 Pa. An opposing force is required on the bottom plate B to keep it stationary. The same shear stress of 0.1 Pa is found at any level in the fluid along the velocity profile C. The distance between the plates (h) is 1.0 cm.

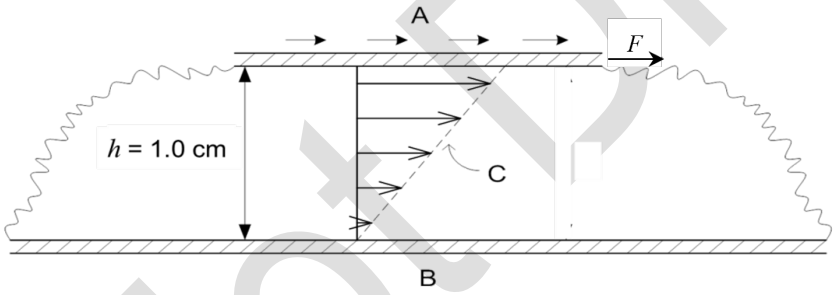

Key

A moving plate

B stationary plate

C velocity profile

F acting force on the moving plate A

h distance between the plates (1 cm)

Figure 1—Fluid-filled Gap between Parallel Plates Showing Effects of Upper Plate Sliding Past Lower Plate

Shear stress, τ, shall be expressed mathematically by Equation (3) as:

$$\tau = \frac{F}{A} \tag{3}$$

where in consistent units (see 1.3):

τ is the shear stress;

F is the force acting on the surface area subject to stress;

A is the surface area subjected to stress.

4.3.2 Horizontal pipe case

In a horizontal pipe, the force, F, pushing a column of liquid through the pipe shall be expressed as the pressure on the end of the liquid column times the cross-sectional area and by Equation (4):

$$F = P\frac{\pi\, d_{\mathrm{i}}^2}{4} \tag{4}$$

where in consistent units (see 1.3):

F is the applied force;

d_{i} is the internal diameter of the pipe;

P is the pressure on the end of the liquid column.

The fluid contact area inside the pipe, A, shall be given by Equation (5):

$$A = \pi\, d_{\mathrm{i}} L \tag{5}$$

where in consistent units (see 1.3):

A is the surface area of the fluid contact;

d_{i} is the internal diameter of the pipe;

L is the length of the pipe.

Thus, from Equation (3), the shear stress at the wall of the pipe, τ_{w}, shall be expressed in consistent units by Equation (6):

$$\tau_{\mathrm{w}} = \frac{F}{A} = \frac{d_{\mathrm{i}} P}{4L} \tag{6}$$

4.3.3 Annulus case

In an annulus of known inner and outer diameters, the shear stress is expressed in the same manner using the pressure times the annular cross-sectional area and the annular fluid contact area.

In a horizontal pipe, the force, F, pushing a column of liquid through an annular section shall be given by Equation (7) :

$$F = P\frac{\pi\, d_{\mathrm{h}}^2}{4} - P\frac{\pi\, d_{\mathrm{p}}^2}{4} = \frac{\pi\, P}{4}\left(d_{\mathrm{h}}^2 - d_{\mathrm{p}}^2\right) = \frac{\pi\, P}{4}\left(d_{\mathrm{h}} + d_{\mathrm{p}}\right)\left(d_{\mathrm{h}} - d_{\mathrm{p}}\right) \tag{7}$$

where in consistent units (see 1.3):

P is the pressure on the end of the liquid column.

d_p is the outside diameter for the inner pipe;

d_h is the hole diameter or casing inside diameter;

and the surface area by Equation (8)

$$A = \pi\, d_h L + \pi\, d_p L = \pi\, L\left(d_h + d_p\right) \tag{8}$$

so that, the shear stress at the wall in an annulus case shall be given by Equation (9),

$$\tau_w = \frac{F}{A} = \frac{\frac{\pi\ P}{4}\left(d_h + d_p\right)\left(d_h - d_p\right)}{\pi\ L\left(d_h + d_p\right)}$$

and then,

$$\tau_w = \frac{F}{A} = \frac{P\left(d_h - d_p\right)}{4L} \tag{9}$$

where in consistent units (see 1.3):

τ_w is the shear stress at the wall;

P is the pressure on the end of the liquid column;

d_p is the outside diameter of the inner pipe;

d_h is the hole diameter or casing inside diameter;

L is the length of the pipe.

4.4 Shear Rate

4.4.1 Definition

Shear rate (γ) is a velocity gradient measured across the diameter of a pipe or annulus. It is the rate at which one layer of fluid is sliding past another layer. As an example, consider the example illustrated in Figure 1. The fluid layer near the bottom plate B is motionless while the fluid layer near the top plate A is moving at almost 1 cm/s. Halfway between the plates, the fluid velocity is the average 0.5 cm/s.

The *velocity gradient* is the rate of change of velocity (ΔV) along the velocity profile. For the simple case shown in Figure 1, the shear rate is $\Delta V/h$ with units of 1/s or s^{-1}. The reciprocal second, also called the inverse second, is the standard unit for shear rate.

The example in Figure 1 applies to Newtonian fluids (see 3.1.2) where the shear rate is constant throughout. Such is not the case for non-Newtonian fluids (see 3.1.3) whose shear stress changes with shear rate. In laminar flow inside a pipe, for example, the shear rate for non-Newtonian fluids is highest next to the pipe wall.

An average shear rate may be used for some calculations, but the shear rate itself is not constant across the flow channel. Frictional pressure loss calculations require calculating the shear rate at the wall.

It is important to express the shear-rate concept mathematically so that models and calculations can be developed. Shear rate ($\dot{\gamma}$) shall be defined by Equation (10) as:

$$\gamma = \frac{\Delta V}{\Delta h} \tag{10}$$

where in consistent units (see 1.3):

γ is the shear rate;

ΔV is the flow velocity change between fluid layers;

Δh is the distance between fluid layers.

4.4.2 Newtonian Fluid

4.4.2.1 Shear rate at the wall —Pipe case

In a pipe, the shear rate at the pipe wall (γ_{wp}) for a Newtonian fluid can be expressed as a function of the average velocity inside the pipe (V_{p}) and the pipe internal diameter (d_{i}).

V_{p}, the average velocity inside the pipe, shall be defined by Equation (11),

$$V_{\mathrm{p}} = \frac{Q}{A} = \frac{4Q}{\pi\ d_{\mathrm{i}}^2} \tag{11}$$

and, the shear rate at the pipe wall, γ_{wp}, shall be defined and calculated using Equation (12),

$$\gamma_{\mathrm{wp}} = \frac{8V_{\mathrm{p}}}{d_{\mathrm{i}}} = \frac{32}{\pi} \times \frac{Q}{d_{\mathrm{i}}^3} = \frac{10.186 \times Q}{d_{\mathrm{i}}^3} \tag{12}$$

where in consistent units (see 1.3):

γ_{wp} is the shear rate at the pipe wall for a Newtonian fluid;

Q is the volumetric flow rate;

A is the pipe internal surface area;

d_{i} is the pipe internal diameter;

V_{p} is the average velocity inside the pipe.

4.4.2.2 Shear rate at the wall—Annulus case

In a concentric annulus of outside diameter (OD) (d_h) and inside diameter (ID) (d_p), the wall shear rate for a Newtonian fluid can be expressed as per Equation (13):

$$\gamma_{wa} = \frac{12 V_a}{d_h - d_p} \tag{13}$$

in which the average velocity, V_a, shall be calculated using equation (14) :

$$V_a = \frac{Q}{A} = \frac{4Q}{\pi\left(d_h^2 - d_p^2\right)} = \frac{4Q}{\pi\left(d_h + d_p\right)\left(d_h - d_p\right)} \tag{14}$$

where in consistent units (see 1.3):

γ_{wa} is the shear rate at the annulus wall for a Newtonian fluid;

Q is the volumetric flow rate;

A is the annulus surface area;

d_p is the pipe outside diameter;

d_h is the hole diameter or casing inside diameter;

V_a is the average fluid velocity in annulus.

4.4.3 Non-Newtonian Fluids

Relationships that correct pipe and annular shear rates for non-Newtonian behavior are given in Sections 5 and 7.

4.5 Shear Stress/Shear Rate Relationship

In summary, the *shear stress* (τ) is the force per unit area required to sustain fluid flow. *Shear rate* (γ) is the rate at which the fluid velocity changes with respect to the distance from the wall. *Viscosity* (μ) is the ratio of the shear stress to shear rate.

Mathematical relationships called rheological models are used for non-Newtonian fluids to describe the non-linear relationship between shear rate and shear stress. Numerous models have been developed to describe the flow behavior of fluids; virtually all are based on empirical measurements. However, a select few are universally applied to drilling fluids. These are discussed later in this section.

4.6 Fluid Characterization

4.6.1 General

Fluids can be classified by their rheological behavior. Fluids whose viscosity remain constant with changing shear rate under otherwise constant conditions are known as *Newtonian* fluids. *Non-Newtonian* fluids are those fluids whose viscosity varies with changing shear rate.

The distinction between Newtonian and non-Newtonian fluids can be illustrated by using a Couette-type direct indicating viscometer described in Section 5. If the 600 r/min dial reading (R_{600}) is twice the 300 r/min reading (R_{300}), the fluid exhibits Newtonian flow behavior. If R_{600} is less than twice R_{300}, the fluid is non-Newtonian and shear-thinning (see 4.6.3).

As discussed later, temperature and pressure affect the viscosity of fluids (as well as density). Therefore, the test temperature and pressure shall be documented with the measured data to properly evaluate the drilling fluid flow behavior. It is common to test fluids at several pressures and temperatures and to make adjustments for downhole conditions. The testing device and test protocol are also important.

Pertinent mathematical models used for hydraulic calculations are shown in later sections.

4.6.2 Newtonian Fluids

Fluids for which shear stress is directly proportional to shear rate are called Newtonian fluids. Water, glycerin, light oils, and brines are examples of Newtonian fluids. For some areas, brines or other Newtonian fluids are used for field drilling applications.

A single viscosity measurement characterizes a Newtonian fluid at a given temperature and pressure.

4.6.3 Non-Newtonian Fluids

4.6.3.1 General

Fluids for which shear stress is not directly proportional to shear rate are called non-Newtonian. Most drilling fluids are non-Newtonian.

Drilling fluids are considered shear thinning when they exhibit lower viscosity at higher shear rates than at lower shear rates. This feature is particularly beneficial for drilling because it provides much higher viscosity in the low-shear rate environment present in the annulus and assists in better cuttings transport.

Some non-Newtonian fluids exhibit shear-thickening behavior in laminar flow. The viscosity of these fluids increases with increasing shear rate. Shear-thickening behavior would not be beneficial for drilling fluid applications. Time independent shear-thickening fluids are called dilatant fluids.

4.6.3.2 Shear-thinning fluids

One type of shear-thinning fluid begins to flow as soon as a shear force or pressure, regardless of how slight, is applied. Such fluids are termed *pseudoplastics*. Increasing shear rate causes a progressive decrease in viscosity. Polymer solutions are examples of true Power Law fluids that are described later.

Another type of shear-thinning fluid does not flow until a given shear stress is applied. The shear stress required to initiate flow is called the *yield stress*. These fluids are known as *viscoplastics*. Most drilling fluids fall into his category.

4.6.3.3 Thixotropic and rheopectic fluids

Fluids also can exhibit time-dependent effects. Under constant shear rate, *thixotropic* fluids experience a decrease in viscosity while *rheopectic* fluids experience an increase in viscosity with time. Many drilling fluids exhibit some level of thixotropic behavior, especially bentonite treated water base fluids.

Thixotropic fluids can also exhibit a behavior known as *gelation* or *gel-strength development*. Time-dependent forces cause the fluid to behave as a semi-solid after the fluid has remained static for a period of time. Sufficient force shall be exerted on the gelled fluid to overcome the gel strength and initiate fluid flow.

Some thixotropic and rheopectic fluids exhibit a hysteresis loop where the measured shear stress is dependent on the prior shear history. For thixotropic fluids the shear stress will be higher as the shear rate is increased from lower values and lower (than at the same shear rate) as the shear rate is reduced from higher values. This phenomenon should be taken into account for testing protocols.

4.6.4 Drilling fluid General Characterization

The range of drilling fluid rheological characteristics can vary from elastic, gelled solids at one extreme to purely viscous, Newtonian fluids at the other. These fluids can exhibit Newtonian, pseudoplastic, viscoplastic, or other behavior under specific conditions. It is not unreasonable to assume that all drilling fluids are *viscoelastic*, meaning that they exhibit both viscous and elastic properties to varying degrees. However, the linear-elastic response of drilling fluids is rarely tested, and the topic is beyond the scope of this document.

For practical reasons in the field and in most drilling fluid laboratories, flow properties usually are expressed in simple rheological terms. General statements regarding drilling fluids are subject to exceptions because of their extraordinary complexity.

4.7 Rheological Models

4.7.1 General

Rheological models provide useful data for characterizing fluid flow. Knowledge of rheological models combined with practical experience is necessary to fully understand fluid performance. No single model available at this time completely describes rheological characteristics of drilling fluids over their entire shear rate range. Rheological models are used to take data from measurements at difference shear rates and allow the shear stress and viscosity to be calculated for any value of interest in the circulating system.

Rheological models used for drilling fluids describe only time-independent, purely viscous behavior. A *rheogram*, the plot of shear stress vs shear rate, is used to graphically depict a rheological model. Figure 2 illustrates rheograms plotted on rectangular coordinates for 4 rheological models discussed later in this section. The curves are plotted using viscometer data (dial reading vs rotational speed) measured on a Couette-type direct indicating viscometer. They can be modeled following Equations (15) through, (18) (see 4.7.2 to 4.7.5).

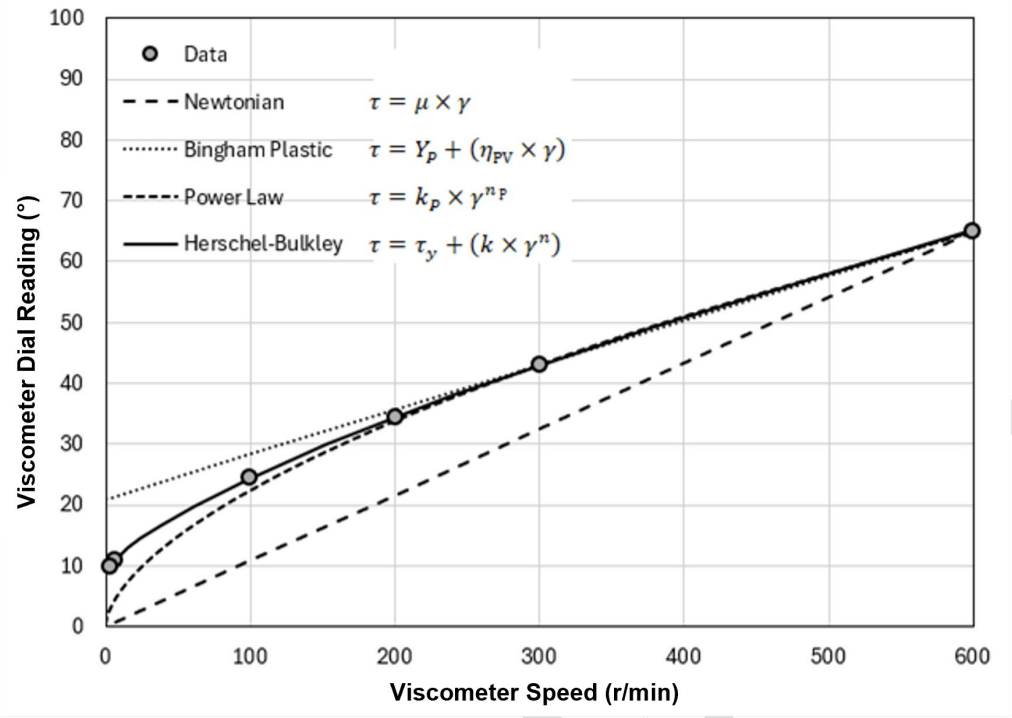

NOTE Newtonian, Bingham Plastic, Power Law and Herschel Bulkley rheological model and their Equations are described respectively under 4.7.2, 4.7.3, 4.7.4 and 4.7.5.

Figure 2—Rheograms of 4 Rheological Models on Rectangular Coordinates

4.7.2 Newtonian Model

The Newtonian model describes fluids for which the shear stress is directly proportional to the shear rate. The ratio shear stress to shear rate is the viscosity , μ, of the fluid. The rheogram on rectangular coordinates is a straight line starting at zero shear rate and stress. Shear stress at 1022 s^{-1} (600 r/min) is twice the value at 511 s^{-1} (300 r/min) on a Couette-type direct indicating viscometer (R1-B1 combination, F1.0 spring) The viscosity can be directly determined from the shear stress at 300 r/min (511 s^{-1})

Shear stress/shear rate relationship shall be described by Equation (15).

$$\tau = \mu \times \gamma \tag{15}$$

where in consistent units (see 1.3):

τ is the shear stress;

μ is the viscosity;

γ is the shear rate.

4.7.3 Bingham Plastic Model

This model describes fluids for which the shear stress/shear rate ratio is linear once a specific shear stress has been exceeded. Two parameters, *plastic viscosity* (η_{PV}) and *yield point* (Y_P), are used to describe this model. Because these parameters are determined at shear rates of 511 s^{-1} and 1022 s^{-1} [300 and 600 r/min, respectively, on a Couette-type direct indicating viscometer (R1B1 rotor/bob combination, F1.0 spring)], this rheological model characterizes fluids in the higher shear rate range where the shear rate/shear stress relationship is linear. The higher shear rates also ensure that the fluid in the gap is fully sheared. A rheogram of the Bingham plastic model on rectangular coordinates is a straight line that intersects the zero shear rate y-axis at a shear stress greater than zero (the yield point).

NOTE Plastic viscosity is commonly known in the industry by the abbreviation PV and the yield point by the abbreviation YP.

Shear stress/shear rate relationship shall be described by Equation (16):

$$\tau = Y_P + (\eta_{PV} \times \gamma) \tag{16}$$

where in consistent units (see 1.3):

τ is the shear stress;

Y_P is the Bingham yield point;

η_{PV} is the plastic viscosity;

γ is the shear rate.

NOTE In USC units, Equation (16) shall be rewritten to consider unit conversion to measured and reported parameters as Equation (19), see 5.2.3.

4.7.4 Ostwald–de Waele Model (Power Law)

This model, universally known as the power law, is used to describe the flow of shear-thinning or pseudoplastic drilling fluids. This model describes fluids for which the rheogram is a straight line when plotted on a log-log graph. Such a line has no y-axis intercept, meaning a power law fluid does not have a yield stress (yield stress is zero). The two required power law constants, flow behavior index (n_P) and power law consistency factor (k_P), for this model are determined from data taken at shear rates of 1022 s^{-1} and 511 s^{-1} [300 and 600 r/min, respectively], on a Couette-type direct indicating viscometer (R1B1 rotor/bob combination and F1.0 spring).

Shear stress/shear rate relationship shall be described by Equation (17):

$$\tau = k_P \times \gamma^{n_P} \tag{17}$$

where in consistent units (see 1.3):

τ is the shear stress;

k_P is the consistency index;

n_{P} is the power law flow behavior index;

γ is the shear rate.

NOTE In USC units, Equation (17) can be rewritten to consider unit conversion to measured and reported parameters see 5.2.4.

4.7.5 Herschel–Bulkley (H-B) Model

Also called the *modified power law*, *yield-power law*, or *yield-pseudoplastic model,* the H-B model is used to describe the flow of pseudoplastic drilling fluids that exhibit a yield stress (τ_{y}) which shall be exceeded to initiate flow. A rheogram of shear stress minus yield stress vs shear rate is a straight line on log-log coordinates. This model is widely used because it:

a) describes the flow behavior of most drilling fluids,

b) includes a yield stress value (τ_{y}) important for hydraulics issues, and

c) includes the Bingham plastic model and power law as special cases with a H-B consistency factor (k) and a H-B flow behavior index (n).

Shear stress/shear rate relationship shall be described by Equation (18):

$$\tau = \tau_{\mathrm{y}} + \left(k \times \gamma^{n}\right) \tag{18}$$

where in consistent units (see 1.3):

τ is the shear stress;

τ_{y} is the Herschel-Bulkley yield stress;

n is the Herschel-Bulkley flow behavior index;

k is the consistency factor;

γ is the shear rate.

NOTE In USC units, Equation (18) can be rewritten to consider unit conversion to measured and reported parameters, see 5.2.5.

4.7.6 Rheological Parameters and API Drilling Fluid Report

Rheological parameters recorded in an API Drilling Fluid Report should include Couette-type direct indicating viscometer readings/measured shear stress values. Two viscometer readings, R_{300} and R_{600}, (or their related measured shear stress values) can be used to calculate Bingham plastic yield point (Y_{P}) and plastic viscosity (η_{PV}) and power law model key parameters: flow behavior index (n_{P}) and consistency factor (k_{P}).

For the H-B model, an additional yield-stress term (τ_y) is required with the H-B flow-behavior index (n) and the consistency factor (k). The H-B yield stress is difficult to measure directly and can be most often calculated.

Additional viscometer readings/shear stress values R_{200}, R_{100}, R_6 *and* R_3 at rotational speed of 200 r/min, 100 r/min, 6 r/min and 3 r/min are often measured and reported. Measurements of dial readings are performed stepwise from the highest to the lowest revolutions per minute. Improved modeling accuracy can be achieved by also measuring the viscometer readings R_{60} and R_{30} (or their related measured shear stress values) at rotational speeds of 60 r/min and 30 r/min.

Gel strengths (β_{10m} and β_{10m}) measured after the fluid has been left static for 10 s and 10 min, respectively, also shall be reported on the API Drilling Fluid Report. The 30-min gel strength (β_{30m}) should be sometimes also measured and reported.

Mathematical treatments of H-B, Bingham plastic, and power law fluids are described in Section 5.

Flow characteristics of a drilling fluid are a function of the viscosity of the base fluid (the continuous phase),any solid particles (both inert and functional), emulsified droplets of nonaqueous fluid (oil) or water/brine, or gases within the fluid (the discontinuous phase),the flow channel characteristics, and the volumetric flow rate. Any interactions among the continuous and discontinuous phases, either chemical or physical, have a marked effect on the rheological parameters of a drilling fluid. The parameters measured and calculated using Couette-type direct indicating viscometer (plastic viscosity and yield point) are indicators commonly used to guide fluid conditioning to obtain the desired performance.

- Plastic viscosity is affected by the addition of any solids, their size, shape and concentration. Higher barite contents for higher drilling fluid weights and excessive colloidal solids lead to higher plastic viscosity, which is undesirable, as it increases pressure loss in the drill string, leading to higher standpipe pressure which may limit flowrates and hydraulic horsepower at the bit. Strategies to reduce plastic viscosity are dilution, processing with solids control equipment, or in some cases by settling.

- Yield point is primarily affected by electrical charges interaction between clays and other solids. Higher yield points indicate increased shear thinning behavior and higher viscosity in the annulus which is desirable for improved hole cleaning, however, higher yields points can also signal undesirable fluid contamination. Strategies to combat high yield point include chemical treatments or dilution.

5 Rheological parameters

5.1 Measurements of Rheological parameters

5.1.1 General

Determination of drilling fluid rheological parameters is important in the calculation of hydraulics, hole-cleaning efficiency, and prediction of weight-material sag in drilling wells. The discussion below only describes the most common instruments used at the wellsite and in drilling fluids laboratories. There are a wide variety of other commercial and research instruments that can be used to determine the rheological properties of drilling fluids. Additionally, fully automated wellsite real time or inline units are becoming more common place. Some of these are based on the Couette-type direct indicating viscometer described in 5.1.3 while others are pipe flow-based viscometers that measure pressure loss at various flow rates to derive equivalent drilling fluid rheological properties.

5.1.2 Orifice-viscometer—Marsh funnel

The Marsh funnel is widely used to measure relative viscosity and to identify changes in viscosity at the rigsite. The measurement, referred to as the funnel viscosity, is the time required in seconds for a finite volume of 1 quart (946 mL) to empty out of the funnel. The Marsh funnel is also a standard test method for clay slurries used in construction and civil engineering. Other orifice-based funnels or cups are used for measuring the viscosity in other industries, such as for paint and protective coatings.

The Marsh Funnel design, dimensions, and testing procedure for measuring funnel viscosity are described in API 13B-1 and API 13B-2.Marsh Funnel viscosity is a rapid, simple test performed routinely at the rigsite for all drilling fluid systems. It is most useful to gauge the relative viscosity against anticipated typical values and to alert rigsite personnel to changes in the drilling fluid properties or conditions. When a change in funnel viscosity is observed, additional rheological testing using a Couette-type direct indicating viscometer may be required to identify the change in fluid rheological properties. No single funnel viscosity measurement can be taken to represent a consistent value for all drilling fluids of the same type or of the same density.

5.1.3 Couette-type direct indicating viscometer

Couette-type direct indicating viscometers are the most common and standard instrument used for measuring the rheological properties of drilling fluids. The test fluid is contained in the annular space between two coaxial cylinders. The outer rotor (sleeve) is driven at a constant rotational speed, thereby applying a torque on the inner cylinder (bob) due to fluid friction.

The resulting torque on the inner cylinder (bob) for mechanical rotational viscometers is measured with a torsion spring that restrains the movement. A dial attached to the bob indicates deflection of the bob in degrees of rotation (dial units) that is proportional to the shear stress. This mechanism is illustrated in Figure 3. Digital Couette-type viscometers use the same geometry and principle; usually an optical encoder measures the deflection of the bob in degrees of rotation, and in some cases a torque sensor is used to measure torque and an equivalent shear stress or dial reading value is displayed digitally or output electronically.

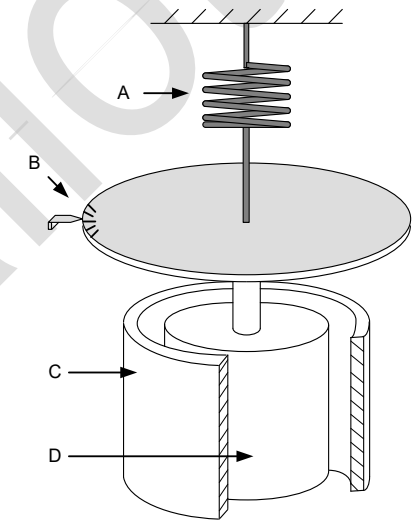

Key

A	torsion spring	C	rotor (sleeve)
B	dial	D	bob

Figure 3—Couette-type, Direct Indicating Viscometer with Dial Readout Schematic

Couette-type direct indicating viscometers used for drilling fluids are called “direct-indicating” or “direct-reading” because they have dimensions and instrument constants such that the Bingham Plastic coefficients, yield point and plastic viscosity, are obtained from viscometer measurements at rotor speeds of 600 r/min (R_{600}) and 300 r/min (R_{300}) using the standard rotor and bob dimensions (known as R1B1) and the standard spring (known as F1.0) see reference [6]. This direct indicating design has a R1 rotor inner diameter of 1.450 in. ±0.001 in. (36.83 mm ±0.02 mm) and a B1 bob diameter of 1.358 in. ±0.001 in. (34.49 mm ±0.02 mm), the diameter ratio (rotor/bob) of 1.0678 .R1B1 combination with a F1.0 spring [torsional stiffness 386 dynes•cm/degree of deflection (10.54 N•m/rad)]) allows the Bingham yield point and plastic viscosity to be calculated by simple subtraction. Also, the dial reading at 300 r/min (R_{300}) is equal to the fluid viscosity in centipoise (cP) at a shear rate of 511 s−1, aptly identifying viscometers of this configuration as “direct-reading*” instruments*. For Newtonian fluids, the dial reading at 300 r/min is equivalent to the viscosity of the fluid.

NOTE A rotor/bob diameter ratio < 1.1 ensures a nominally uniform shear stress across the gap and to keep fluid homogeneous.

The dimensions for the rotor R1, bob B1 and spring F1.0 constant, as described, determine the following:

— 1° deflection of the bob equals a shear stress of approximately 1 lbf/100 ft^2, more exactly 1.067 lbf/100 ft^2; or 0.511 Pa.

— 1 r/min of the rotor equals a shear rate of 1.7023 reciprocal seconds (s^{-1}).

Table 2 lists the types and operating limits of viscometers commonly used to test drilling fluids. Tier 1 units are portable devices used in the field and drilling fluids laboratories. Most are mechanical units like those illustrated in Figure 3, while others are digital. Most are 6, 9, or 12 speed Couette-type viscometer.

Tier 2-4 viscometers are computer-controlled units designed primarily for laboratory use and only used in the field under special circumstances. All of the viscometers listed in Table 2 use the same measurement principle; however, they differ in drive system, shear rate range, test conditions, and method of readout.

Table 2—Types of Couette-type Viscometers for Measuring Drilling Fluid Rheological Properties

Tier	Type	Maximum Pressure	Maximum Temperature
1	Portable (field)	Atmospheric	200 °F[a] (88°C)
2	High temperature	1000–2500 lbf/in.^{2} (6900–17,200 kPa)	500 °F (260 °C)
3	High temperature/high pressure	20,000 lbf/in.^{2} (137,900 kPa)	≥500 °F (≥260 °C)
4	Ultra-high temperature/high pressure	≥30,000 lbf/in.^{2} (206,800 kPa)	≥500 °F (≥260 °C)

[a] If the boiling point of water at the testing facility altitude is less than 212 °F(100 °C), the maximum temperature shall be adjusted accordingly.

Calibration and testing procedures for Tier 1 direct-indicating Couette-type viscometers are provided in API 13B-1 and API 13B-2. Specific operating procedures for other instruments shall be obtained from the respective manufacturers.

5.2 Rheological Models

5.2.1 Principle

The determination of drilling fluid rheological parameters is important for formulating, monitoring, and treating drilling fluids and in the calculation of hydraulics, hole-cleaning efficiency, and mitigation of weight-material sag in drilling wells. Additional details are provided hereafter for the three non-Newtonian rheological models presented in 4.7; Bingham plastic, power law, and Herschel-Bulkley (H-B). The H-B model has become the de facto standard for engineering calculations in the drilling industry and is recommended for field and office use. This H-B model provides accurate calculations for shear stresses at the shear rate of interest with good agreement to the measured data for both water-based and nonaqueous drilling fluids.

It is important to note that the constitutive equations provided in this section cannot be used directly to calculate frictional pressure losses. They first shall be converted to their respective flow equations [5.1, 5.2, 5.3] (Section 7).

5.2.2 Instrumentation Configuration

Use of a Couette-type direct-indicating viscometer with the standard configuration (R1B1, F1.0 spring) (see 5.1.3) is assumed in this section. The temperature at which the measurements are taken is important and should be considered when using the derived rheological parameters. Recommended test temperature guidelines are given in API 13B-1 (water-based drilling fluids) and API 13B-2 (nonaqueous-based fluids).

Drilling fluid rheological properties measured using Couette-type direct-indicating viscometers require instrument conversion factors to obtain values in proper engineering units [5.4]. The following applies to these types of viscometers using the R1B1 rotor and bob dimensions and F1.0 stiffness spring.

a) Shear stress (τ) expressed in lbf/100 ft^2 is determined by multiplying the dial reading, expressed in degrees, by 1.067.

b) Shear rate (γ) expressed in s^{-1} is determined by multiplying the rotor speed expressed in r/min by 1.7023.

Useful conversions from USC units to SI units are: 478 cP = 1.0 lbf•s/ 100 ft^2 , 1mPa•s = 1cP and 0.511 Pa = 1.067 lbf/100 ft².

5.2.3 Bingham Plastic Model

The Bingham Plastic model shown in Equation (16) (see 4.7.3) requires two parameters, *plastic viscosity* (η_{PV}) and *yield point* (Y_P). Using a Couette-type direct indicating viscometer with R1B1 combination and F1.0 spring Equation (16) shall be modified considering reporting units used for η_{PV} and Y_P, shall be shown as Equation (19).

$$\tau = Y_P + \left(\frac{\eta_{PV}}{511}\right) \times \gamma \tag{19}$$

where

τ is the shear stress, expressed in degrees (≈ lbf/100 ft²);

η_{PV} is the plastic viscosity, expressed in degrees/s^{-1} (= centipoises);

Y_P is the yield point in degrees (≈ lbf/100 ft^2);

γ is the shear rate, expressed in reciprocal seconds (s^{-1}).

NOTE The value of 511 in the denominator of Equation (19) is a units conversion from degrees per s^{-1} to centipoises. The Bingham Plastic model for drilling fluids is often written for shear rate having units of r/min with the denominator of the η_{PV} being 300, in that form the value of 300 is a unit conversion from degrees per r/min to centipoises.

Bingham parameters η_{PV} and Y_P should be calculated using viscometer shear stress measurements R_{600} and R_{300}, as shown respectively in Equations (20) and (21).

Although η_{PV} is reported with centipoise units and Y_P with lbf/100 ft^2 units, in Equations (19), (20), and (21), these parameters actually have Couette-type direct indicating viscometer units [degrees/s^{-1} (which are equivalent to centipoises with R1B1, F1.0 spring) and degrees, respectively]. This practice allows the parameters to be reported as integer values for simplicity. The discrepancies from the true units are about 6 % which is often resolved when the two parameters are used for pressure-loss calculations.

$$\eta_{PV} = R_{600} - R_{300} \tag{20}$$

$$Y_P = 2 \times R_{300} - R_{600} \tag{21}$$

where

η_{PV} is the plastic viscosity in centipoises;

Y_P is the yield point in degrees (≈ lbf/100 ft^2);

R_{600} is the dial reading at 600 r/min in degrees;

R_{300} is the dial reading at 300 r/min in degrees.

Using these 2 parameters the shear stress in Equation (19), τ, shall be calculated and expressed in viscometer degrees which are approximatively equivalent to lbf/100 ft². To obtain a value expressed in lbf/100 ft², it shall be required to multiply Y_P in degree value by 1.067.

The Bingham plastic model overestimates shear stresses at low shear rate ranges normally observed in most annular flow. However, η_{PV} and Y_P values derived from this model are particularly useful for reporting, monitoring, design, and treatment of all drilling fluids, even though the Bingham Plastic model itself may not be useful for calculating the annular shear stress values needed to determine annular pressure losses and evaluate other hydraulic characteristics. For certain drilling fluid types, the model provides a reasonably good fit to the viscosity, especially for flocculated or contaminated water-based drilling fluids viscosified with bentonite, like spud mud, where the low shear rate shear stress values are close to the Bingham yield point.

η_{PV} represents the slope of a straight line between dial readings R_{600} (γ = 1022 s^{-1}) and R_{300} (γ = 511 s^{-1}), on rectilinear coordinates (degrees vs γ). It is the viscosity of the fluid in the very high shear-rate linear region of the and is the theoretical minimum viscosity a fluid will have. Y_P is the intersection of the Bingham model straight line with the vertical y-axis (γ = 0). It represents the yield stress required to initiate flow.

It should be noted that with the η_{PV} value reported with centipoise units and the Y_P value reported with lbf/100 ft^2 units, there is often greater than an order of magnitude difference in these values. A one (1) unit change in Y_P is 478 times greater than a one (1) unit change in η_{PV}.

The viscometer data and derived parameters for all rheological models are temperature and pressure dependent, so care should be taken to consider the application of these parameters with the measurement conditions.

5.2.4 Power Law Model

5.2.4.1 General

The power law model provides a reasonable fit for some drilling fluid types, such as polymer water-based drilling fluids with very low yield stress values. However, it underestimates the shear stress values at low shear rates for most drilling fluids as the model forces the yield stress value (zero shear rate value) to be zero. One improved application of the power law model is to determine separately high shear rate and low shear rate flow behavior index (n_P and n_{Pa}) and consistency factor (k_P and k_{Pa}) values [5.5]. The high shear rate n_P and k_P values are determined from the R_{600} and R_{300} shear stress values and applicable to inside pipe calculations while the low shear rate n_{Pa} and k_{Pa} values are determined from the R_{100} and R_{300} shear stress values and applicable to annular calculations and particle settling [5.5].

It is also challenging to use n_P and k_P values to monitor and treat most drilling fluids in the same way that PV and Y_P are used. The flow behavior index (n_P), which varies from about 0.3 to 1.0 for drilling fluids, can help characterize rheological behavior. Lower n_P values suggest higher levels of shear thinning, while n_P = 1 represents Newtonian behavior. Care should be taken when comparing n_P and k_P values from various sources as the units used to report k_P may be different and difficult to convert.

A rheogram plot of dial reading vs shear rate is a straight line on log-log coordinates that passes through points measured at 600 r/min and 300 r/min. The slope of this line is n_P, and k_P is the y-axis intercept at γ = 1 s^{-1}. While Equations (22) and (23) are most frequently used to determine values for n_P and k_P based on measurements at 600 r/min and 300 r/min, curve fitting, or other mathematical methods may be used to fit the full range of shear stress values in order to determine more accurate values for n_P and k_P.

5.2.4.2 High shear rate parameters

The power law model shown in Equation (17) (see 4.7.4) requires two parameters: high shear rate flow behavior index (n_P) and consistency factor (k_P). These parameters should be calculated using Couette-type direct indicating viscometer measurements R_{300} and R_{300}, as shown in Equations (22) and (23).

The high shear rate flow behavior index (n_P) shall be calculated using Equation (22):

$$n_P = 3.32 \times \log_{10}\left(\frac{R_{600}}{R_{300}}\right) \tag{22}$$

and the power law consistency factor (k_P) using Equation (23):

$$k_{\mathrm{P}} = \frac{R_{300}}{511^{n_{\mathrm{P}}}} \tag{23}$$

where

n_{P} is the power law flow behavior index (high shear), dimensionless;

R_{600} is the dial reading at 600 r/min, expressed in degrees;

R_{300} is the dial reading at 300 r/min, expressed in degrees;

k_{P} is the power law consistency factor (high shear), expressed in degrees•s$^{n_{\mathrm{P}}}$ (≈ lbf•s$^{n_{\mathrm{P}}}$/100 ft^2).

NOTE The value of 511 in the denominator of Equation (23) is a unit conversion from degrees per s^{-1} to centipoises.

Using these parameters the shear stress in Equation (17), τ, shall be calculated and expressed in Couette-type direct indicating viscometer degrees which are approximatively equivalent to lbf/100 ft².

NOTE k_{P} as calculated using Equation (23) is obtained in viscometer degrees, which is approximatively equivalent to lbf•s$^{n_{\mathrm{P}}}$/100 ft². To obtain an exact value expressed in lbf•s$^{n_{\mathrm{P}}}$/100 ft², it is necessary to multiply k_{P} in degrees•s$^{n_{\mathrm{P}}}$ by 1.067. Then, τ should be calculated in lbf/100 ft².

5.2.4.3 Low shear rate parameters

Low shear rate flow behavior index (n_{Pa}) and consistency factor (k_{Pa}) should be calculated using Couette-type direct indicating viscometer measurements R_{100} and R_3, as shown in Equations (24) and (25).

The low shear rate flow behavior index (n_{P}) should be calculated using Equation (24):

$$n_{\mathrm{Pa}} = 0.657 \times \log_{10}\left(\frac{R_{100}}{R_3}\right) \tag{24}$$

and the low shear rate power law consistency factor (k_{Pa}) using Equation (25):

$$k_{\mathrm{Pa}} = \frac{R_{100}}{170.3^{n_{\mathrm{Pa}}}} \tag{25}$$

where

n_{Pa} is the low shear power law flow behavior index, dimensionless;

R_{100} is the dial reading at 100 r/min, expressed in degrees;

R_3 is the dial reading at 3 r/min, expressed in degrees;

k_{Pa} is the low shear power law consistency factor expressed in degrees•s$^{n_{Pa}}$ (≈ lbf•s$^{n_{Pa}}$/100 ft^2).

NOTE 1 The value of 170.3 in the denominator of Equation (25) is a unit conversion from degrees per s^{-1} to centipoises.

NOTE 2 k_{Pa} as calculated using Equation (25) is obtained in viscometer degrees, which is approximatively equivalent to lbf•s$^{n_{Pa}}$/100 ft². To obtain an exact value expressed in lbf•s$^{n_{Pa}}$/100 ft², it is necessary to multiply k_{Pa} in degrees•s$^{n_{Pa}}$ by 1.067. Then, τ should be calculated in lbf/100 ft².

5.2.5 Herschel-Bulkley (H-B) Rheological Model

5.2.5.1 General

The Herschel-Bulkley constitutive equation shown in Equation (18) (see 4.7.5) utilizes three parameters: n (flow behavior index), k (consistency factor), and τ_y (yield stress) [5.6, 5.3]. The H-B model can be thought of as a power law model with a yield stress, because the values for the H-B model are simply a power law curve shifted up by the yield stress value. The H-B rheological model provides an improved method to calculate the shear stress of interest for nearly all drilling fluids.

The yield stress is the shear stress required to initiate flow. The H-B yield stress, τ_y, is analogous to the Bingham yield point but is more accurate. It cannot be measured directly with a Couette-type direct indicating viscometer but can be estimated from low shear measurements several different ways. This value is often referred to as one of the following: tau-zero, true yield point, low-shear-rate yield point (LSRYP), or low-shear yield point ($LSYP$). It can also be mathematically estimated with curve-fit algorithms by fitting Equation (18) by assuming different values for τ_y within the limits of 0 (power law) and Y_P (Bingham Plastic).

The flow behavior index, n, and the consistency factor, k, can be calculated as shown in Equations (26) and (27) from viscometer measurements R_{600} and R_{300} using a value for the H-B yield stress, τ_y. Approximations of H-B yield stress, τ_y, are discussed in 5.2.5.2 and numerical calculation methods for all three H-B parameters in 5.2.5.3.

$$n = 3.32 \times \log_{10}\left(\frac{R_{600} - \tau_y}{R_{300} - \tau_y}\right) \tag{26}$$

$$k = \frac{\left(R_{300} - \tau_y\right)}{511^n} \tag{27}$$

where

n is the H-B flow behavior index, dimensionless;

k is the H-B consistency factor in degrees•s^n (≈ lbf•s^n/100 ft^2);

R_{600} is the dial reading at 600 r/min in degrees;

R_{300} is the dial reading at 300 r/min in degrees;

τ_y is the H-B yield stress in degrees (≈ lbf/100 ft^2).

NOTE The value of 511 in the denominator of Equation (27) is a unit conversion from degrees per s^{-1} to centipoises.

Using these parameters the shear stress in Equation (18), τ, shall be calculated and expressed in Couette-type direct-indicating viscometer degrees which are approximatively equivalent to lbf/100 ft².

NOTE H-B parameters as calculated using Equations (26) and (27) or estimated should provide a value based on Couette-type direct indication viscometer degrees, which is approximatively for k a value expressed in lbf•s^n and for in τ_y a value expressed in lbf/100 ft². To obtain a value for k expressed in lbf•s^n /100 ft² it should be required to multiply k in degrees•s^n/100 ft² by 1.067. Then, τ should be calculated in lbf/100 ft², providing τ_y should be also converted in lbf/100 ft² (degrees x 1.067).

5.2.5.2 Determination of H-B yield stress—Approximation methods

As detailed above, values for the H-B parameters n (flow behavior index) and k (consistency factor) can be determined from the Couette-type direct indicating viscometer measurements without any computer processing. However, these viscometers are not able to measure τ_y directly. In fact, measurement of τ_y is challenging even using sophisticated viscometers.

A commonly used approximation for τ_y, known as the low shear (rate) yield point ($LSYP$) [5.3], can be calculated from viscometer readings R_6 and R_3 as shown in Equation (28).

$$\tau_y \approx LSYP = 2R_3 - R_6 \quad (28)$$

where

τ_y is the H-B yield stress in degrees (≈ lbf/100 ft^2);

$LSYP$ is the low shear yield point expressed in degrees (≈ lbf/100 ft²);

R_6 is the dial reading at 6 r/min in degrees;

R_6 is the dial reading at 3 r/min in degrees.

While not as accurate as using the $LSYP$ value from Equation (28) for τ_y, the R_3 viscometer dial reading can also be used as a simplification.

Yield stress τ_y can be more accurately determined by measurement on oilfield digital viscometers that operate at shear rates as low as 0.017 s^{-1}(i.e. 0.01 r/min). Special-purpose viscometers that directly measure τ_y are also available but not widely used.

5.2.5.3 Determination of drilling fluid H-B parameters— Numerical solution

Numerical regression techniques using unweighted [5.6, 5.7] or weighted parameters [5.8] are preferred for determining all three H-B parameters more accurately. Spreadsheets or computer programs are required for this purpose. These fitting methods have the distinct advantage of using more data pairs over the full shear

rate range of measurements. Increased accuracy can be obtained by using additional data pairs within the shear rate range for annular flow conditions (e.g. shear stress values at R_{60} and R_{30}).

The weighted-parameter least-squares method is potentially superior but is more complex to solve. The weighted-parameter method more consistently preserves the original values for R_{600} and R_{300} as it applies a higher weighting to the "relatively more precise" high shear rate data.

Many widely used H-B parameter numerical solutions [5.6, 5.7] include calculating or estimating the corrected shear rate at the bob wall due to non-Newtonian behavior and the influence of n. There is no explicit analytical solution for the shear rate at the bob wall for H-B fluids and a non-linear regression or approximations should be used [5.9]. This shear rate at the bob wall is then used for each shear stress measurement with each iteration of n values during the fitting analysis using the new data pairs. Depending on the numerical method used and whether or not the corrected shear rate at the bob wall is used, the reported H-B parameter values may differ slightly for any given set of measured data.

Another numerical solution involves selection of a third data value in addition to R_{600} and R_{300} and using a simple convergence approach to determine τ_y. Possible choices include either R_6 or R_3. Values for τ_y are sequentially tested until the calculated and measured values for the chosen parameter converge. Original values for R_{600} and R_{300} are preserved by definition. H-B parameters n and k can then be calculated directly using Equations (26) and (27), respectively. τ_y values should be constrained within 0 (inclusive) and Y_P (inclusive).

6 Prediction of Downhole Behavior of Drilling Fluids

6.1 Principle

The downhole behavior of fluid properties should be considered to accurately calculate the hydraulics of drilling fluids. This is especially important when nonaqueous drilling fluids (NADF) are used. The downhole behavior of drilling fluids is dependent on static and dynamic temperatures, pressures, rheological properties, and density. Each of these areas are discussed in this Section 6.

6.2 Temperature Predictions of Circulating Drilling Fluids

6.2.1 Principle

The prediction of bottomhole circulating temperature (T_{bhc}) is necessary for use in hydraulic and drilling fluid density modeling, especially when NADFs are used. The prediction of circulating temperatures in a wellbore is a very complex task, however, as many operational and physical parameters are required. A simplified calculation procedure is presented here that requires a minimum of input parameters and is generally sufficiently accurate to predict circulating temperatures.

This model [6.1, 6.2], which can be easily programmed in a spreadsheet program, gives acceptable results within the following ranges for the bottomhole static temperature (T_{bhs}) and geothermal gradient (ψ_g):

— bottomhole static temperature: 166 °F to 414 °F (74 °C to 212 °C);

— geothermal gradient: 0.83 °F/100 ft to 2.44 °F/100 ft (1.51 °C/100 m to 4.45 °C/100 m).

6.2.2 Temperature Prediction Input Parameters

For the prediction of downhole circulating temperatures, T_{bhc}, expressed in degrees Fahrenheit, input parameters shall be required for Equations (29) to (35) as follows:

a) true vertical depth (D_{tvd}), expressed in feet;

b) bottomhole static temperature (T_{bhs}), expressed in degrees Fahrenheit par 100 feet

c) for offshore wells, water depth (D_w), expressed in feet; for land wells, D_w = 0;

d) geothermal gradient ($\psi_{g)}$), expressed in degrees Fahrenheit par 100 feet;

e) geothermal gradient adjusted for water depth (ψ_{gw}), expressed in degrees Fahrenheit par 100 feet

f) surface temperature (T_0) measured at 50-ft depth or approximated by the annual mean surface temperature, expressed in degrees Fahrenheit.

6.2.3 Bottomhole Circulating Temperature Calculations

Temperature calculation methods for land and offshore wells should be as follows.

a) For land wells with a known bottomhole static temperature (T_{bhs}) expressed in °F, the bottomhole circulating temperature (T_{bhc}) can be calculated using the following method [6.1].

1) Calculate geothermal gradient ψ_g expressed in °F/100 ft as given by Equation (29).

$$\psi_g = 100 \times \frac{(T_{bhs} - T_0)}{D_{tvd}} \tag{29}$$

2) Estimate T_{bhc} expressed in °F using Equation (30).

$$T_{bhc} = \left(3354 \times \frac{\psi_g}{100}\right) + \left[T_{bhs} \times \left(1.342 - 22.28 \times \frac{\psi_g}{100}\right)\right] - 102.1 \tag{30}$$

b) For land wells with a known geothermal gradient (ψ_g), T_{bhc} can be calculated by the following.

1) Calculate T_{bhs} expressed in °F as given by Equation (31).

$$T_{bhs} = T_0 + \left(\frac{D_{tvd} \times \psi_g}{100}\right) \tag{31}$$

2) Estimate T_{bhc} expressed in °F using Equation (30).

c) For offshore wells with a known T_{bhs}, the above method can be used once the geothermal gradient has been adjusted for the presence of a water column.

1) Calculate the geothermal gradient adjusted for the water depth (ψ_{gw}) expressed in °F/100 ft using Equation (32).

$$\psi_{\text{g}} = 100 \times \frac{\left(T_{\text{bhs}} - T_0\right)}{\left(D_{\text{tvd}} - D_{\text{w}}\right)} \tag{32}$$

2) Estimate T_{bhc} expressed in °F using Equation (30).

d) For offshore wells with a known geothermal gradient, Equations (33) and (30) can be used after adjusting for water depth:

1) Calculate T_{bhs} expressed in °F as given by Equation (33).

$$T_{\text{bhs}} = T_0 + \frac{\psi_g}{100} \times \left(D_{\text{tvd}} - D_{\text{w}}\right) \tag{33}$$

2) Estimate T_{bhc} expressed in °F using Equation (30).

6.2.4 Static Temperature Profile

A static temperature profile for a well shall be constructed. Temperatures for a static well should be collected and predicted using the following data.

a) Surface temperature.

1) For land wells:

The annual mean surface temperature serves as the static temperature value at D_{tvd} = 0.

NOTE If the annual mean temperature is unknown, use the static temperature at 50-ft depth as T_0.

2) For offshore wells:

Adjustments in the geothermal gradients are required to account for water depth.

Static temperatures in a seawater column and then temperature at mudline (T_{ml}), expressed in degrees Fahrenheit, can be predicted as a function of water depth, D_{w}, expressed in feet, by Equation (34) or (35):

— For water depths ≤ 3000 ft:

$$T_{\text{ml}} = 154.43 - 14.214 \times \ln\left(D_{\text{w}}\right) \tag{34}$$

— For water depths > 3000 ft:

$$T_{\mathrm{ml}} = 41.714 - \left(3.714 \times 10^{-4}\right) D_{\mathrm{w}} \tag{35}$$

b) Construction of the predicted static temperature profile.

While a well is being drilled, estimates for T_{bhs} should be made using a known geothermal gradient or the geothermal gradient is estimated using a known T_{bhs}. Several data points should be collected as functions of D_{tvd} while the well is being drilled.

A straight-line fit between the collected data points can give a predicted static temperature profile by depth. These values or averages of them over a desired depth interval can then be inserted into the models that predict the downhole static rheological properties and density of drilling fluids as outlined later.

6.2.5 Dynamic Temperature Profile

Dynamic circulating temperatures for a well can be predicted in a similar manner to those used above in predicting static temperatures. Dynamic circulating temperature profile should be constructed using the following steps.

a) Using the values for T_{bhc} and the geothermal gradients ψ_{g} the T_{bhc} for each of the points can be calculated using the Equations in 6.2.3.

b) Flowline temperature (T_{fl}) is routinely measured and serves as the dynamic circulating temperature at depth D_{tvd} = 0. This value can be used to calibrate the circulating temperature predictions made from the Equations in 6.2.3.

c) A straight-line fit between the collected data points predicts dynamic temperature profile by depth.

These values or averages of them over a desired depth interval can then be inserted into the models that predict the downhole dynamic rheological properties and density of drilling fluids as outlined later in this section.

6.3 Prediction of Downhole Rheological Properties

6.3.1 Principle

Accurate prediction of downhole rheological properties of drilling fluids is important for the optimization of hydraulic and hole-cleaning capabilities of drilling fluids. With enhanced prediction of downhole properties, standard hydraulics calculations such as circulating pressure losses, surge and swab pressures, and hole-cleaning efficiencies can be more accurately determined. This increased accuracy can be of critical value in well sections where the differentials between pore pressures and formation fracture gradients are small. For certain drilling fluid types such as NADFs, downhole rheological properties can be significantly different from those measured under surface conditions. As a result, the usefulness of hydraulics calculations made with surface-measured rheological parameters can be limited.

6.3.2 Effects of Temperature and Pressure

The effects of temperature and pressure on rheological properties shall be taken into account. When considered separately, the generalized effects of temperature and pressure on downhole rheological properties can be summarized as follows:

- The effect of increased temperature usually decreases the viscosity of drilling fluids. The temperature effects on fluid viscosity are generally non-linear.

- The effect of increased pressure usually increases the viscosity of drilling fluids. The pressure effects on fluid viscosity are generally exponential.

- The combined effects of temperature and pressure on drilling fluids depend on the fluid type. Usually drilling fluid viscosity is lower downhole as compared to the surface measured values.

High temperature high pressure (HTHP) applications and deepwater cases where fluids in long risers are exposed to cold seawater are special cases where downhole modeling of drilling fluids and brines enhance the accuracy of hydraulic calculations.

The effects of temperature and pressure on downhole fluid rheological properties are most pronounced for NADFs. By way of example, the viscosity profiles of several nonaqueous base fluids as a function of temperature are presented in Figure 4. The non-linear reduction in fluid viscosity with increasing temperature is evident.

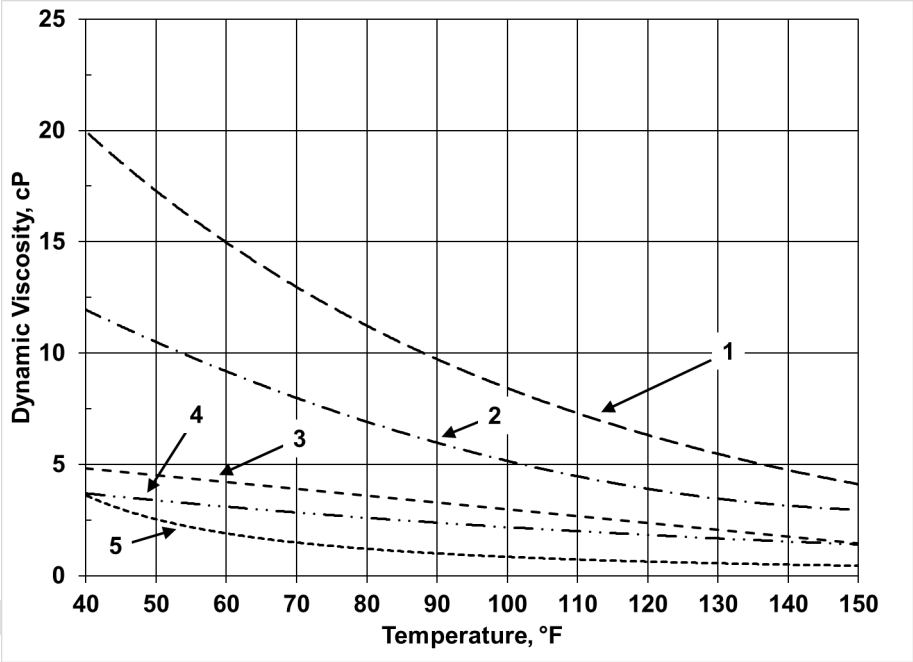

Key

1 ester synthetic fluid
2 PAO synthetic fluid
3 IO C16-18 synthetic fluid
4 LAO C14-16 synthetic fluid
5 diesel oil

Figure 4—Viscosity of Several Nonaqueous Base Fluids as Function of Temperature

6.3.3 Test Matrix

Testing is required to determine downhole rheological properties. Measurements using HTHP viscometers are recommended for improved predictions of downhole viscosity. Viscometers capable of testing at elevated temperatures and pressures are described in Section 5 of this document.

A comprehensive test matrix should be planned and developed before any testing is undertaken. The test matrix should include several key conditions.

a) A common test matrix involves dividing the well into individual sections based on changes in hole angle, wellbore geometry, estimated circulating temperatures (see 6.2), etc...

b) For each wellbore section, determine the average pressure and temperature conditions.

   Construct a test matrix incorporating the temperature and pressure ranges from the wellbore plus add a buffer on each side of the temperature and pressure ranges so that slightly more severe conditions than the original conditions can be tested. For example, given a wellbore having temperature and pressure conditions of 80 °F to 260 °F and 500 lbf/in.^{2} to 7000 lbf/in.^{2}, respectively, construct a testing matrix similar to that shown in Table 3.

Table 3—Example HTHP Viscometer Test Matrix

Temperature °F	**Pressure**, lbf/in.^{2}				
	0	2000	4000	6000	8000
70	data	data	data	data	data
120	data	data	data	data	data
170	data	data	data	data	data
220	data	data	data	data	data
270	data	data	data	data	data

NOTE Alternatively, the number of laboratory measurements can be reduced by testing only at the average temperature and pressure conditions predicted for each of the wellbore sections. Consequently, the reduced number of tests would be represented as a near diagonal in the test matrix above (see shaded cells).

c) For each temperature/pressure combination in the test matrix, record (at the minimum) $R_{600,}$ $R_{300,}$ $R_{200,}$ $R_{100,}$ $R_{6,\text{ and}}$ R_3. Gel-strength measurements (β_{10s} *and* $\beta_{10\min}$) also should be included. Use of the standard configuration (R1B1 combination and spring F1.0) on the viscometer is recommended.

   NOTE R_{60} and R_{30} can be also recorded and are recommended for a numerical determination of H-B parameters.

d) Calculate the drilling fluid rheological parameters (see Section 5) using the test data and the H-B rheological model.

e) Insert the fluid rheological parameters calculated above into the well sections determined as in 7.4 and run the hydraulics calculations (pressure losses, swab/surge, etc.) for each section.

6.4 Prediction of Downhole Pressures and Density

6.4.1 Principle

Accurate prediction of downhole pressures is important in drilling and completion operations, especially in those situations where there is a narrow window between pore pressure and fracture gradient. As with drilling fluid rheological properties, drilling fluid density is affected by downhole temperatures and pressures. To more accurately model ECD and equivalent static density (ESD), the local drilling fluid density profile at each wellbore location along the entire wellbore length should be determined using downhole conditions. The methods presented assume that the suspended solids are incompressible.

For certain drilling fluid types, such as NADFs, the drilling fluid density under downhole conditions can be significantly different from that measured at ambient surface conditions.

The method used to determine the density and pressure at any point in the wellbore is to divide the well into short intervals or cells and to calculate the local temperature and pressure at each cell so that a local density and rheology can be determined [6.3, 6.4], see Annex B Table B.2.

For static conditions, the local cell density and change in true vertical depth (TVD) are used to determine the hydrostatic pressure contribution of each cell, then these are summed from surface to any depth to obtain the pressure at that depth, see 6.4.5.2.

For dynamic conditions, the hydrostatic pressure contribution and annular pressure loss (calculated from the local rheology) are added for each cell then summed over then entire circulating path from surface to any depth, see 6.4.5.3.

6.4.2 Effects of Temperature and Pressure on Density

6.4.2.1 Summary

The effect of both temperature and pressure shall be considered to predict the downhole fluid density. When considered separately, the generalized effects of temperature and pressure on downhole drilling fluid density can be summarized as follows.

a) The effect of increased temperature will decrease density and reduced temperatures increase density. Temperature effects on non-aqueous fluid density are generally linear or near linear.

b) The effect of increased pressure will increase drilling fluid density. Pressure effects on density generally follow a 2nd order polynomial at any given temperature.

6.4.2.2 Temperature and pressure effects on drilling fluids density

The magnitude of temperature and pressure effects on drilling fluid density depends on the base fluid type and fluid composition. For many drilling fluids and wellbore conditions, the combination of temperature and pressure work in opposite directions and tend to reduce the overall change in density. NADFs are affected to a greater degree than water-based fluids.

The effects of temperature and pressure on the density of water, water-based drilling fluids, and brines are usually moderate and less than for NADFs. Monovalent brines are less affected by temperature and pressure than divalent brines. Hence for some water-based drilling fluids and monovalent brines, the use of fluid density measured at surface may be acceptable for use in downhole simulations for some wells.

The effects of downhole temperature and pressure on the density of divalent brines such as calcium chloride can be significant and warrant these changes being considered. In 6.4.2.2, data for a 19.3 wt% calcium chloride solution is presented to allow modelling temperature and pressure effects of this commonly used brine phase for non-aqueous drilling fluids.

The effects of temperature and pressure on downhole fluid density are most pronounced for nonaqueous liquids and NADFs. The effects of temperature and pressure on a synthetic-based drilling fluid are shown in Figure 5. The data clearly show the temperature and pressure effects. Because the data are well-ordered, a general mathematical model can describe these effects in a numerical fashion. Since different nonaqueous fluids behave slightly differently with changes in temperature and pressure, individual correlations should be constructed to mathematically describe fluid behavior more accurately.

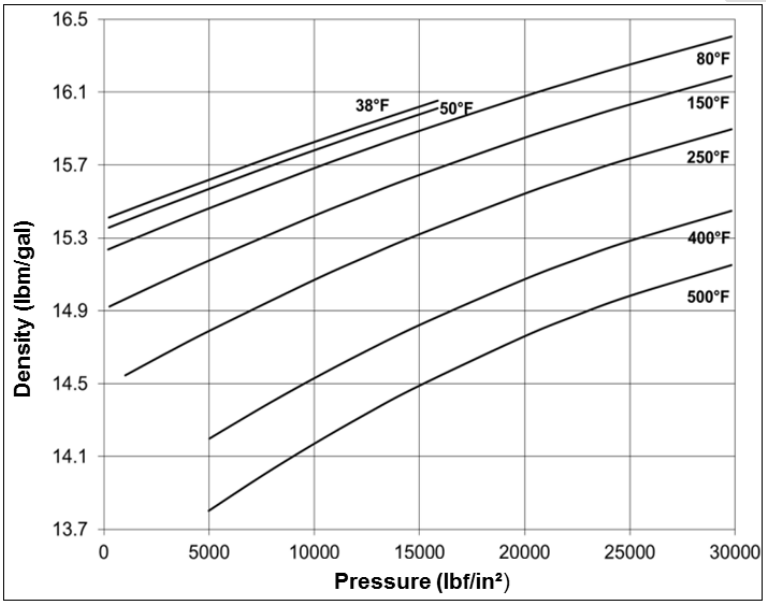

Figure 5—Isothermal Plot of a 15.3 lbm/gal Synthetic-based Drilling Fluid

6.4.3 Modeling the Effects of Temperature and Pressure on Drilling Fluid Density

6.4.3.1 General

The downhole density of drilling fluids can be accurately predicted using a compositional model that considers the compressibility and thermal expansion of the liquid and solid phases in the drilling fluid [6.5, 6.6]. Drilling fluid is generally composed of base fluid (nonaqueous, water, or brine), suspended solids (weighting agent, drill solids, and insoluble additives) and added chemicals. The volume of added chemicals and their contribution to changes in density is small as compared to the volume changes of the base fluid and other liquids. For this exercise the added chemicals are assumed to be part of the base fluid and corrected solids volumes as measured by a retort. The volume change for suspended solids is even less, so the volume fraction of solids is considered to be incompressible.

Example calculations for the Equations provided in Section 6.4 are included in Annex B.

6.4.3.2 NADF case

For a NADF, the fluid density (ρ_{total}) can be calculated from the fractional volumetric mass of the components (φ_{base} for base fluid, φ_{brine} for brine, and φ_{solids} for solids] of the whole-NADF and their respective densities (ρ_{base}, ρ_{brine}, and $_{\text{solids}}\rho$) using Equation (36). Similarly, the density for water-based fluids can be calculated using a compositional model of the base fluid, other NADF liquids, and solids.

$$\rho_{\text{total}} = \varphi_{\text{base}}\rho_{\text{base}} + \varphi_{\text{brine}}\rho_{\text{brine}} + \varphi_{\text{solids}}\rho_{\text{solids}} \tag{36}$$

With the sum of the fractional component volumes equal to 1.0, the volume fraction of (suspended) solids of the whole-NADF shall be expressed by Equation (37).

$$\varphi_{\text{total}} = \varphi_{\text{base}} + \varphi_{\text{brine}} + \varphi_{\text{solids}} = 1 \quad \text{or} \quad \varphi_{\text{solids}} = 1 - \left(\varphi_{\text{base}} + \varphi_{\text{brine}}\right) \tag{37}$$

Under downhole conditions of higher pressure and temperature, the drilling fluid volume changes due to the combined effects of expansion and contraction of the base fluid and the brine, resulting in a change in density. The compressibility and the thermal expansion of the solids are generally negligible compared to volumes changes of the liquids.

For a NADF, drilling fluid density at any pressure and temperature [$\rho_{(P\text{-}T)}$] can be calculated from base fluid and brine density at ambient temperature and pressure (respectively (ρ_{base} and ρ_{brine}) and at desired pressure P and temperature T (respectively ($\rho_{\text{base}(P\text{-}T)}$ and $\rho_{\text{brine}(P\text{-}T)}$), using their volume fractions at ambient conditions (respectively φ_{base} and φ_{brine}) plus the solids density and volume fraction (ρ_{solids}, φ_{solids}) using Equation (38). Volume fractions are expressed in decimal values (from 0 to 1) and density can be expressed in any consistent density units.

$$\rho_{(P-T)} = \frac{\varphi_{\text{base}}\rho_{\text{base}} + \varphi_{\text{brine}}\rho_{\text{brine}} + \varphi_{\text{solids}}\rho_{\text{solids}}}{1 + \varphi_{\text{base}}\left(\frac{\rho_{\text{base}}}{\rho_{\text{base}(P-T)}} - 1\right) + \varphi_{\text{brine}}\left(\frac{\rho_{\text{brine}}}{\rho_{\text{brine}\,(P-T)}} - 1\right)} \tag{38}$$

When the drilling fluid density at ambient temperature and pressure is known, the density of the solids fraction, ρ_{solids}, should be calculated using Equation (42). When the drilling fluid density at ambient is not known and when a drilling fluid density at another temperature and pressure is known, the density of the solids fraction, ρ_{solids}, can be calculated by rearranging Equation (38) to solve for the density of the solids fraction.

From the drilling fluid retort analysis, the volume fraction of the individual components of the whole drilling fluid shall be measured: φ_{base}, φ_{water} and φ_{ds} (volume fraction of base fluid, pure water, and dried retort solids respectively). These retort values sum to 1.0 as shown in Equation (39).

$$\varphi_{\text{total}} = \varphi_{\text{base}} + \varphi_{\text{brine}} + \varphi_{\text{ds}} = 1 \tag{39}$$

To calculate the volume fraction of solids (φ_{solids}) , and then the density of solids (ρ_{solids}), the volume fractions of dried retort solids (φ_{ds}) and water shall be corrected for the volume of soluble salt from the brine which is contained in the retort volume fraction of dried solids. API 13B-2 contains the procedure to determine the mass fraction of soluble salt plus corrections for brines which contain both sodium and calcium chloride.

6.4.3.3 NADF with only calcium chloride brine

For a NADF which contains only calcium chloride, the density of the brine at ambient conditions, ρ_{brine}, in grams per milliliter, shall be calculated using Equation (40).

$$\rho_{\text{brine}} = 0.99707 + \left[7.923 \times 10^{-3} \left(w_{\text{CaCl}_2}\right)\right] + \left[4.964 \times 10^{-5} \left(w_{\text{CaCl}_2}\right)^2\right] \quad (40)$$

where

w_{CaCl_2} is the NADF aqueous-phase mass fraction of calcium chloride, expressed as a percentage of the total aqueous-phase mass.

For a NADF which contains only calcium chloride in the aqueous phase, the volume fraction of brine, φ_{brine}, shall be calculated using Equation (41).

$$\rho_{\text{brine}} = \frac{100 \times \varphi_{\text{water}}}{\varphi_{\text{water}} \times \left[100 - \left(w_{\text{CaCl}_2}\right)\right]} \quad (41)$$

where

φ_{water} is the volume fraction of pure water from the retort;

ρ_{brine} is the NADF brine density, expressed in grams per milliliter;

w_{CaCl_2} is the NADF aqueous-phase mass fraction of calcium chloride, expressed as a percentage of the total aqueous-phase mass.

6.4.3.4 NADF corrected solids from retort analysis

The corrected volume fraction of solids, φ_{solids}, for a NADF shall be calculated using Equation (42).

$$\varphi_{\text{solids}} = 1 - \left(\varphi_{\text{base}} + \varphi_{\text{brine}}\right) \quad (42)$$

where

φ_{solids} is the volume fraction (corrected) of solids of the whole-NADF

φ_{base} is the volume fraction of base fluid of the whole-NADF;

φ_{brine} is the volume fraction of brine of the whole-NADF.

The density (corrected) of solids for a NADF shall be calculated using Equation (43). It may be used with any consistent density units.

$$\rho_{\text{solids}} = \frac{\rho_{\text{total}} - \left[\left(\varphi_{\text{base}} \times \rho_{\text{base}}\right) + \left(\varphi_{\text{brine}} \times \rho_{\text{brine}}\right)\right]}{\varphi_{\text{solids}}} \quad (43)$$

where

ρ_{solids} is the density (corrected) of the solids;

φ_{base} is the volume fraction of base fluid of the whole-NADF;

φ_{brine} is the volume fraction of brine of the whole-NADF;

φ_{solids} is the volume fraction (corrected) of solids of the whole-NADF;

ρ_{total} is the density of the whole-NADF at ambient condition, expressed in lbm/gal;

ρ_{brine} is the density of the brine at ambient conditions, expressed in lbm/gal;

ρ_{base} is the density of the base fluid at ambient conditions, expressed in lbm/gal .

6.4.3.5 Base fluid and brine density at temperature and pressure

Base fluid and brine density at any temperature and pressure ($\rho_{\text{base(P-T)}}$ and $\rho_{\text{brine(P-T)}}$) can be calculated using Equation (44). With the proper coefficients, Equation (41) is suitable for NADFs and most brines used for drilling fluids. It is not as accurate for water and lower-salinity brines that do not behave linearly with temperature [6.7].

$$\rho_{\text{base}(P\text{-}T)} \text{ or } \rho_{\text{brine}(P\text{-}T)} = \left(a_1 + b_1 P + c_1 P^2\right) + \left(a_2 + b_2 P + c_2 P^2\right) \times T \quad (44)$$

Pressure and temperature coefficients presented in Table 4 can be used in Equation (44) to determine values expressed in pounds mass per gallon of $\rho_{\text{base(P-T)}}$ and $\rho_{\text{brine(P-T)}}$ for any combination of temperature, T, expressed in degrees Fahrenheit , and pressure, P, expressed in pounds force per square inch, within the range of validity indicated. Each of the six coefficients (a_1, b_1, c_1, a_2, b_2 and c_2) to be used in Equation (44) shall be calculated by multiplying the actual fluid density (ρ) at ambient with the six coefficients listed in scientific notation in Table 4, before inserting into the equation. If the actual fluid density at ambient is unavailable, the average density value from Table 4 should be used.

The data for mineral oils, synthetics, and diesels represent average values [6.10] measured on a commercial pressure volume temperature (PVT) pycnometer [6.8, 6.9]. This method is useful for general calculations, especially when planning a well, when the individual base fluid is unknown, or when base fluid specific PVT data is not available. The 19.3 %wt $CaCl_2$ brine data were measured using the same pycnometer and test procedures. Data for individual base fluids also are available in the literature [6.5, 6.6, 6.8 to 6.11] and often from the manufacturer. The average values in Table 4 were determined by normalizing the coefficients of each base fluid with its density at ambient conditions.

For NADFs with a brine phase significantly different than 19.3 %wt. $CaCl_2$, other coefficients for Equation (44) or another calculation method [6.7, 6.1 to 6.13] should be used, especially if the volume fraction of the brine phase

is greater than 10%. Density data for calcium chloride is available in literature [6.14] that can be used to develop calculation methods for the coefficients used in Equation (44) based on the exact weight percent or molality.

Table 4—Temperature and Pressure Coefficients for Determining Fluid Density Using Equation (44)

Multiply listed coefficients by ρ fluid density (lbm/gal)	**Mineral Oils** [6.10]	**Synthetics** [6.10]	**Diesels** [6.10]	**DI Water** [6.8]	**$CaCl_2$ Brine** [6.9] **19.3 %wt**
Average Pressure Coefficients					
a_1, lbm/gal	ρ × 1.03E+00	ρ × 1.02E+00	ρ × 1.04E+00	ρ × 1.03E+00	ρ × 1.02E+00
b_1, (lbm/gal)/(lbf/in.^{2})	ρ × 4.55E-06	ρ × 4.67E-06	ρ × 4.47E-06	ρ × 1.95E-06	ρ × 1.71E-06
c_1, (lbm/gal)/(lbf/in.^{2})^2	ρ × −3.63E-11	ρ × −4.03E-11	ρ × −4.25E-11	ρ × 8.28E-12	ρ × 1.13E-11
Average Temperature Coefficients					
a_2, (lbm/gal)/°F	ρ × −4.13E-04	ρ × −4.24E-04	ρ × −3.98E-04	ρ × −4.63E-04	ρ × −3.15E-04
b_2, [(lbm/gal)/(lbf/in.^{2})] /°F	ρ × 9.53E-09	ρ × 9.33E-09	ρ × 8.95E-09	ρ × 7.17E-09	ρ × 3.50E-09
c_2, [(lbm/gal)/(lbf/in.^{2})^2] /°F	ρ × −1.41E-13	ρ × −1.22E-13	ρ × −1.25E-13	ρ × −1.06E-13	ρ × −6.49E-14
Average Densities					
ρ, lbm/gal	6.706	6.494	6.935	8.454	9.8
Range of Validity					
Max. pressure, lbf/in.^{2}	30,000	30,000	30,000	30,000	30,000
Min. temperature, °F	40	40	40	84	76
Max. temperature, °F	600	600	600	500	500

6.4.4 Modeling Static and Dynamic Downhole Pressures and Equivalent Density.

6.4.4.1 Principle

As described in 6.4.1, the method used to determine the equivalent density and pressure at any point in the wellbore is to divide the well into short intervals or cells and to calculate the local temperature and pressure at each cell so that local density and rheology can be determined. The pressure change of each cell is then summed from surface to the depth of interest, see the example in Annex B Table B.2.

6.4.4.2 Static downhole pressures

For static conditions, the local drilling fluid density for each cell, $\rho_{(P\text{-}T),i}$ shall be calculated from Equation (38) using the local temperature and pressure. Values for the static temperature at each cell can be determined using the method described in 6.2. The hydrostatic pressure changes for each cell, $\Delta P_{\mathrm{ha},i}$, expressed in lbf/in.², shall be calculated using the local cell fluid density and the change in TVD using Equation (45).

$$\Delta P_{\mathrm{ha},i} = 0.052 \times \rho_{(P-T),i} \times \Delta D_{\mathrm{tvd},i} \tag{45}$$

NOTE Coefficient 0.052 is a unit conversion and rounded for ease of use. A more exact value is 12/231 or 0.051948052.

where

$\rho_{(P\text{-}T),i}$ is the local drilling fluid density for each i cell, expressed in lbm/gal

$\Delta D_{\text{tvd},i}$, is the change in total vertical depth for each i cell, expressed in ft

For both static and dynamic conditions, after drilling with high rates of penetration (ROP) and when the effect of suspended cuttings in annulus is important, such as for poor hole cleaning in a vertical section, when cuttings have not been circulated from the well, the increase effective density due to the cuttings concentration [value between brackets in Equation (46)] should be used to calculate the change in hydrostatic pressure of each cell, $\Delta P_{\text{hac,i}}$, expressed in lbf/in.², shall be calculated using Equation (46). To determine the cuttings concentration, c_{a}, see 9.4.1.7.

$$\Delta P_{\text{hac},i} = 0.052 \times \left[\left(1 - c_{\text{a}}\right) \rho_{(P\text{-}T),i} + 8.345 \times \left(c_{\text{a}}\, \rho_{\text{c}}\right) \right] \times \Delta D_{\text{tvd},i} \tag{46}$$

where

c_{a} is the cuttings volume concentration (decimal fraction);

$\rho_{(P\text{-}T),i}$ is the local drilling fluid density for each i cell, expressed in lbm/gal;

ρ_{c} is the relative density of the cuttings in grams per milliliter

$\Delta D_{\text{tvd},i}$ is the change in total vertical depth for each i cell, expressed in feet

NOTE For complex wells, it may be necessary to calculate the cuttings concentration for each significantly different annular dimension.

The hydrostatic pressure at any depth should be then determined by summing the hydrostatic pressure contribution of each cell from the surface to that depth. This can be done without considering cuttings using Equation (47) to determine P_{ha}, or using Equation (48) to determine P_{hac}, for including the effect of cuttings.

$$P_{\text{ha}} = \sum_{i=1}^{n} \Delta P_{\text{ha},i} = \Delta P_{\text{ha},1} + \Delta P_{\text{ha},2} + \Delta P_{\text{ha},3} + \cdots + \Delta P_{\text{ha,n}} \tag{47}$$

where

$\Delta P_{\text{ha,i}}$ is the annular hydrostatic pressure change without cuttings for each successive i cell, expressed in lbf/in.²

and,

$$P_{\text{hac}} = \sum_{i=1}^{n} \Delta P_{\text{hac},i} = \Delta P_{\text{hac},1} + \Delta P_{\text{hac},2} + \Delta P_{\text{hac},3} + \cdots + \Delta P_{\text{hac,n}} \tag{48}$$

where

$\Delta P_{hac,i}$ is the annular hydrostatic pressure change with cuttings for each successive i cell, expressed in lbf/in.².

NOTE For managed pressure drilling (MPD) and well control operations the imposed annular surface pressure should be included.

6.4.4.3 Equivalent static densities

The equivalent static density in annulus without considering cuttings, ESD_{a}, expressed in pounds per gallon shall be calculated from the static hydrostatic annular pressure at any depth and at the TVD using Equation (49).

$$ESD_{\mathrm{a}} = \frac{P_{\mathrm{ha}}}{0.052 \times D_{\mathrm{tvd}}} \tag{49}$$

where

P_{ha} is the annular hydrostatic pressure, expressed in lbf/in.².

D_{tvd} is the total vertical depth, expressed in feet

NOTE For MPD and well control operations the imposed annular surface pressure should be included.

The equivalent static density in annulus with cuttings, ESD_{ac}, expressed in pounds per gallon shall be calculated from the static hydrostatic annular pressure with cuttings at any depth and the TVD using Equation (50).

$$ESD_{\mathrm{ac}} = \frac{P_{\mathrm{hac}}}{0.052 \times D_{\mathrm{tvd}}} \tag{50}$$

where

P_{hac} is the annular hydrostatic pressure with cuttings, expressed in lbf/in.².

D_{tvd} is the total vertical depth, expressed in feet

6.4.4.4 Dynamic downhole pressures

Under circulating dynamic conditions, the downhole pressure at any depth is calculated in a similar manner to static conditions where the pressure change for each cell is summed from surface to the depth of interest. Under dynamic conditions the pressure increase for each cell is determined by adding the hydrostatic pressure change to the annular frictional pressure loss using local values for temperature, pressure, and rheology. The circulating temperature at each cell can be determined using the method described in 6.2. For each cell, the local density is calculated from Equation (38) using the local temperature and pressure. The rheology for each cell can be determined using the methods described in 6.3. The annular friction pressure loss for each cell, $P_{a,i}$, can then be calculated using the procedures in 7.4.12.

The downhole circulating annular pressure at any depth, P_{dca}, expressed in lbf/in.² should be then determined by summing the hydrostatic pressure contribution of each cell including cuttings, $\Delta P_{\mathrm{ha,i}}$, with the annular friction pressure loss for each cell, $P_{\mathrm{a,i}}$ from surface to that depth using Equation (51).

$$P_{\mathrm{dac}} = \sum_{i=1}^{n} \left(\Delta P_{\mathrm{hac},i} + P_{\mathrm{a},i} \right)$$

$$P_{\mathrm{dac}} = \left(\Delta P_{\mathrm{hac},1} + P_{\mathrm{a},1} \right) + \left(\Delta P_{\mathrm{hac},2} + P_{\mathrm{a},2} \right) + \left(\Delta P_{\mathrm{hac},3} + P_{\mathrm{a},3} \right) + \cdots + \left(\Delta P_{\mathrm{hac,n}} + P_{\mathrm{a,n}} \right) \quad (51)$$

NOTE For MPD and well control operations the imposed annular surface pressure should be included.

where

$\Delta P_{\mathrm{hac,i}}$ is the annular hydrostatic pressure change including cuttings for each successive i cell, expressed in lbf/in.².

$P_{\mathrm{a},i}$ is the annular friction pressure loss for each successive i cell, expressed in lbf/in.².

NOTE Effect of cuttings to the downhole circulating pressure can be neglected substituting $\Delta P_{\mathrm{hac,i}}$ by $\Delta P_{\mathrm{ha,i}}$, annular pressure changes for each successive i cell.

As described in 6.4.4, for fast drilling situations or for where the effect of suspended cuttings in annulus is important, such as for poor hole cleaning in a vertical section, the increased hydrostatic pressure due to the cuttings concentration shall be included in the calculation of $\Delta P_{\mathrm{hac,i}}$ for each cell.

6.4.5 Modelling volume changes between static and dynamic conditions

The change in volume between dynamic and static conditions due to changes in temperature and pressure is often of value. For example, when circulation is stopped and the wellbore reverts to static temperature and pressure conditions, it is important to know the volume of fluid needed to fill the well due to thermal contraction or the volume of flowback to expect due to thermal expansion. A similar change in volume will happen when going from static to dynamic conditions but is normally not of interest. The dynamic to static change in volume for each cell due to temperature and pressure is $(Vol_2 - Vol_1)_i$ or ΔVol_i. Since the reciprocal of density is specific volume (volume per unit mass), this volume change can be calculated from the change in density and starting volume for each cell. From conservation of mass for each cell, the starting volume times the starting density ($Vol_1 \times \rho_{(\mathrm{P1\text{-}T1})}$) shall equal the ending volume times the ending density ($Vol_2 \times \rho_{(\mathrm{P2\text{-}T2})}$). Equation (52) should be derived from this conservation of mass relationship. And the total wellbore volume change can then be determined from the summation of the changes for each cell over the entire wellbore using Equation (53).

The change in volume for each cell, ΔVol_{i}, expressed in barrels shall be calculated using Equation (52).

$$\Delta Vol_{\mathrm{i}} = Vol_{i+1} - Vol_{\mathrm{i}} = Vol_{\mathrm{i}} \left(\frac{\rho_{\mathrm{i}} - \rho_{\mathrm{i+1}}}{\rho_{\mathrm{i+1}}} \right) \quad (52)$$

where

ΔVol_{i} is the change in volume for each successive i cell, expressed in barrels.

Vol_{i} is the volume of the cell i, expressed in barrels.

$Vol_{\mathrm{i+1}}$ is the volume of the successive cell i+1 ,expressed in barrels.

ρ_{i} is the local drilling fluid density in the cell i, expressed in lbm/gal

$\rho_{\mathrm{i+1}}$ is the local drilling fluid density in the successive cell i+1, expressed in lbm/gal

The total volume change in the wellbore (ΔVol_{wb}) , expressed in barrels, shall be calculated using Equation (53).

$$\Delta Vol_{\mathrm{wb}} = \sum_{i=1}^{n} \Delta Vol_i = \Delta Vol_1 + \Delta Vol_2 + \Delta Vol_3 + \cdots + \Delta Vol_{\mathrm{n}} \quad (53)$$

where

ΔVol_i, is the change in volume for each successive i cell, expressed in barrels.

7 Pressure-loss Modeling

7.1 Principle

The purpose of Section 7 is to provide methods and Equations to calculate frictional pressure losses and hydrostatic pressures through the different elements of the circulating system of a drilling well. The information is suitable for hydraulics analyses, planning, and optimization.

It is also useful for modeling special well-construction operations such as well control, cementing, tripping, and casing runs. Equations in this Section 7 are applicable to water-, oil-, and synthetic-based fluids; they do not address air/gas, foam, and other aerated, multi-phase or highly compressible fluids. All drilling fluid properties used in methods and Equations in this section assume that downhole temperature and pressure effects are already accounted for and using Equations and models presented in Section 6. Where appropriate, downhole density and rheology values should be used in Equations in this Section 7.

7.2 Basic Relationships

7.2.1 Circulating Pressures

Pressures in the circulating system can be defined by fundamental relationships for standpipe (pump) pressure and bottomhole pressure that are valid under static and dynamic conditions.

Pump pressure ($P_{\mathrm{p,}}$) should be equal to the sum of frictional pressure losses [surface connections (P_{sc}), drill string (P_{ds}), downhole tools and motors (P_{dt}), bit (P_{b}), annular (P_{a}), surface back pressure (P_{cl}, chock line)] , and hydrostatic-pressure differential between the annulus (P_{ha}), and drill string (P_{hd}), and calculated using Equation (54), all pressures are expressed in lbf/in.².

$$P_{\mathrm{p}} = P_{\mathrm{sc}} + P_{\mathrm{ds}} + P_{\mathrm{dt}} + P_{\mathrm{b}} + P_{\mathrm{a}} + P_{\mathrm{cl}} + P_{\mathrm{c}} + P_{\mathrm{ha}} - P_{\mathrm{hd}} \quad (54)$$

Pressure at the bottom of the well (P_{bh}) should be the sum of the annular frictional pressure losses (P_a), surface back pressure (P_{cl}), and annular hydrostatic pressure (P_{ha}), calculated using Equation (55), all pressures are expressed in lbf/in.².

$$P_{bh} = P_a + P_{cl} + P_c + P_{ha} \quad (55)$$

7.2.2 Hydrostatic pressure—Conventional well

Hydrostatic pressure depends on true vertical depth (D_{tvd}) and the density profile of the drilling fluid column in the well. An effective annular hydrostatic pressure can be determined by including the volume percent of drilled cuttings. The process to estimate average cuttings concentration (c_a in decimal fraction) is presented in 9.4.1.3.

For conventional wells, the hydrostatic pressure can be approximated by using the drilling fluid density measured at the surface (ρ_s). Note that temperature and pressure effects on downhole density of drilling fluids should be ignored if the surface density is used to calculate hydrostatic pressure.

Hydrostatic pressures for conventional wells, expressed in lbf/in.², shall be calculated using following Equations (56) to (58).

a) Drill string (pipe) hydrostatic pressure (P_{hd}) using Equation (56).

$$P_{hd} = 0.052 \times \rho_s D_{tvd} \quad (56)$$

b) Annular hydrostatic pressure without cuttings (P_{ha}) using Equation (57).

$$P_{ha} = 0.052 \times \rho_s D_{tvd} \quad (57)$$

c) Annular hydrostatic pressure with cuttings (P_{hac}) using Equation (58).

$$P_{hac} = 0.052 \times \left[\left(1 - c_a\right) \rho_s + 8.345 \times \left(c_a \rho_c\right) \right] \times D_{tvd} \quad (58)$$

Where

ρ_s is the drilling fluid density at surface, expressed in lbm/ft;

D_{tvd} is the total vertical depth, expressed in ft;

c_a is the cuttings volume concentration (decimal fraction);

ρ_c is the relative density of the cuttings, dimensionless .

NOTE Coefficient 0.052 is for unit conversion, rounded for ease of use. A more exact value is 12/231 or 0.051948052.

7.2.3 Hydrostatic pressure—High pressure, extreme Temperature well

In high-pressure and extreme-temperature (hot and cold) wells, the density profile is significantly affected by temperature and pressure. Accurate hydrostatic pressures in the drill string and annulus ($P_{hd}$and P_{ha},

respectively) in these types of wells shall be calculated using equivalent static densities (ESD_{p} and ESD_{ac}) defined at the true vertical depth of interest (D_{tvd}). and using the following Equations (59) to (62).

a) Drill string (pipe) hydrostatic pressure (P_{hd}) using Equation (59).

$$P_{\mathrm{hd}} = 0.052 \times ESD_{\mathrm{p}}\, D_{\mathrm{tvd}} \tag{59}$$

b) Annular hydrostatic pressure without cuttings (P_{ha}) using Equation (60).

$$P_{\mathrm{ha}} = 0.052 \times ESD_{\mathrm{a}}\, D_{\mathrm{tvd}} \tag{60}$$

c) Annular hydrostatic pressure with cuttings (P_{hac}) using Equation (61) or Equation (62).

$$P_{\mathrm{hac}} = 0.052 \times ESD_{\mathrm{ac}}\, D_{\mathrm{tvd}} \tag{61}$$

or

$$P_{\mathrm{hac}} = 0.052 \times \left[\left(1 - c_{\mathrm{a}}\right) ESD_{\mathrm{a}} + 8.345 \times c_{\mathrm{a}}\, \rho_{\mathrm{c}} \right] D_{\mathrm{tvd}} \tag{62}$$

Where

ESD_{p} is the equivalent static density in drill string (pipe), expressed in lbm/gal;

ESD_{a} is the equivalent static density in annulus (without cuttings), expressed in lbm/gal;

ESD_{ac} is the equivalent static density in annulus including cuttings, expressed in lbm/gal;

D_{tvd} is the total vertical depth, expressed in ft;

c_{a} is the cuttings volume concentration (decimal fraction);

ρ_{c} is the relative density of the cuttings (dimensionless)

NOTE Coefficient 0.052 is for unit conversion, rounded for ease of use. A more exact value is 12/231 or 0.051948052.

Since cuttings usually have a higher density than the drilling fluid, cuttings suspended by the drilling fluid in the annulus add to the effective drilling fluid density and hence increase ECD. Cuttings held in suspension contribute to an increase in effective drilling fluid density in the same manner as for a vertical well. In directional or extended-reach wells, cuttings that settle on the low side of the hole in inclined sections are supported by the wellbore and do not add to the effective hydrostatic pressure.

7.3 Surface-connection Pressure Loss

Pressure loss through surface connections (P_{sc}) depends on pipe geometry, surface drilling fluid density (ρ_{s}) and flow rate (Q). Common practice is to categorize surface-connection piping into five general cases and to use the appropriate proportionality constant (C_{sc}) from Table 5 to estimate the pressure loss which shall be calculated, expressed in lbf/in.² using Equation (63) [7.9].

$$P_{sc} = C_{sc}\,\rho_s \left(\frac{Q}{100}\right)^{1.86} \tag{63}$$

where

C_{sc} is the sum of coefficients from Table 5 and related to surface-connections elements;

ρ_s is the drilling fluid density at surface, expressed in lbm/gal;

Q is the flow rate, expressed in gal/min.

Table 5—C_{sc} Values for Surface-connection Elements per Case

Case	Case Elements				C_{sc}
	Standpipe	Hose	Swivel	Kelly	
1	40 ft × 3.0 in. ID	45 ft × 2.0 in. ID	4 ft × 2.0 in. ID	40 ft × 2.25 in. ID	1.00
2	40 ft × 3.5 in. ID	55 ft × 2.5 in. ID	5 ft × 2.5 in. ID	40 ft × 3.25 in. ID	0.36
3	45 ft × 4.0 in. ID	55 ft × 3.0 in. ID	5 ft × 2.5 in. ID	40 ft × 3.25 in. ID	0.22
4	45 ft × 4.0 in. ID	55 ft × 3.0 in. ID	6 ft × 3.0 in. ID	40 ft × 4.00 in. ID	0.15
5	100 ft × 5.0 in. ID	85 ft × 3.5 in. ID	22 ft × 3.5 in. ID		0.15

NOTE The proportionality constant, C_{sc}, may also be determined by directly measuring the pressure loss through surface-connection piping at a known flow rate with a known density drilling fluid and then re-arranging the terms in Equation (63).

7.4 Drill-string and Annular Frictional Pressure Loss

7.4.1 Principle

Flow rate, flow regime, rheological properties, and channel geometry are among the key parameters that impact frictional pressure losses in the drill string and annulus. The process to model these pressures, complex in its own right for H-B fluids, is further complicated in HTHP and deepwater wells by the sensitivity of drilling fluid density and rheological properties to downhole temperatures and pressures.

7.4.2 Section Lengths for Pressure-loss Calculations

An efficient method [7.2, 7.15, 8.1] to incorporate downhole conditions is to subdivide the drill string and annulus into the short segments (or "cells") of length L like those used to numerically integrate the density profile (see Section 6). For the most part, equations and parameter values presented in 7.4 apply to these individual cells. Geometric sections or casing intervals commonly used for conventional wells also can be used for critical wells; however, relevant parameters such a downhole density and rheology should be properly averaged over each segment length.

7.4.3 Fluid Velocity

Average (or bulk) velocities in drill string (V_p) and in annulus (V_a) are inversely proportional to the cross-sectional area of the respective fluid conduit. Average bulk velocities expressed in feet per minute should be calculated using the following Equations (64) and (65).

a) Average fluid velocity in pipe (V_{p}) given by Equation (64).

$$V_{\mathrm{p}} = 24.51 \times \frac{Q}{d_{\mathrm{i}}^{2}} \tag{64}$$

b) Average fluid velocity in annulus (V_{a}) given by Equation (65).

$$V_{\mathrm{a}} = 24.51 \times \frac{Q}{\left(d_{\mathrm{h}}^{2} - d_{\mathrm{p}}^{2}\right)} \tag{65}$$

Where

Q is the flow rate, expressed in gallons per minute;

d_{i} is the pipe internal diameter , expressed in inches;

d_{p} is the pipe outside diameter , expressed in inches;

d_{h} is the hole or casing internal diameter, expressed in inches.

In deepwater drilling, booster pumps often are used to supplement flow in the riser to assist with hole cleaning. For these cases, flow rate in the riser/drill-string annulus should be the sum of the conventional and the booster flow rates.

7.4.4 Hydraulic Diameter

The hydraulic-diameter concept is used to relate fluid behavior in an annulus to that in a circular pipe. There are several different expressions [1] used for the annular hydraulic diameter (d_{hyd}), but the most widely used is derived from the hydraulic radius, the ratio of the cross-sectional area to the wetted perimeter of the annular section (see 3.1.1). Hydraulic diameters, d_{hyd}, expressed in inches, shall be given by following Equations (66) and (67).

a) Pipe hydraulic diameter by Equation (66).

$$d_{\mathrm{hyd}} = 4 \times \frac{\left(\pi d_{\mathrm{i}}^{2} \diagup 4\right)}{\pi d_{\mathrm{i}}} = d_{\mathrm{i}} \tag{66}$$

b) Annular hydraulic diameter, by Equation (67).

$$d_{\mathrm{hyd}} = 4 \times \frac{\frac{\pi}{4}\left(d_{\mathrm{h}}^2 - d_{\mathrm{p}}^2\right)}{\pi\left(d_h + d_p\right)} = d_h - d_p \tag{67}$$

Where

d_{i} is the pipe internal diameter, expressed in inches;

d_{p} is the pipe outside diameter, expressed in inches;

d_{h} is the hole or casing internal diameter, expressed in inches.

7.4.5 Rheological Parameters

Rheological parameters used for pressure-loss modeling are measured on field and HTHP laboratory viscometers (see Section 5). These values should be adjusted for the expected downhole temperatures and pressures in each well segment (see Section 6) in order to yield quality results.

H-B parameters n (flow behavior index) and k (consistency factor) in each downhole segment can be calculated using viscometer readings R_{600}, R_{300} and τ_{y} as shown previously in Equations (26), (27), and (28) or using a numerical regression calculation (see 5.2.5.3).

The ratio (R) , decimal fraction H-B yield stress/Bingham yield point ($\tau_{\mathrm{y}}/Y_{\mathrm{P}}$) should be given by Equation (68) is an additional parameter useful for characterizing rheological behavior.

$$R = \frac{\tau_{\mathrm{y}}}{Y_{\mathrm{P}}} = \frac{\tau_{\mathrm{y}}}{\left(2\,R_{300} - R_{600}\right)} \quad \text{(for} \quad Y_{\mathrm{P}} > 0\text{)} \tag{68}$$

where

τ_{y} is the H-B yield stress, expressed in degrees [see 5.2.3, Equation (28)];

Y_{P} is the Bingham yield point, expressed in degrees [see 5.2.2, Equation (21)];

R_{600} is the dial reading at 600 r/min in degrees;

R_{300} is the dial reading at 300 r/min in degrees.

NOTE R = 0 for power law fluids, R = 1 for Bingham plastic fluids, and 0 < R < 1 for H-B fluids.

7.4.6 Shear Rate Geometry Correction Factors

The Newtonian (or “nominal”) shear rate (γ) first shall be converted to shear rate at the wall (γ_{w}) in order to calculate pressure loss. This is accomplished using correction factors that adjust for the geometry difference

between the flow conduit (pipe or annulus) and Couette-type direct indicating viscometers used to measure rheological properties. [7.3]

The shear rate correction factor for well geometry (B_a) is dependent on the fluid flow behavior index (n). It is convenient to use a geometry index (α) so that flow in pipes and annuli can be considered in a single expression. For simplicity and without significant loss of accuracy, the annulus can be treated as an equivalent slot (α = 1). Equation (69) should be used to calculate B_a (dimensionless).

$$B_a = \left[\frac{(3-\alpha)n+1}{(4-\alpha)n}\right]\left[1+\frac{\alpha}{2}\right] \tag{69}$$

where

α = 0 for the geometry index for a pipe;

α = 1 for the geometry index for an annulus,

n is the flow behavior index (H-B) (dimensionless) [see 5.2.5.1 Equation (26)].

Shear rate correction also applies to field viscometers using a viscometer correction factor B_x. Unfortunately, closed analytical solutions do not exist for H-B fluids, and complex numerical methods are inaccurate at very low shear rates. Practically speaking, it can be assumed that the viscometer correction factor $B_x \approx 1$. Alternatively, B_x for power law fluids [7.4] can be used if it is important to preserve exact solutions for these fluids. For the standard rotor/bob combination R1B1, B_x for power law fluids varies from 1.0 (for n_P = 1.0) to 1.1569 (for n_P = 0.3). Equation (70) should be used to calculate B_x (dimensionless).

$$B_x = \left[\frac{x^{2/n_P}}{n_P x^2}\right]\left[\frac{x^2-1}{x^{2/n_P}-1}\right] \approx 1 \tag{70}$$

where

x = 1.0678 for the viscometer standard R1B1 combination;

n_P is the power law flow behavior index, dimensionless [see 5.2.4.2 Equation (22)].

The well geometry and viscometer shear rate correction factors can be combined into a single geometry factor (G_f) that can be used to convert nominal shear rate to wall shear rate. Dimensionless geometry factor, G_f, shall be given by Equation (71); for many cases, it is acceptable to assume $B_x \approx 1$.

$$G_f = \frac{B_a}{B_x} \approx 1 \tag{71}$$

where

B_a is the well geometry correction factor [see Equation (69)];

B_x is the viscometer geometry correction factor [see Equation (70)]

7.4.7 Shear Rate at the Wall

Shear rate at the wall (γ_w) expressed in reciprocal seconds, shall be as given by Equation (72), calculated by multiplying nominal shear rate by the geometry factor (G_f). This equation is applicable for pipes and annuli for appropriate values of fluid velocity (V) and hydraulic diameter (d_{hyd}).

$$\gamma_w = \frac{1.6 \times G_f \, V}{B_x} \tag{72}$$

where

V is the average flow velocity expressed in feet per minute [see 7.4.3 Equation (64) or (65)];

G_f is the geometry factor [see 7.4.6, Equation (71)];

B_x is the viscometer correction factor [see 7.4.5 Equation (70)].

7.4.8 Shear Stress at the Wall (Flow Equation)

Frictional pressure loss is directly proportional to the shear stress at the wall, τ_w, defined by the fluid-model-dependent flow equation. Flow equations are developed by applying the Weissenberg–Rabinowitch–Mooney relation [5.1, 5.2] to the constitutive models presented in Section 5. Results for Bingham plastic fluids and H-B fluids are complex and require iterative solutions to determine τ_w; however, they can be approximated by an expression of the same recognizable form as their respective constitutive equations. [7.5] In Equation (73), τ_y is the Couette-type direct indicating viscometer dial reading and τ_w is the wall shear stress; α = 0 for pipes and α = 1 for annuli; and n and k can be calculated using Equation (26) and Equation (27) (see 5.2.5.1). For a Couette-type direct indicating viscometer, flow and shear stress equation at the wall can be written as given by Equation (73), expressed in “direct-indicating viscometer units”.

$$\tau_v = \left(\frac{(4-\alpha)}{(3-\alpha)}\right)^n \tau_y + k\gamma_w^n \tag{73}$$

where

τ_v is the shear stress at the wall expressed in degrees per reciprocal seconds;

α is the viscometer geometry index, dimensionless (see 7.4.6);

n is the H-B flow behavior index , dimensionless;

τ_y is the H-B yield stress in degrees per reciprocal seconds;

γ_w is the shear rate at the wall expressed in reciprocal seconds;

k is the H-B consistency factor expressed in lbf•s^n/100 ft².

For $\tau_y = 0$, the flow equation in Equation (73) reduces to the exact solution for power law fluids.

For $\tau_y = Y_P$, then $n = 1$ and the flow equation reduces to the simplified Bingham plastic expression historically used in drilling.

The shear stress at the wall, τ_w, expressed in lbf/100 ft² shall be given by Equation (74).

$$\tau_w = 1.067\,\tau_v \tag{74}$$

7.4.9 Flow Regime

7.4.9.1 Reynolds Numbers

Flow patterns and friction factors in fluid conduits are characterized by laminar, transitional, and turbulent flow regimes.

Dimensionless generalized Reynolds number (N_{ReG}) applies to both pipes and annuli [7.3]. A convenient form of the equation involves the shear stress at the wall (τ_w), defined in 7.4.8. Dimensionless N_{ReG} shall be given by Equation (75).

$$N_{ReG} = \frac{\rho V^2}{19.36 \times \tau_w} \tag{75}$$

where

ρ is the fluid density expressed in lbm/gal;

V is the average flow velocity, expressed in ft/min;

τ_w is the shear stress at the wall, expressed in lbf/100 ft².

The critical Reynolds number ($N_{Re,crit}$) is the value of N_{ReG} where the regime changes from laminar to transitional flow [7.16] , it shall be given by Equation (76).

$$N_{Re,crit} = 3470 - 1370\,n \tag{76}$$

where

n is the H-B flow behavior index, dimensionless.

7.4.9.2 Critical velocity

While not required to calculate pressure losses, critical velocity is still an important hydraulics parameter. Critical velocity (V_{crit}) is the bulk velocity where the Reynolds number (N_{ReG}) as per 7.4.9.1, equals the critical Reynolds number ($N_{Re,crit}$) as per Equation (76). Unfortunately, iterative methods are required to calculate

V_{crit} for H-B fluids. A close approximation, however, can be achieved by the empirical relationship in Equation (77) based on critical velocity for power law fluids (V_{critP}), critical velocity for Bingham plastic fluids (V_{critB}) and R the ratio H-B yield stress/ Bingham yield point from Equation (68). Critical velocity for a fluid, expressed in feet per minute, shall be calculated using Equation (77).

$$V_{crit} = V_{critP} + (V_{critB} - V_{critP}) R^{\sqrt{V_{critP}/V_{critB}}} \tag{77}$$

With for the critical velocity parameters calculated using for power law fluids Equations (78) and (79), or for Bingham fluids Equations (80) and(81):

a) V_{critP}**,** Critical velocity for power law fluids shall be given by Equation (78).

$$V_{critP} = \left[\frac{28{,}274 \times (2.533 - n_P) k_P}{\rho} \times \left(\frac{1.6\, G_P}{d_{hyd}} \right)^{n_P} \right]^{\frac{1}{2-n_P}} \tag{78}$$

where G_P the geometry shear rate correction factor (power law) should be calculated by Equation (79).

$$G_P = \left[\frac{(3-\alpha) n_P + 1}{(4-\alpha) n_P} \right] \left[1 + \frac{\alpha}{2} \right] \tag{79}$$

and,

ρ is the fluid density, expressed in lbm/gal;

n_P is the power law flow behavior index, dimensionless;

k_P is the power law consistency factor, expressed in lbf•s^{n_P}/100 ft².

d_{hyd} is the hydraulic diameter (see 7.4.4); expressed in inches.

α is the viscometer geometry index, dimensionless (see 7.4.6).

b) V_{critB}, Critical velocity for Bingham plastic fluids shall be given by Equation (80).

$$V_{critB} = \frac{67.86}{\rho} \left[\beta + \sqrt{\left(\beta^2 + 9.42\, \rho Y_P \frac{(4-\alpha)}{(3-\alpha)} \right)} \right] \tag{80}$$

where β the intermediate variable should be defined as per Equation (81).

$$\beta = \frac{\eta_{PV}\left(1+\frac{\alpha}{2}\right)}{d_{hyd}} \tag{81}$$

and,

ρ is the fluid density, expressed in lbm/gal;

d_{hyd} is the hydraulic diameter (see 7.4.4); expressed in inches.

n_P is the power law flow behavior index, dimensionless;

k_P is the power law consistency factor, expressed in lbf•s^{n_P}/100 ft².

Y_P is the yield yield point (Bingham), expressed in lbf/100 ft²;

η_{PV} is the plastic viscosity, expressed in centipoises;

α is the viscometer geometry index, dimensionless (see 7.4.6).

7.4.10 Critical Flow Rate

The critical flow rate (Q_{crit}) expressed in gallons per minute is the flow rate at which the velocity equals the critical velocity (V_{crit}) (expressed in feet per minute).

a) In a pipe, it shall be calculated by Equation (82).

$$Q_{crit} = \frac{V_{crit}\, d_i^2}{24.51} \tag{82}$$

b) In an annulus, it shall be calculated by Equation (83).

$$Q_{crit} = \frac{V_{crit}\left(d_h^2 - d_p^2\right)}{24.51} \tag{83}$$

Where

d_i is the pipe internal diameter , expressed in inches;

d_p is the pipe outside diameter, expressed in inches;

d_h is the hole or casing internal diameter, expressed in inches.

7.4.11 Friction Factor

7.4.11.1 Fanning friction factor

Pressure loss for a fluid in pipes and annuli is proportional to the dimensionless Fanning friction factor (f), which is a function of generalized Reynolds number, flow regime, and fluid rheological properties.

a) Laminar-flow

Laminar-flow friction factors (f_{lam}) for pipes and concentric annuli are combined into a single relationship when using the generalized Reynolds number (N_{ReG}) defined in 7.4.9.1 and can be calculated using Equation (84).

$$f_{\text{lam}} = \frac{16}{N_{\text{ReG}}} \tag{84}$$

b) Transitional-flow

An empirical equation consistent with critical Reynolds number ($N_{\text{Re,cr}}$) defined in 7.4.9.1 can be used to determine transitional-flow friction factor (f_{trans}), it can be calculated using Equation (85).

$$f_{\text{trans}} = \frac{16\, N_{\text{ReG}}}{N_{\text{Re,cr}}^2} \tag{85}$$

c) Turbulent-flow

The Blasius form of the turbulent-flow friction factor (f_{turb}) for non-Newtonian fluids should be a function of generalized Reynolds number (N_{ReG}) and power law flow behavior index (n_{P}), f_{turb} can be calculated using Equation (86) where constants a and b, calculated using Equations (87) and (88), are based on curve fits of data taken on power law fluids [7.16].

$$f_{\text{turb}} = \frac{a}{N_{\text{ReG}}^b} \tag{86}$$

Where a and b shall be calculated using respectively Equations (87) and (88):

$$a = \frac{\log_{10}\left(n_{\text{P}}\right) + 3.93}{50} \tag{87}$$

and

$$b = \frac{1.75 - \log_{10}\left(n_{\text{P}}\right)}{7} \tag{88}$$

where

n_P is the power law flow behavior index , dimensionless (see 5.2.4.2);

7.4.11.2 Friction factor and pipe roughness.

Pipe roughness elevates the friction factor in fully developed turbulent flow; however, relative roughness for most wellbore geometries is low, and Reynolds numbers in pipes and annuli rarely reach the high values where effects of roughness are particularly significant [1].

7.4.11.3 Drag reduction.

Viscoelastic fluids in turbulent flow exhibit lower frictional factors and pressure losses, and delayed onset of turbulence. [7.13] This drag-reduction phenomenon can be observed in the field as a greatly reduced pump pressure when circulating certain clean, polymer fluids. The reductions in pressure loss can be very significant and values of >70 % reduction have been observed for dilute polymer systems. However, pump pressures systematically return to normal as long-chain polymers are mechanically degraded and low-gravity (drilled) solids build up in the drilling fluid. Various analytical and empirical techniques have been proposed to model this behavior, but none have been universally adopted for drilling fluids.

7.4.11.3 Generalized friction factor determination

The following method [7.8] can be used to determine the friction factor (f) for all Reynolds numbers and flow regimes. This technique involves an intermediate term (f_{int}) based on transitional and turbulent-flow friction factors (f_{trans} and f_{turb}) and laminar-flow friction factor (f_{lam}). Friction factor (f) should be calculated using Equation (89) and intermediate Equation (90).

$$f = \left(f_{int}^{12} + f_{lam}^{12} \right)^{\frac{1}{12}} \tag{89}$$

where

$$f_{int} = \left(f_{trans}^{-8} + f_{turb}^{-8} \right)^{\frac{-1}{8}} \tag{90}$$

and,

f_{lam} is the laminar-flow friction factor (see 7.4.11.1 item a), dimensionless;

f_{trans} is the transitional-flow friction factor (see 7.4.11.1 item b), dimensionless;

f_{turb} is the turbulent-flow friction factor (see 7.4.11.1 item c), dimensionless.

7.4.12 Frictional Pressure Loss

7.4.12.1 Principle

Frictional pressure losses in the drill string and annulus are equal to the sum of the losses in the individual segments described in 7.4.1. The Fanning equation is used to calculate incremental pressure losses; however, the various parameters should be defined for each segment (j) in the drill string and annulus.[1]

Frictional pressure losses expressed in lbf/in.² can be calculated with for following case :

a) P_{ds} Drill string (pipe) frictional pressure loss using Equation (91).

$$P_{\mathrm{ds}} = \sum \left(\frac{1.076\, f \rho_{\mathrm{p}} V_{\mathrm{p}}^2 L}{10^5\ d_{\mathrm{i}}} \right)_j \tag{91}$$

b) P_{a} Annular friction pressure loss using Equation (92).

$$P_{\mathrm{a}} = \sum \left(\frac{1.076\, f \rho_{\mathrm{a}} V_{\mathrm{a}}^2 L}{10^5\ d_{\mathrm{hyd}}} \right)_j \tag{92}$$

Where

f is the fanning friction factor, dimensionless, see 7.4.11.2;

ρ_{p} is the fluid density in the drill string expressed in lbm/gal;

ρ_{a} is the fluid density in annulus, expressed in lbm/gal;

V_{a} is the average fluid velocity in drill string , expressed in ft/min;

V_{p} is the average fluid velocity in annulus, expressed in ft/min;

L is the length of the drill string or annular segment , expressed in feet;

d_{i} is the drill string (pipe) internal diameter , expressed in inches;

d_{hyd} is the hydraulic diameter of the annular section pipe, expressed in inches.

Drill-string eccentricity in directional wells reduces annular pressure loss in laminar and turbulent flow. A widely used method [7.6] to estimate this reduction involves multiplication of concentric-annulus pressure loss in each segment by an empirically derived ratio depending on flow regime: eccentric annulus laminar pressure ratio (R_{lam}) or eccentric annulus turbulent pressure ratio (R_{turb}) should be calculated using respectively Equation (93) and Equation (94). Eccentricity (e) is defined as the displacement of the radii divided by the difference in radii. The value of e is 0 for a concentric annulus and 1.0 for a fully eccentric annulus when the pipe (or tool-joint) touches the low side of the hole.

$$R_{\mathrm{lam}} = 1.0 - 0.072 \times \left(\frac{e}{n}\right)\left(\frac{d_{\mathrm{p}}}{d_{\mathrm{h}}}\right)^{0.8454} - 1.5 \times e^2 \sqrt{n}\left(\frac{d_{\mathrm{p}}}{d_{\mathrm{h}}}\right)^{0.1852} + 0.96 \times e^3 \sqrt{n}\left(\frac{d_{\mathrm{p}}}{d_{\mathrm{h}}}\right)^{0.2527} \tag{93}$$

$$R_{\text{turb}} = 1.0 - 0.048 \times \left(\frac{e}{n}\right)\left(\frac{d_{\text{p}}}{d_{\text{h}}}\right)^{0.8454} - \frac{2}{3} \times e^2 \sqrt{n}\left(\frac{d_{\text{p}}}{d_{\text{h}}}\right)^{0.1852} + 0.285 \times e^3 \sqrt{n}\left(\frac{d_{\text{p}}}{d_{\text{h}}}\right)^{0.2527} \quad (94)$$

where

e is the annular eccentricity, expressed as a decimal fraction;

n is H-B flow behavior index, dimensionless;

d_{p} is the drill string outside diameter, expressed in inches;

d_{h} is the hole or casing internal diameter, expressed in inches.

Eccentric annular friction pressure loss, $P_{\text{a,ecc}}$, for a laminar or a turbulent flow, expressed in lbf/in.², can be calculated using Equation (95)

$$P_{\text{a,ecc}} = \left(R_{\text{lam}} \; or \; R_{\text{turb}}\right) \times P_{\text{a}} \quad (95)$$

where

P_{a} is the annular pressure loss expressed in lbf/in.².

7.4.12.2 Laminar frictional pressure loss case

Substitution of the laminar-flow friction factor (f_{lam}) defined in 7.4.11.1 item a) into the general equations defined in 7.4.12 yields simplified relationships for laminar-flow pressure loss that also can be derived by force-balance analysis [1]. Equations (96) and (97) are equivalent to the derived Equation (10) in 4.3.7. The individual parameters should be defined for each well segment (*j*).

a) P_{ds} Drill string (pipe) frictional pressure loss in laminar flow, expressed in lbf/in.² should be given by Equation (96):

$$P_{\text{ds}} = \sum\left(\frac{\tau_{\text{w}} L}{300\, d_{\text{i}}}\right)_j \quad (96)$$

b) P_{a} Annular friction pressure loss in laminar flow, expressed in lbf/in.² should be given by Equation (97):

$$P_{\text{a}} = \sum\left(\frac{\tau_{\text{w}} L}{300\, d_{\text{hyd}}}\right)_j \quad (97)$$

Where

τ_w is the shear stress at the wall, expressed in lbf/100 ft²;

L is the length of the drill string or annular segment , expressed in feet;

d_i is the drill string (pipe) internal diameter, expressed in inches;

d_{hyd} is the hydraulic diameter of the annular section (see 7.4.4), expressed in inches.

7.4.12.3 Minimum pressure to break circulation

Laminar-flow pressure-loss Equations (96) and (97) in 7.4.12.2 can be used to estimate the minimum pressure required to break circulation after a long static period. The pressure to break drilling fluid gel and circulation can be calculated by substituting the fluid's 10-min gel strength (β_{10m}) for the wall shear stress (τ_w) under no-flow conditions. The β_{10m} value could represent an average for the entire well or preferably should be adjusted for temperature and pressure if temperature and pressure dependent rheology data are available. The calculation for the annulus is more important as excessive pressure could lead to lost circulation after long static periods with high-gel strength fluids. Equations (98) and (99) assume the flow rate is very low and do not consider frictional pressure losses.

a) $P_{ds\text{-}min}$ Minimum drill string (pipe) pressure loss to break drilling fluid gel and circulation in drill string (pipe), expressed in lbf/in.² should be given by Equation (98).

$$P_{ds\text{-}min} = \sum\left(\frac{\beta_{10m} L}{300\, d_i}\right)_j \tag{98}$$

b) $P_{a\text{-}min}$ Minimum annular pressure loss to break drilling fluid gel and circulation in annulus, expressed in lbf/in.² should be given by Equation (99).

$$P_{a\text{-}min} = \sum\left(\frac{\beta_{10m} L}{300\, d_{hyd}}\right)_j \tag{99}$$

Where

β_{10m} is the drilling fluid gel strength expressed in lbf/100 ft²;

L is the length of the drill string or annular segment , expressed in feet;

d_i is the drill string (pipe) internal diameter, expressed in inches;

d_{hyd} is the hydraulic diameter of the annular section (see 7.4.4), expressed in inches.

7.4.13 Special Considerations

Tool joints can affect frictional pressure losses in the drill string and annulus for several reasons, the most obvious of which is the diameter difference between tool joints (both OD and ID) and the pipe. For internally

constricted tool joints, drill string pressure loss can increase due to contraction and expansion effects as fluid enters and exits the tool joints [7.10]. Also, if full turbulence is achieved in the tool joint, the drill pipe joint may be too short to allow complete fluid recovery to nominal flow regime in the pipe. Field data support that this can result in the elevation in the turbulent flow friction factor [7.1].

Drill string rotation invariably increases annular pressure loss in the field. Unfortunately, relationships are not readily available that consider combined effects of rotation, non-Newtonian fluid behavior, eccentricity, and hydrodynamic/drill string instabilities. Centrifugal flows between the rotating drill string and the wellbore or casing may form translating or propagating spiral vortices called Taylor vortices. The formation of Taylor vortices increases viscous dissipation and the annular frictional pressure loss. Part of the pressure increase in directional wells may be attributed to cuttings or sagged density material incorporated into the main flow stream. Most hydraulics studies on the subject have focused on slim-hole geometry where narrow annular clearances can magnify the effects of rotation [7.7].

Frictional pressure losses for coiled tubing on the reel are higher than for straight tubing due to imposed secondary flows [7.11]. A number of correlations have been published to compensate for this effect by adjusting friction factors in laminar and turbulent flow [7.12]. However, most of these modifications are empirically derived and are difficult to generalize due to their high sensitivity to drilling fluid characteristics.

7.5 Bit Pressure Loss

7.5.1 General

Pressure loss through bit nozzles (P_b) is based on a kinetic energy change. Drilling fluid density through the bit nozzles (ρ_b) can be replaced by surface drilling fluid density (ρ_s) for conventional wells. If downhole tools include provisions for fluid bypass, actual flow rate through the nozzles (Q) should be adjusted accordingly. P_b expressed in lbf/in.², should be calculated by Equation (100).

$$P_b = \frac{\rho_b Q^2}{12{,}042\, C_d^2\, TFA^2} = 8.3 \times 10^{-5} \left[\frac{\rho_b Q^2}{C_d^2\, TFA^2} \right] \tag{100}$$

where

TFA is the total flow area (see 7.5.2), expressed in square inches;

C_d is the jet-nozzle discharge coefficient (see 7.5.3), dimensionless;

ρ_b is the fluid density through bit nozzles, expressed in lbm/gal;

Q is the flow rate through the bit nozzles, expressed in gal/min.

7.5.2 Total Flow (Nozzle) Area

Total flow area (TFA) is proportional to the sum of the squares of the various nozzle diameters. By convention, nozzle diameters (d_n) are defined in 1/32 in. TFA (with i nozzles) expressed in square inches, shall be calculated using Equation (101).

$$TFA = 0.76699 \times 10^{-3} \left(d_{n1}^2 + d_{n2}^2 + d_{n3}^2 + \cdots + d_{ni}^2 \right) \tag{101}$$

7.5.3 Jet-nozzle Discharge Coefficient

The jet-nozzle discharge coefficient (C_d) varies with the diametric ratio (output diameter/input diameter) and the fluid Reynolds numbers passing through the nozzles [7.14]. There is significant evidence to update the long-standing C_d value of 0.95 to 0.98, given the flow rates, drilling fluid densities, and nozzle ratios typical to oilfield operating conditions. Dimensionless C_d to take in account should be provided by Equation (102).

$$C_d = 0.98 \tag{102}$$

7.6 Downhole-tools Pressure Loss

7.6.1 General

Bottomhole assemblies, logging-while-drilling tools, and other downhole tools invariably increase pressure losses inside the drill string and annulus.

7.6.2 Miscellaneous Downhole Equipment

Pressure losses through turbines, thrusters, jars, rotary steerable systems (RSSs), and measurement while drilling (MWD) tools (P_{dt}) depend strongly on the internal design of the individual tools, as well as the fluid density and viscosity. Vendor-published pressure losses are usually based on flow loop or rigsite tests run over a limited range of conditions. Pressure losses inside these tools generally are in turbulent flow, so that data from suppliers can be adjusted to provide a closer fit to well conditions. These adjustments should include a drilling fluid density correction determined by dividing the drilling fluid density at the bit (ρ_b) by the reference drilling fluid density ($\rho_{Ref\text{-}dt}$) provided by the tool manufacturer and a proportionality constant referring to manufacturer data. P_{dt} expressed in lbf/in.², shall be calculated using Equation (103).

$$P_{dt} = \frac{\rho_b}{\rho_{Ref\text{-}dt}} C_{dt} Q^{1.86} \tag{103}$$

where

P_b is the drilling fluid density at the bit , expressed in lbm/gal

$\rho_{Ref\text{-}dt}$ is the reference drilling fluid density (tool manufacturer) expressed in lbm/gal

Q is the flow rate through the bit nozzles, expressed in gal/min.

C_{dt} is the proportionality constant which can be is determined from Equation (104).

$$C_{dt} = \frac{P_{Ref\text{-}dt}}{(Q_{Ref})^{1.86}} \tag{104}$$

And with, provided by the tool manufacturer:

$P_{Ref\text{-}dt}$ is the reference pressure loss through the tool, expressed in lbf/in.²;

Q_{Ref} is the reference flow rate through the tool, expressed in gal/min.

7.6.3 Positive-displacement Motors

Pressure drop of positive-displacement motors (PDMs) consists of the no-load pressure drop (bit off-bottom) and the operating pressure drop (added to the no-load pressure drop when the bit is on bottom and cutting rock). No-load pressure drop is a function of flow rate, drilling fluid density, and PDM characteristics. Operating pressure drop of a PDM is not strongly dependent on flow rate. It is determined by bit torque that is the product of weight-on-bit and bit aggressiveness. Operating pressure drop is best obtained from the PDM manufacturer's data handbook.

7.7 Choke-line Pressure Loss

7.7.1 Single Line

Circulating through the choke-line on wells with subsea blowout preventer (BOP) stacks imposes additional pressure on the annulus. Pressure-loss calculations for pipe in 7.5 can be used to model choke-line losses.

7.7.2 Multiple Lines

Choke and kill lines sometimes are used simultaneously to reduce back pressure on the annulus during well-control operations. For two lines with identical diameters, return flow would be split equally, and the resulting net pressure loss would be roughly one-fourth of that through a single line.

7.8 Casing Pressure

7.8.1 General

Casing pressure is the surface back pressure applied on the annular side under both static and dynamic conditions.

7.8.2 Casing Pressure While Shut In

In a well-control situation, casing pressure (P_{cs}) is the shut-in casing pressure and bottomhole pressure (P_{f}) is the formation pressure. P_{cs} expressed in lbf/in.², shall be calculated using Equation (105).

$$P_{\text{cs}} = P_{\text{f}} - P_{\text{ha}} \tag{105}$$

where

P_{ha} is annular hydrostatic pressure, expressed in lbf/in.².

P_{f} is formation pressure, expressed in lbf/in.².

7.8.3 Casing Pressure While Circulating

Annular back pressure can be applied during circulation to manage the pressure barrier in a well. In many wells, this drilling method can be used to control the bottomhole pressure, improve wellbore integrity, and permit drilling more efficiently with reduced risk, less non-productive time, and enhanced wellbore stability. Low and high-pressure rotating control devices (RCDs) are incorporated to seal the annulus above the choke line.

7.9 Equivalent Circulating Density

The ECD at total depth (TD) is equivalent to the bottomhole pressure equation (see 7.2.2 and 7.2.3) expressed as a drilling fluid density gradient. Equations presented here can be used to calculate ECD at any depth if annular ESD_{a} is defined at the depth of interest (D_{tvd}) and the annular pressure loss (P_{a}) is calculated from surface to D_{tvd}. For conventional wells, ρ_{s} can substitute for ESD_{a}. Cuttings concentration (c_{a}) and cuttings relative density (specific gravity) (ρ_{c}) can be determined from equations presented in Section 9 to allow to calculate annular ECD with cuttings (ECD_{ac}.) .

NOTE Annular ECD with cuttings, ECD_{ac}, can be called equivalent dynamic density (EDD).

Equations (106) and (107) shall be used respectively to calculate ECDs, without cuttings (ECD_{a}) and with cuttings (ECD_{ac}), expressed in lbm/gal.

a) Annular ECD_{a} without cuttings:

$$ECD_{\mathrm{a}} = ESD_{\mathrm{a}} + \frac{\left(P_{\mathrm{a}} + P_{\mathrm{cl}} + P_{\mathrm{c}}\right)}{0.052\, D_{\mathrm{tvd}}} \tag{106}$$

b) Annular ECD_{ac} with cuttings:

$$ECD_{\mathrm{ac}} = ESD_{\mathrm{ac}} + \frac{\left(P_{\mathrm{a}} + P_{\mathrm{cl}} + P_{\mathrm{c}}\right)}{0.052\, D_{\mathrm{tvd}}} \tag{107}$$

Where

ESD_{a} is the equivalent static density in annulus (without cuttings); expressed in lbm/gal;

ESD_{ac} is the equivalent static density in annulus with cuttings; expressed in lbm/gal;

P_{a} is the annular pressure loss, expressed in lbf/in.²;

P_{cl} is the chock line pressure loss, expressed in lbf/in.²;

P_{c} is the casing pressure, backpressure on annulus, expressed in lbf/in.²;

D_{tvd} is the true vertical depth, expressed in feet.

8 Swab/Surge Pressures

8.1 Principle

The purpose of this section is to provide equations and procedures to calculate changes in pressure created by movement of the pipe in a liquid-filled wellbore. While surge and swab calculations are generally performed while the wellbore is not being circulated, the methods can also be applied to circulating conditions.

Swab/Surge effects are influenced by the following:

- geometry of the well,
- fluid properties as a function of pressure and temperature, and
- acceleration, velocity, and deceleration of the string.

Pressure changes can be induced by the following mechanisms:

a) frictional pressure loss due to the displacement of the fluid,

b) pressure changes generated by the inertia of the drilling fluid column, and

c) pressures resulting from breaking the drilling fluid gels.

Not included in this section are considerations for the drilling-fluid compressibility, elasticity of the string, and elasticity of the well.

8.2 Effective Velocity

8.2.1 String Speed

The drill or casing sting velocity used for calculating the surge and swab pressure is the maximum velocity which occurs while running or pulling each stand or joint, instead of the average values. Using an average string speed substantially underestimates the maximum swab and surge pressures.

8.2.2 Displaced Fluid

The displaced fluid is the volume of fluid flow caused by pipe displacement and is a function of the geometry of the well and the string, and the tripping speed.

The two distinct modes of displaced fluid flow for surge and swab calculations are the open-pipe mode where fluid flows in both the annulus and pipe bore and the closed-pipe mode where fluid only flows in the annulus. The open-pipe mode would only occur when not circulating (pumps off).

Closed-pipe mode occurs when drill pipe float valves or conventional casing float collars are present such that no fluid flow into the pipe bore occurs. A drill string with a downhole motor or plugged jet nozzles is also a closed-pipe mode condition, even when no float valve is used.

Open-pipe mode occurs when running open ended pipe or any other situation where fluid flow can flow into the pipe bore, including flow paths such as bit nozzles (no float valve) or autofill casing equipment.

8.2.3 Effective Annular Fluid Velocity—Closed-pipe Mode

The *effective annular velocity* ($V_{\mathrm{a,eff}}$) is the combination of the annular velocity due to the displaced fluid plus a fluid velocity component due to the moving of the drill or casing string exterior wall.

The fluid velocity component due to string boundary movement is a function of the ratio of pipe diameter to hole diameter. From this ratio, a proportionality constant, called the *clinging factor* (C_{g}), is used to calculate the average fluid velocity caused by the string velocity. Tabulated, graphical, and equations for clinging factors for various rheological models under laminar and turbulent flow are available, see Bibliography [8.1 to 8.3]. A

conservative estimate for the clinging factor, C_g, is a value of 0.45 for the most common pipe and hole diameters. For pipe diameter to hole diameter ratios < 0.4, a calculated clinging factor value should be used.

The resulting effective annular fluid velocity for closed-pipe mode shall be provided by Equation (108), $V_{a,eff}$, expressed in ft/min.

$$V_{a,eff} = \frac{d_p^2}{d_h^2 - d_p^2} V_{ds} + C_g V_{ds} = V_{ds}\left(\frac{d_p^2}{d_h^2 - d_p^2} + C_g\right) \quad (108)$$

where

C_g is the clinging factor, dimensionless;

d_p is the drill string (pipe) outside diameter, expressed in inches;

d_h is the hole diameter or casing inside diameter, expressed in inches;

V_{ds} is the velocity of the drill string (pipe), expressed in ft/min.

8.2.4 Effective Annular Fluid Velocity —Open-pipe, Pump-on Mode

The effective fluid velocity for surge and swab when circulating is to add the annular velocity due to circulation to the effective fluid velocity for the closed-pipe mode, this condition is often referred to as the open-pipe, pump on mode even though no reverse fluid flow occurs into the pipe bore. The resulting effective annular fluid velocity when circulating (open-pipe , pump-on mode), $V_{a\text{-}circ,eff}$, expressed in ft/min shall be calculated using Equation (109).

$$V_{a\text{-}circ,eff} = V_a \pm V_{a,eff} = V_a \pm V_{ds}\left(\frac{d_p^2}{d_h^2 - d_p^2} + C_g\right) \quad (109)$$

where

V_a is the velocity in the annulus resulting from pump flow, expressed in ft/min;

$V_{a,eff}$ is the effective annular fluid velocity for closed-pipe mode, expressed in ft/min [see Equation (108)]

V_{ds} is the velocity of the drill string (pipe), expressed in ft/min;

C_g is the clinging factor, dimensionless;

d_p is the drill string (pipe) outside diameter, expressed in inches;

d_h is the hole diameter or casing inside diameter, expressed in inches;

$\pm$ is the sign for surge and swab, the positive sign is for surge and the negative sign is for swab.

NOTE $V_{ds}\left(\frac{d_p^2}{d_h^2 - d_p^2} + C_g\right)$ is the effective fluid velocity value for closed-mode, $V_{a,eff}$, see Equation (108).

8.2.5 Effective Annular Fluid Velocity —Open-pipe, Pump-off Mode

The effective fluid velocity for the open-pipe, pumps off mode requires an iterative procedure to determine the ratio of annular flow to total flow, f_a. Once this ratio is determined, the effective velocity in the annulus and inside the pipe should be calculated using Equation (110) and Equation (111).

a) $V_{a\text{-open,eff}}$, Effective fluid velocity for open-pipe, pump-off, in the annulus, expressed in ft/min.

$$V_{a\text{-open,eff}} = V_{ds}\left[f_a \times \frac{\left(d_p^2 - d_i^2\right)}{\left(d_h^2 - d_p^2\right)} + C_g\right] \tag{110}$$

b) $V_{ds\text{-open,eff}}$, Effective fluid velocity for open-pipe, pump-off in the drill string (pipe), expressed in ft/min.

$$V_{ds\text{-open,eff}} = V_{ds}\left[\left(1 - f_a\right) \times \frac{\left(d_p^2 - d_i^2\right)}{d_i^2} + 1\right] \tag{111}$$

Where

V_{ds} is the velocity of the drill string (pipe), expressed in ft/min;

f_a is the ratio of annular flow rate to total displaced flow rate, dimensionless;

C_g is the clinging factor, dimensionless;

d_p is the drill string (pipe) outside diameter, expressed in inches;

d_h is the hole diameter or casing inside diameter, expressed in inches;

d_i is the drill string (pipe) inside diameter, expressed in inches.

To determine the f_{an} in open-pipe mode, pumps-off case, the annular pressure loss and pipe bore pressure loss shall be equal. This requires that each of the pressure loss values should be calculated at different f_{an} values until they are equal using an iterative technique for the annular flow ratio, see Bibliography [8.1].

8.2.6 Drilling Fluid Properties as Function of Pressure and Temperature

Drilling fluid properties are temperature and pressure dependent, so the properties used for swab and surge calculations should follow the methods described in Section 6.

8.3 Calculate Pressure Changes

8.3.1 Frictional Pressure Loss

Section 7 includes details for frictional pressure loss calculations in laminar and turbulent flows, as well as the effects of drill string eccentricity.

8.3.2 Acceleration Pressure Drop

The component of surge pressure due to the inertia of the drilling fluid is caused by the tendency of drilling fluid to resist changes in motion.

a) Closed-pipe mode

For the closed-pipe mode, the inertial pressure surge (P_{ss}), expressed in lbf/in.² should be obtained from Equation (112).

$$P_{ss,av} = (0.052\,\rho) \times L \times \left(\frac{a_{ds}}{g}\right) \times \frac{d_p^2}{\left(d_h^2 - d_p^2\right)} = \frac{\rho L \times a_{ds}}{619} \times \frac{d_p^2}{\left(d_h^2 - d_p^2\right)} \quad (112)$$

where

a_{ds} is the acceleration of the drill string, expressed in ft/s²;

L is the length of drill string or annular segment, expressed in feet;

ρ is the fluid density, expressed in lbm/gal;

d_p is the drill string (pipe) outside diameter, expressed in inches;

d_h is the hole diameter or casing inside diameter, expressed in inches;

619 is the unit conversion factor including g the gravitational acceleration (32.1705 ft/s²).

b) Open-pipe, pump-off mode

For open-pipe mode and pump off, the average inertial pressure surge ($P_{ss,av}$), expressed in lbf/in.² can be calculated using Equation (113).

$$P_{ss,av} = (0.052\,\rho) \times L \times \left(\frac{a_{ds}}{g}\right) \times \frac{\left(d_p^2 - d_i^2\right)}{\left(d_h^2 - d_p^2 + d_i^2\right)} = \frac{\rho L \times a_{ds}}{619} \times \frac{\left(d_p^2 - d_i^2\right)}{\left(d_h^2 - d_p^2 + d_i^2\right)} \quad (113)$$

where

a_{ds} is the acceleration of the drill string, expressed in ft/s²;

L is the length of drill string or annular segment, expressed in feet;

ρ is the fluid density, expressed in lbm/gal;

d_{p} is the drill string (pipe) outside diameter, expressed in inches;

d_{i} is the drill string (pipe) inside diameter, expressed in inches;

d_{h} is the hole diameter or casing inside diameter, expressed in inches;

619 is the unit conversion factor including g, the gravitational acceleration (32.1705 ft/s²).

Equations (108) and (109) assume that the fluid is incompressible and therefore may slightly over-predict the inertia effect. A suggested estimate for pipe acceleration is 4.5 ft/s², if a measured value is not available.

Equation (109) assumes that the fluid inside and outside of the drill string has same velocity, which can under or over-predict the inertia effect inside and outside the pipe when the fluid velocities inside and outside the pipe are different. However, for open-pipe tripping, the pressure surge caused by inertial effects are generally small.

8.3.3 Breaking the Gel Strength

The surge pressure required to break the gel strength, $P_{\mathrm{a\text{-}min}}$, may be estimated using the definition of shear stress as a function of pressure as shown in Equation (114) and expressed in lbf/in². Pressures required to break gel strength buildup are normally lower than the surge pressures at peak velocities.

$$P_{\mathrm{a\text{-}min}} = \sum\left(\frac{\beta_{10\mathrm{min}}\, L}{300\, d_{\mathrm{hyd}}}\right)_j \tag{114}$$

where

j is an individual wellbore section or element;

$\beta_{10\mathrm{min}}$ is the 10 min gel strength, expressed in lbf/100 ft²;

L is the length of an individual j drill string or annular segment, expressed in feet;

d_{hyd} is hydraulic diameter (see 7.4.4), expressed in inches.

NOTE Longer time gels may be used if available.

8.4 Calculation Procedure

8.4.1 Set Up Common Process

The procedures for calculating pressure change due to tripping and its effect on the overall hydrostatic pressure is outlined in this section. To maintain the equivalent drilling fluid density above the formation pressure and below the fracture pressure, it is necessary to determine a safe trip speed. A safety margin can be used to ensure the maximum trip speed is still within the allowable range.

The common process set-up should be as follow.

a) *Define the point of interest (*POI*).*

The POI is the depth in the well that is most critical with respect to the pressures while tripping. It can be the casing shoe, at TD, or at a known weak zone in the open hole.

b) *Divide well in sections.*

The well needs to be divided into short sections to account for the pressure loss due to the geometry and the downhole fluid properties. Set the initial position of the bit for short trip. For full trip, the bit is placed at well total depth (tripping out) or at the surface (tripping in).

c) *Bracket running or pulling velocities.*

Select a range of speeds to be evaluated.

d) *Determine the drilling fluid properties.*

Drilling fluid properties can be determined using the procedures described in Section 5 and Section 6.

e) *Transform the Pressure to Equivalent Drilling Fluid Density (EMW).*

Calculate EMW at the POI for a given running speed. Procedure to calculate pressure is prescribed in 8.4.2 through8.4.4.

f) Compare EMW with Fracture Gradient and iterate running speed within the range prescribed in item c) to determine maximum allowable speed.

g) *Change position of the bit.*

Recalculate the well geometry sections based on the new bit position. Update drilling fluid properties as prescribed in item d). Iterate through all bit positions until final tripping depth is reached.

8.4.2 Calculate Pressures for Closed-pipe mode Tripping

Following steps shall be completed to determine the total pressure at the depth of interest (POI):

a) determine the fluid to be displaced,

b) assume laminar flow,

c) determine the clinging factor,

d) determine the effective velocity,

e) calculate the frictional pressure loss,

f) recalculate turbulent frictional pressure loss if flow is not laminar, and

g) calculate the total pressure at the POI.

8.4.3 Calculate Pressures for Open-pipe, Pumps-on mode Tripping

Following steps shall be completed to determine the total pressure at the depth of interest:

a) determine the fluid to be displaced,

b) assume laminar flow,

c) determine the clinging factor,

d) determine the effective velocity,

e) add pump flow rate to determine a combined velocity,

f) calculate the frictional pressure loss,

g) recalculate turbulent frictional pressure loss if flow is not laminar, and

h) calculate the total pressure at the POI.

8.4.4 Calculate Pressure for Open-pipe, Pumps-off mode Tripping

The analysis for an open-string configuration requires the determination of the flow distribution between the annulus and the string. After an initial guess for the flow distribution, pressure due to tripping can be calculated for each flow conduit. The flow distribution is adjusted until the pressure loss in each path is equal, see Bibliography [8.1].

a) determine the fluid to be displaced,

b) determine the clinging factor,

c) guess initial value for annular fraction of the total displacement flow rate f_{a},

d) determine the effective velocity in pipe and annulus using Equations (110) and (111),

e) calculate the frictional pressure loss in pipe and annulus,

f) balance the pressure loss in pipe and annulus through iterations of f_{a} value,

g) calculate the total pressure at the POI.

8.5 Transient Swab/Surge Analysis

Tripping pressures are not steady-state for several reasons. The pipe is set in motion and then brought to a stop as soon as a complete joint of casing or a stand of pipe is run in or pulled from the hole. Furthermore, the fluid is compressible, and so are the various conduits through which it flows under pressure. The unsteady flow causes pressure transients or surges that propagate in the fluid at the speed of sound. Fully dynamic surge models are more complex and require more computer resources than steady-state surge models. Movement of the pipe does not translate to the bottom due to the elasticity of the pipe and wellbore friction. Comprehensive transient surge/swab analysis is outside the scope of this document although references on this subject are included, see Bibliography [8.1 to 8.4].

9 Hole Cleaning

9.1 Description of the Challenge

Removal of cuttings from the wellbore is essential to drilling operation. Comprehensive detailed hole cleaning calculations for complex wells is outside the scope of this document although references on this subject are included, see Bibliography [9.9 to 9.17]. This section is provided to give the user useful tools for evaluating and achieving adequate hole cleaning.

Failure to effectively transport the cuttings can result in a number of drilling problems including:

a) excessive pick-up/slack-off weights and over-pull on trips,

b) high rotary torque,

c) stuck pipe,

d) hole pack-off,

e) excessive ECDs and cuttings accumulation,

f) lost circulation,

g) slow rates of penetration, and

h) difficulty tripping. running casing, and logging.

Successful hole cleaning relies upon integrating optimum drilling fluid properties, hydraulics, drill-string mechanics, and good drilling practices. This needs to be supported by careful monitoring and observation at the rigsite.

When difficulties are encountered, it is essential to understand the factors affecting hole cleaning to determine the most appropriate remedial actions. For example, poor hole cleaning resulting in high cuttings concentrations and cuttings beds in the annulus can be detected using downhole annular pressure measurements and by monitoring torque and drag against modelled conditions, see Bibliography [9.1, 9.2].

9.2 Hole-cleaning Practices and Remedial Options

9.2.1 Recommended Drilling Practices

The overall success of any hole-cleaning campaign is a combination of good planning and execution. It is recommended to develop a set of appropriate drilling practices to assist with achieving adequate hole cleaning and efficient drilling operations. Table 6 provides guidance on the parameters and controls that may be used to achieve best practices for hole cleaning. Table 6 is neither prescriptive nor fully exhaustive, it is provided to acknowledge the importance of appropriate drilling practices and provide a starting framework for an engineer planning an operation.

Table 6—Example Hole Cleaning Operational Practices

Downhole Annular Pressure Monitoring	Downhole annular pressure measurement is an excellent tool for monitoring hole cleaning. Comparison between actual and predicted values may indicate when preventative actions or extra hole cleaning measures should be taken. A recommended actionable condition is when the measured *ECD* reaches 0.2 lbm/gal (24 kg/m^3) over the *ECD* prediction with cuttings loading. This *ECD* prediction should be calibrated from measurements during clean hole conditions and from following trends throughout the hole section.
Flow Rate	Values should be based on calculations from this document or from industry standard recommendations for a given hole size and angle. For difficult wells, the flow rate selection should consider the planned drill string rotation and any potential sliding.
Rotation	Values should be based on this document or industry standard recommendations for a given hole size and angle. For difficult wells, the selected drill string rotation should consider the planned flow rate. Maximum revolutions per min should be based on drilling experience, drill string mechanics, and hole conditions.
Connections	Minimize or avoid back reaming as a standard procedure. Perform two surveys per stand. Once stand is down, circulate for 5 min (so cuttings are above the bottom hole assembly (BHA), shut pumps off/pumps on, perform survey, make connection. Stage rotation and pump flow rate gradually to break gels prior to full circulation.
ROP	Maintain steady *ROP* and control instantaneous drill rate to avoid overloading annulus with cuttings. Maximum suggested instantaneous *ROP* is 150 ft/h (45 m/h). Avoid overloading the annulus with cuttings and use downhole pressure measurement trends to detect increases in *ECD/EDD.*
Monitor Trends	Watch trends between surface vs downhole parameters (weight on bit, temperature, and torque/drag). Record pick-up, slack-off, rotating weights, and torque/drag and compare them to calculated values and trends.
Cuttings Monitoring	Monitor the amount, shape and size of cuttings over the shakers. Small, rounded cuttings indicate that cuttings are not being transported efficiently. Methods and equipment are available to quantitatively measure the cuttings return rate at the shakers which can be compared with the volume predicted from ROP. Watch for any sign of cavings over the shakers.
Critical Drilling Fluid Properties	The drilling fluid properties are critical to the hydraulics and *ECD* control. Trend graphs of the critical properties (for all tests) should be monitored daily. If necessary, stop and condition the drilling fluid before continuing to drill. Record drilling fluid density in and out of the hole every 15 min and log for trend analysis. Perform a minimum of two full drilling fluid checks per day. Circulate multiple bottoms-up before tripping or running casing. Condition drilling fluid properties prior to running casing and cementing.
Hole Cleaning Sweeps	Hole cleaning sweeps are not a substitute for good hole cleaning parameters (fluid properties, circulation rate, drill string rotation, and drilling practices). General recommendations for hole cleaning sweeps are: — Only pump a sweep after the hole has been conventionally cleaned with circulation and rotation, so as not to overload the annulus with cuttings. — Only allow one sweep in the hole at any time. — Monitor the effectiveness of sweeps using downhole annular pressure measurement or torque and drag monitoring. Also record the change in cuttings load as the sweep exits the well. — For high angle and horizontal intervals, high density and low viscosity sweeps may be beneficial for helping to reduce stationary cuttings beds. For high-density sweeps, 3-4 lbm/gal (360-480 kg/m^3) over baseline drilling fluid density is recommended while being sure not to exceed fracture initiation pressure. For both high density and low viscosity sweeps the sweep volume should be sufficient to cover 400 ft (120 m) of annular length. Sweeps should be pumped with the maximum circulation rate and pipe rotation parameters and while reciprocating the drill string. — Viscous sweeps are not effective for high angle and horizontal intervals but work well in vertical intervals.
Wiper Trips	Only perform wiper trips as a means of monitoring hole condition. If the hole dictates, short trip at TD ensures that drilling fluid density margin is sufficient to come out of the hole. Use torque and drag monitoring and annular pressure measurement to indicate if a wiper or clean-up trip is needed.
Hole Pack-off	Slow or stop pump, work pipe with slow circulation until full circulation is established.

9.2.2 Circulation Prior to Tripping

Simple predictions are not available for determining the rate of cuttings removal and the length of time needed to circulate prior to tripping for complex and high-angle wells. Because cuttings are transported slower than the circulating drilling fluid, it is essential that a sufficient number of bottom-up circulations are performed prior to tripping. For deviated and horizontal intervals, a single bottoms-up is usually not sufficient to remove all cuttings from the well.

The minimum on-bottom circulation time prior to tripping is influenced by hole size, inclination, ROP, bit type, RPM and flow history (i.e. drilling fluid properties and flow rate). These factors affect the height of cutting beds and the accumulation of cuttings in horizontal and high angle intervals.

Before tripping, monitor the shakers for sufficient time to ensure the cuttings return rate is reduced to an acceptable background level. If available, use downhole annular pressure data to determine whether the ECD has been reduced to an acceptable value and in line with calculated values.

9.2.3 Impact of Drill String Rotation

Movement of the drill string (rotation and/or reciprocation) can mechanically disturb cuttings beds and assist hole cleaning for high angle intervals. Rotation is critical for achieving good hole cleaning as it mobilizes cuttings beds back into the higher velocity flow profile on the high side of the hole for near horizontal intervals. The influence of drill pipe rotation is more pronounced in viscous drilling fluids and in smaller hole sizes (i.e. <12 ¼ in.). In cases where the pipe is not rotated (e.g. slide drilling), cuttings beds form more easily and are more difficult to remove.

The normal recommended range of drill pipe rotational speeds is 120 r/min to 200 r/min for horizontal intervals. In practice, there needs to be a balance between the beneficial effects on hole cleaning and possible detrimental effects (e.g. vibration causing premature failures of downhole equipment). Excessive rotary speed values should also be avoided in unstable formations since mechanical interaction can cause wellbore degradation and instability.

9.2.4 Guidelines on Sweeps

Drilling fluid properties and drilling parameters should always be optimized to provide adequate hole cleaning. Sweeps alone cannot provide adequate hole cleaning and are often ineffective. Excessive use of sweeps should be avoided as they may change the desired drilling fluid density and viscosity of the active drilling fluid system.

High-viscosity (and preferably higher-density) sweeps are effective at removing cuttings in vertical and shallow angle intervals <30°. Sweeps which incorporate fibrous materials are similarly effective in these more vertical intervals. For horizontal and intervals above 30° inclination, weighted sweeps or low-viscosity sweeps are occasionally beneficial. High-density sweeps are recommended to be formulated at 3 to 4 lbm/gal (360 kg/m^3 to 480 kg/m^3) above baseline drilling fluid density. The volume of high-density or low viscosity sweeps is dictated by hydrostatic considerations, but the recommended sweep volume should cover at least 400-ft (120-m) of annular length.

9.3 Cuttings Transport

9.3.1 Forces Acting on Cuttings

In vertical and near-vertical sections, cuttings are effectively carried by being distributed and suspended in the flowing drilling fluid. The viscous drag and annular fluid velocity act to overcome the cuttings settling tendency, resulting in a net upward movement of the cuttings.

In high-angle and horizontal intervals, the gravitational force acting on the cuttings causes the formation of cuttings beds on the low side of the hole. The annular fluid velocity creates a drag force that tends to move the cuttings bed along the wellbore, while a fluid lift force acts to move the upper portion of the exposed cuttings bed into the higher velocity flow stream on the high side. Gravitational force on the drill pipe forces the pipe towards the low side of the hole resulting in a skewed annular velocity profile since fluid always seeks the path of least resistance. Pipe rotation is beneficial in these high angle intervals as the pipe generally is closer to the cuttings bed and fluid movement due to pipe rotation stirs up the cuttings into the higher velocity flow profile on the high side.

9.3.2 Flow Patterns

Flow patterns in the annulus depend strongly upon inclination, flow rate, and drilling fluid viscosity. Low viscosity fluids with low yield points and yield stresses tend to promote turbulence and cuttings saltation. High-viscosity fluids with high yield points and yield stresses increase the fluid drag force and tend to promote the cuttings to be suspended and for cuttings beds to slide.

9.3.3 Cuttings Transport in Vertical vs High-angle Wells

Figure 6 is a schematic representation of the transport mechanisms for a range of well inclinations assuming no pipe rotation. In highly deviated wells, cuttings tend to settle on the low side wall and form cuttings beds. These cuttings are often transported along the low side of the hole either as a continuous moving bed or in separated beds/dunes.

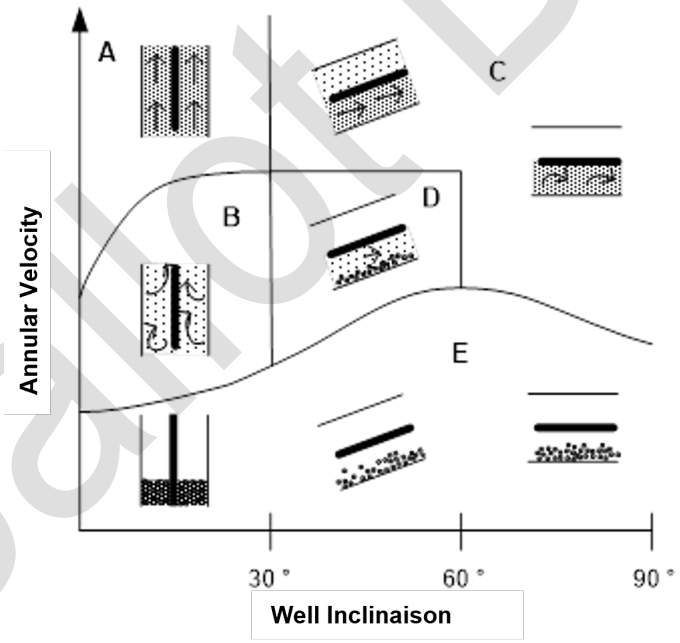

Key

A Zone A—efficient hole cleaning
B Zone B—slow cuttings removal
C Zone C—good hole cleaning with moving cuttings bed
D Zone D—some hole cleaning—cuttings bed formed
E Zone E—difficult hole cleaning

Figure 6—Cuttings Transport Mechanisms in Vertical and Deviated Wells

At inclinations less than 30°, cuttings are effectively suspended and transported by the fluid drag acting on the particles and beds do not form (Zones A and B). For such cases, conventional transport calculations based on vertical slip velocities are applicable. For these more vertical angles, annular velocity requirements are significantly less than for higher angle intervals of similar hole size.

Inclinations between 30° and 60° are considered the transition or critical range for hole cleaning where cuttings are no longer transported predominantly suspended in the flowing fluid and unstable cuttings beds and dunes form on the low side of the wellbore. These can potentially slide back down the well causing the annulus to pack-off. Transport behavior in this interval (Zone C and D) is complex with some cuttings being transported while suspended in the fluid, by saltation, by moving or sliding beds, as ripples or dunes, or as slugs of cuttings.

For inclinations above 60°, cutting beds form almost instantaneously, are more stable (immobile) and difficult to remove. Studies have shown that for most conditions there is a stationary bed on the bottom of the wellbore with a fluidized moving bed above the stationary bed at the bed/drilling fluid interface which is where the main fluid flow velocity profile occurs at the top of the wellbore. (Zone C). For these high angle intervals, drill pipe rotation is critical to mechanically disturb the cuttings beds and stir them up into the higher velocity flowing drilling fluid at the top of the hole.

Zones for easiest cuttings transport are Zone A and Zone B. Probability is high for excessive thick cuttings bed formation in Zone E where the lower annular velocity can lead to tight-hole or stuck pipe.

Analytical and numerical methods have been used with some success to model complex drill cuttings transport and fluid flow at all angles and with eccentric annuli. In practice, the complexity of cuttings transport in deviated wells and transient drilling conditions rule out the use of pure analytical approaches to modeling heterogeneous cuttings/drilling fluid mixtures. Most modeling approaches used today are based on empirical methods of using laboratory data to fit physics-based models, see Bibliography [3, 9.3 to 9.17].

9.4 Modeling Hole Cleaning in Vertical and Low-angle Wells

Cuttings removal in vertical intervals has been studied for over 75 years. These studies are showing:

a) the importance utilizing a sufficient flow rate, rotation, and fluid properties to keep the drill cuttings concentration below 5%,

b) effect of particle shape and particle flow regime (laminar, transition, or turbulent) on slip velocity while cuttings fall in the flowing fluid,

c) effect of fluid viscosity and density, and

d) the influence of hole size and pipe rotation on transport.

Several methods for evaluating hole cleaning for vertical intervals are listed in the Bibliography [3, 9.3 to 9.8]. For complex wells with highly deviated and horizontal intervals, differences in the results from these models and hole cleaning in the vertical interval is not normally a critical zone of concern.

9.4.1 Vertical Hole-cleaning Model 1 [9.7]

9.4.1.1 Principle

Hole cleaning in vertical and near-vertical intervals is generally modeled by comparing the annular fluid velocity with the slip velocity of the cuttings. Provided the annular velocity of the fluid is higher than the cuttings slip velocity, there will be a net upward movement of the cuttings. The rate that cuttings accumulate in the annulus

will be a function of this net upward velocity of the cuttings and the rate that cuttings are produced (a function of bit size and penetration rate).

The slip velocity of the cuttings (V_s) can be estimated by a number of empirical calculations, see Bibliography [3, 9.3 to 9.8] A useful and simple method is presented here, Bibliography [9.7]. The first step involves calculating the shear stress on a disk-shaped cutting as it falls edgewise through the drilling fluid.

Shear stress, τ_c, due to cutting slip shall be given by Equation (115).

$$\tau_c = 7.9 \times \left[h_c \left(8.345\, \rho_c - \rho \right) \right]^{1/2} \tag{115}$$

where

τ_c is the shear stress on the falling cutting, expressed in lbf/100 ft^2;

h_c is the cutting thickness, expressed in inches;

ρ_c is the cutting relative density (specific density) dimensionless;

ρ is the fluid density, expressed in lbm/gal.

If the shear stress on the cutting (τ_c) is lower than drilling fluid yield stress (τ_y), then the cutting does not settle. Otherwise, the drilling fluid shear rate (γ_c) required to equal the cutting shear stress (τ_c) can be estimated for a H-B fluid by using Equation (116) and expressed in s^{-1} .

$$\gamma_c = \left[\frac{\tau_c}{k} - \left(\frac{3}{2} \right)^n \frac{\tau_y}{k} \right]^{1/n} \tag{116}$$

NOTE Alternatively this shear rate value can be determined graphically from shear stress vs shear rate at the shear stress value for τ_c or by using by using a power law calculation for this shear stress.

9.4.1.2 Cuttings slip velocity and cuttings transport ratio

The rate at which the cuttings slip depends on the flow regime of the fluid surrounding the cutting. If the annular flow regime is turbulent, then the flow around the cutting also will be turbulent. Otherwise, the flow regime surrounding the cutting is determined by comparing γ_c to a critical shear rate (γ_b) defined for a N_{Re} = 100 (turbulent-transition) using Equation (117).

$$\gamma_b = \frac{186}{d_c \sqrt{\rho}} \tag{117}$$

where

γ_b is the shear rate corresponding to a N_{Re} = 100, expressed in sec^{-1};

ρ is the fluid relative density, dimensionless;

d_c is the cuttings diameter, expressed in inches.

For $\gamma_c < \gamma_b$ laminar-transitional flow is assumed, and the cuttings slip velocity V_s, expressed in feet per minute shall be calculated by Equation (118).

$$V_s = 1.22\,\tau_c \left(\frac{d_c\,\gamma_c}{\sqrt{\rho}} \right) \tag{118}$$

where

γ_c is the cutting shear rate required to equal the cutting shear stress (τ_c) [see Equation (116)], expressed in sec^{-1};

τ_c is the shear stress on the falling cutting, expressed in lbf/100 ft^2;

d_c is the cuttings diameter, expressed in inches;

ρ is the fluid relative density, dimensionless.

For $\gamma_c > \gamma_b$, turbulent flow is assumed, and the cuttings slip velocity V_s, expressed in feet per minute, shall be calculated by Equation (119).

$$V_s = \frac{16.62\,\tau_c}{\sqrt{\rho}} \tag{119}$$

where

τ_c is the shear stress on the falling cutting, expressed in lbf/100 ft^2;

d_c is the cuttings diameter, expressed in inches;

ρ is the fluid relative density, dimensionless.

Effectiveness of cleaning a vertical well can be gauged by comparing cuttings slip velocity and fluid annular velocity using the cuttings transport ratio R_t, a decimal ratio which shall be calculated using Equation (120):

$$R_t = \frac{V_u}{V_a} = \frac{V_a - V_s}{V_a} \tag{120}$$

where

V_u is the net upward cuttings velocity, in feet per minute, and shall be defined by Equation (121):

$$V_{\mathrm{u}} = V_{\mathrm{a}} - V_{\mathrm{s}} \tag{121}$$

and

V_{a} is fluid velocity in the annulus, expressed in feet per minute;

V_{s} is cuttings slip velocity, expressed in feet per minute.

9.4.1.3 Hole cleaning in vertical wells

General rules-of-thumb for adequate hole cleaning in vertical wells are a transport ratio R_t > 0.5 and in-situ cuttings concentration (c_a) lower than 0.05 or 5 %.

To determine the cuttings concentration in the vertical annulus, the cuttings concentration as a volume fraction, (c_a), can be determined using Equation (122). This equation is derived from the volumetric rate of cuttings being generated at the bit being equal to the volumetric rate of cuttings exiting the well under steady state conditions.

$$c_{\mathrm{a}} = \frac{d_{\mathrm{b}}^2 \times ROP}{1471 Q R_{\mathrm{t}}} = \frac{d_{\mathrm{b}}^2 \times ROP}{60\left(d_{\mathrm{b}}^2 - d_{\mathrm{p}}^2\right)\left(V_{\mathrm{a}} - V_{\mathrm{s}}\right)} \tag{122}$$

where

c_a is the in-situ cuttings volume concentration , expressed as a decimal fraction;

d_b is the bit diameter, expressed in inches;

ROP is the rate of penetration expressed in feet per hour,

Q is the flow rate, expressed in gallons per minutes

R_t is the cuttings transport ratio, expressed as a decimal fraction;

d_p is the pipe outside diameter, expressed in inches;

V_{a} is fluid velocity in the annulus, expressed in feet per minute;

V_{s} is cuttings slip velocity, expressed in feet per minute.

NOTE For complex wells, it may be necessary to calculate the cuttings concentration for each significantly different vertical annular dimensions.

9.4.2 Hole-cleaning Model 2 [9.8]

9.4.2.1 Carrying Capacity Index (*CCI*)

There are three drilling fluids-related hole-cleaning variables that can be controlled at the drilling rig:

- drilling fluid density,
- drilling fluid viscosity, and
- annular velocity.

Increasing any one of these variables generally improves hole cleaning. An empirical equation has been developed from field observations to predict good hole cleaning in vertical and near-vertical wells.

The Carrying Capacity Index (CCI) [10.1] shall be calculated using Equation (123), and:

a) when CCI is equal to or greater than 1, good hole cleaning is expected and cuttings tend to be sharp-edged and large;

b) when CCI has a value of around 0.5, hole cleaning is marginal and cuttings may be more rounded and smaller;

c) when CCI has a value below 0.4, hole cleaning is poor and cuttings can be expected to be grain-sized.

$$CCI = \frac{\rho k_1 V_a}{400{,}000} = 2.5 \times 10^{-6} \left(\rho k_1 V_a \right) \tag{123}$$

where

ρ is the fluid relative density, dimensionless;

V_a is fluid velocity in the annulus, expressed in feet per minute;

k_1 is the power law viscosity at one (1) s^{-1}, expressed in centipoises.

k_1 Is an indication of the viscosity at low shear rates and shall be calculated using Equation (124)

$$k_1 = 511^{\left(1-n_p\right)} \times R_{300} \tag{124}$$

with the power law flow behavior index, n_p , calculated using Equation (125)

$$n_P = 3.32 \times \log_{10} \left(\frac{R_{600}}{R_{300}} \right) \tag{125}$$

where

n_p is the power law flow behavior index, dimensionless;

R_{600} is the dial reading at 600 r/min in degrees;

R_{300} is the dial reading at 300 r/min in degrees.

9.4.2.2 *CCI* Evaluation Summary

A summary of evaluating CCI in vertical and near-vertical wells is as follows.

a) Use Equations (124) and (125) to determine value of k_1 from R_{600} and R_{300}.

b) Use flow rate and maximum hole diameter to determine annular velocity.

c) Determine CCI using Equation (123).

If CCI is less than 1.0 or the cuttings discharged are small or have rounded edges, the needed to increase in equivalent viscosity, k_1, at 1 s^{-1} to provide sufficient carrying capacity shall be calculated using Equation (126).

$$k_1 = \frac{4\times10^5 \times R_{300}}{\rho V_a} \tag{126}$$

where

R_{300} is the dial reading at 300 r/min in degrees;

ρ is the fluid relative density, dimensionless;

V_a is fluid velocity in the annulus, expressed in feet per minute.

To increase the k_1 value (viscosity at low shear rate) and improve hole cleaning in near vertical intervals it is preferred to utilize additives which increase the shear thinning (lower n value) and have a minimum increase in η_{PV} .

9.5 Modeling Hole Cleaning in Directional Wells

9.5.1 General

Presenting comprehensive methods for evaluating hole cleaning in complex wells with highly deviated and horizontal sections is outside the scope of this document. Cuttings transport between these intervals is interrelated and strongly influenced by cuttings size, flow regime, localized annular velocity profiles, ROP, rotation, and fluid properties. For detailed calculation methods to evaluate cuttings transport in highly deviated and horizontal sections, the Bibliography includes references [9.9 to 9.17].

A simple chart-based method [9.16] for high-angle wells is described below which is based on the fluid forces acting on cuttings within a settled bed and is applicable to hole angles > 30°. The model takes into account both lift and drag forces to predict the minimum flow rate required to prevent formation of stationary cuttings beds. The model was originally developed from flow loop data and has been validated in the field against numerous high-angle and horizontal wells, where the primary measure of good hole cleaning has been the absence of operational problems associated with poor hole cleaning.

The main features of this model are:

a) allows for rheological properties and flow regime,

b) models washed-out hole,

c) assumes the drill pipe is rotated at 100 r/min, and

d) predicts flow rate requirements with changing ROP.

9.5.2 Chart-based Model—Drilling Fluid

This model demonstrates that either thick or thin fluids can be used to clean high-angle sections. Studies have shown that cuttings removal in these sections occurs through a combination of saltation and cuttings transport at the bed interface or by cuttings beds sliding. This complex behavior is caused by fluid lift and the drag forces acting on the settled cuttings. In laminar flow, drag dominates, while in turbulent flow lift is more important. These forces indicate that the effect of fluid rheology and of flow regime are interdependent. Intermediate viscosity drilling fluids provide the worst conditions and should be avoided. In situations where ECD is not a limiting factor, high-viscosity fluids with high yield point/plastic viscosity ($Y_{\mathrm{P}} / \eta_{\mathrm{PV}}$) ratios are preferred.

Figure 7 shows how increasing the drilling fluid yield point causes the flow regime to change from turbulent to laminar. Intermediate values of Y_{P} should be avoided since they can produce the worst conditions for cuttings transport. The higher Y_{P} (and hence laminar flow) regime is often preferred because the higher viscosity drilling fluid provides better cuttings suspension and improved transport.

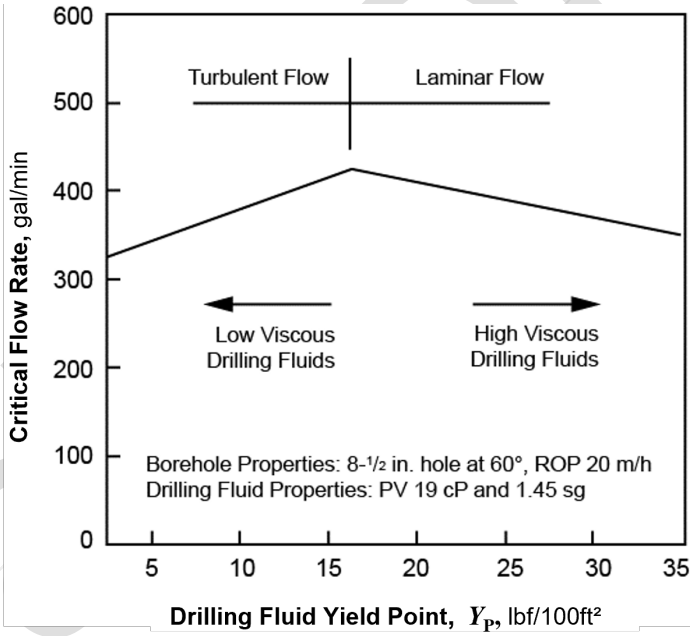

Figure 7—Effect of Yield Point on Critical Flow Rate

Under conditions where ECD is a limiting factor, the use of thin fluids in turbulent flow should be considered. Thin fluids reduce annular frictional pressure losses and hence result in lower ECDs. Turbulent flow in the annulus should be avoided with weakly consolidated formations due to the increased risk of hole erosion (see Section 10). Extra care is also required with low viscosity drilling fluids due to the increased risk of barite sag.

9.5.3 Graphical method

A simple graphical method is presented for estimating the maximum ROP for adequate hole cleaning in high-angle wells for a particular $Y_{\mathrm{P}} / \eta_{\mathrm{PV}}$, fluid density and flow rate.

The charts in Figure 8 and Figure 9 apply to 8 1/2-in. hole sections. Similar charts for 17 1/2-in. and 12 1/4-in. hole sizes are available [9.16]. The method assumes that the drill pipe is rotated at 100 r/min. If the drill pipe is not rotated, then a significantly higher flow rate is required to clean the hole. Alternatively, it may prove necessary to use remedial drilling practices to clean the hole after an extended period of slide drilling.

The procedure shall be as follows.

a) Enter the rheology factor (RF) chart (Figure 8) with the appropriate values of Y_{P} and η_{PV} values at 120 °F and atmospheric pressure. Read the value of the RF.

b) Calculate the transport index (TI) based on the drilling fluid flow rate and drilling fluid density given by Equation (127) (dimensionless).

$$TI = \frac{Q \times \rho \times RF}{834.5} = 1.198 \times 10^{-3} \left(Q \times \rho \times RF\right) \tag{127}$$

where

Q is the flow rate , expressed in gallons per minute;

ρ is the fluid relative density, dimensionless;

RF is the rheology factor, dimensionless.

c) Determine the maximum ROP using Figure 9. From the value of TI calculated from Equation (127) and the maximum hole angle, find the maximum ROP that can be sustained while still maintaining adequate hole cleaning.

NOTE A similar method from the same authors, using a different equation for TI and using different hole cleaning charts (with ROP vs hole angle) can be found in Bibliography [9.17].

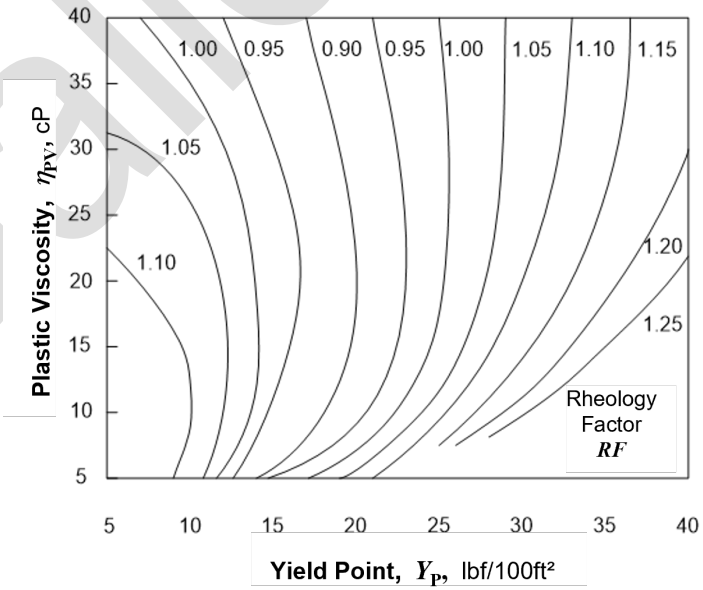

Figure 8—Rheology Factor (RF) Chart for 8 1/2-in. Holes [9.16]

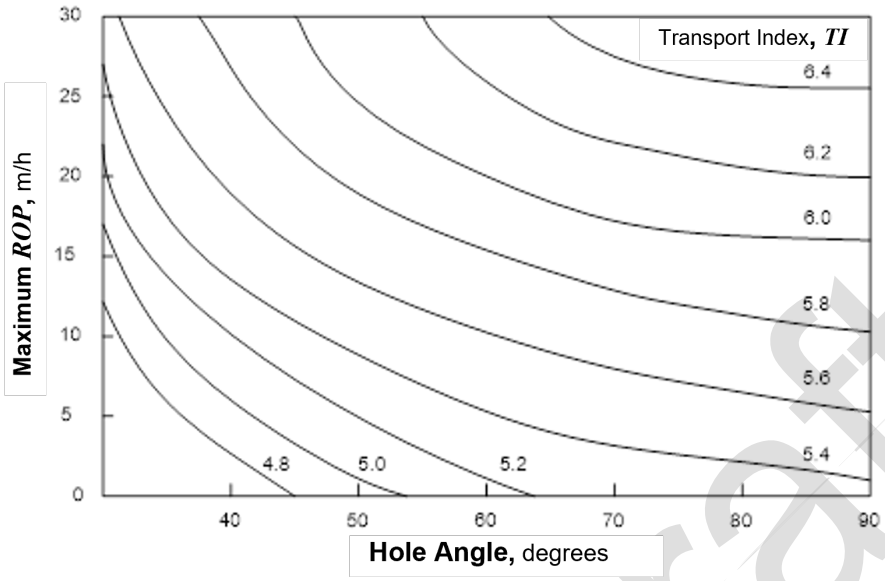

NOTE To convert Maximum ROP in ft/h, divide m/h by 0.3048.

Figure 9—Hole-cleaning Chart for 8½-in. Holes [9.16]

For ERD field experience has shown that the combination of adequate flow rate and drill pipe rotation is needed to maintain good hole cleaning. This field experience has led to a recommended range of values for having acceptable hole cleaning for ERD applications. Typical ranges for these ERD recommendations for common hole sizes are listed in Table 7. The drill pipe size can strongly affect the best flow rate and rotation, especially in the smaller hole sizes, and should be considered when selecting those parameters.

Table 7—Recommended Range of Flow Rate and Rotation for ERD

Hole Size in.	Flow Rate gal/min	Rotation r/min
17 ½	900 – 1400	>150
12 ¼	750 – 1100	>120
9 ⅞	600-900	>120
8 ½	400-600	>100
6 ½	150-250	>75

It is possible to estimate the cuttings contribution to equivalent drilling fluid density for a simple vertical well. This is based on the cuttings feed rate, the drilling fluid flow rate, and the transport ratio (R_t) defined in Equation (120), see Section 9.4.1.2. Transport ratio is a measure of how fast the cuttings are carried in the drilling fluid compared with the annular fluid velocity. If no slip occurs, then the transport ratio is 1. The reciprocal of transport ratio can be used as a guide for the number of bottoms-up required to bring cuttings to the surface.

In the case of a deviated well, no simple method exists to calculate the cuttings contribution to ECD. It is, however, possible to use results from downhole annular pressure measurements to estimate the cuttings contribution to static drilling fluid density. These data are normally only available from memory data since the pumps shall be off to record the static drilling fluid density.

9.6 Weight-material Sag

In weighted drilling fluids, the separation of weighting material can lead to local fluctuations in fluid density. This is commonly referred to as barite sag. It can be particularly pronounced in high-angle wells and lead to significant variations in return drilling fluid density as drilling fluid is circulated to surface. A more detailed description of weight-material sag is provided in API 13B-2. As described in Section 6.4, the density of NADFs is strongly affected by temperature. For this reason, when monitoring barite sag, it is critical to make all measurements at a uniform temperature or to adjust the density to the same reference temperature.

10 Hydraulics Optimization

10.1 Optimization Objectives

10.1.1 Principle

The goal of bit hydraulics optimization is to maximize the hydraulic energy available at the bit to remove generated cuttings as quickly and efficiently as possible. This can help maximize ROP by minimizing cuttings regrinding. Optimized hydraulics design is defined here as the determination of the jet nozzle sizes and flow rates to satisfy an optimization criterion. Criteria include the maximizing bit hydraulic horsepower or hydraulic impact force at the bit.

Constraints in the optimization process include:

- rig capability limitations, namely maximum available standpipe pressure and maximum horsepower of the rig pumps,
- wellbore limitations, namely minimum required and maximum available flow rates for wellbore stability and hole-cleaning requirements, and
- downhole-tool limitations.

The goal of bit hydraulics optimization is to determine the flow rate, total nozzle flow area (TFA), and jet nozzle sizes to deliver maximum bit hydraulic horsepower or impact force within the limitation of maximum pump pressure and hydraulic horsepower available from the rig pumps.

If a cutting is removed before the next tooth reaches the cutting, the bottom of the borehole is being sufficiently cleaned. The drilling rate for a roller cone drill bit increases as a function of the square of the weight on a roller cone drill bit until rate of cuttings generation is too rapid for the drilling fluid to remove all of the cuttings. At this point, called the founder point, the drilling rate will not continue to increase as rapidly when the weight on the bit is increased. Increasing hydraulic parameters very far below the founder point will not significantly increase drilling rate. In fact, under these circumstances, increased flow rate may increase the bottomhole pressure and decrease drilling rate. With high pressure differentials, cuttings are more difficult to remove after they are formed, and the founder point will decrease [10.1 to 10.5].

Including drilling rate as a mathematical parameter in the optimization process is beyond the scope of this document.

10.1.2 Maximizing Hydraulic Horsepower and Impact Force at the Bit

Bit hydraulic horsepower and jet impact force are maximized so that cuttings and debris beneath the drill bit are forced away from the bottom of the hole before being reground. This raises the founder point. The hydraulic

horsepower at the bit (HHP_b) and bit jet impact force (F_j) shall be calculated respectively by Equation (128) and Equation (129).

$$HHP_b = \frac{QP_b}{1714} \tag{128}$$

$$F_j = 0.0182 \times C_d Q \sqrt{\rho P_b} \tag{129}$$

where

Q is the flow rate, expressed in gal/min;

P_b is the pressure loss through the bit, expressed in lbf/in.^{2};

C_d is the jet nozzle discharge coefficient = 0.98;

ρ is the fluid relative density, dimensionless.

Hydraulic horsepower (HHP) can be expressed as ρQV^2, and jet impact force (F_j) can be expressed as ρQV. The optimum flow rate for the maximum bit hydraulic horsepower will be lower than the optimum flow rate for the maximum jet impact force. Since hydraulic horsepower is related to the square of the velocity, jet velocity is more important than flow rate. No comparison studies have been reported in the literature comparing drilling rates for these two optimum techniques under identical conditions at the rig.

Theory for the optimization was developed for roller cone bits. Polycrystalline diamond compact (PDC) bit experience shows that the penetration rates are best for a certain value of hydraulic horsepower or hydraulic horsepower per square inch (HSI). In this latter case, nozzle sizes are selected to achieve a specified HSI value instead of the maximum HSI .

10.1.3 Maximizing Jet Velocity

Some drilling programs select flow rates by using the maximum possible jet velocity (V_j), which occurs at the lowest flow rate that provides adequate hole cleaning and barite-sag mitigation. Low flow rates minimize parasitic losses and provide maximum pressure and jet velocity through the bit nozzles. Field guidelines recommend nozzle velocities above 230 ft/s (70 m/s) to reduce the possibility of plugged jet nozzles. The jet velocity (V_j) shall be given by Equation (130).

$$V_j = C_d \sqrt{\frac{P_b}{8.074 \times 10^{-4}\ \rho}} = 35.19 \times C_d \sqrt{\frac{P_b}{\rho}} \tag{130}$$

where

C_d is the jet nozzle discharge coefficient = 0.98;

P_b is the pressure loss through the bit, expressed in lbf/in.^{2};

ρ is the fluid relative density, dimensionless.

10.1.4 Annular Velocity

Annular velocity moves cuttings from the bottom of the hole to the surface. Increasing annular velocity increases annular pressure loss and ECD and, therefore, can have an adverse effect on drilling rate. See Section 9 for hole-cleaning guidelines.

With PDC bits, HSI is more important than the nozzle velocity. Higher HSI values should be required as the shale reactivity of the formation increases.

10.2 Calculations

10.2.1 System Parasitic Pressure

The system parasitic pressure loss (SPP, P_{x}) which includes all pressure losses expressed in lbf/in.² in the circulating system excluding the bit, can be simulated using Equation (54). Since most of the flow is turbulent, P_{x} also can be defined using the following power law relationship, Equation (131), discussed in 10.2.2.

$$P_{\mathrm{x}} = K_{\mathrm{x}} Q^{u} \tag{131}$$

where

K_{x} is the parasitic pressure loss coefficient, expressed in (lbf/in.²)/(gal/min)^{u};

Q is the flow rate, expressed in gallon per minute;

u is the slope of logarithmic system parasitic pressure loss, dimensionless.

10.2.2 Hydraulic Optimization

Hydraulic optimization should be applied using the following procedure [10.1].

a) Caliper the individual nozzles. Since the bit pressure drop is inversely proportional to d_{n}^{4}, small variations in bit diameter nozzle can have a big impact.

b) Calibrate the rig pumps to achieve accurate flow rate measurements.

c) Determine the SPP loss characteristics of the circulating system.

   1) *On the rig*—Measure the standpipe pressure (P_{p}) for the range of flow rates. Flow rates of interest should be on the high end to minimize the chance of laminar flow in the drill string. Determine the SPP loss (P_{x}) for each flow rate (Q) by calculating the respective bit pressure loss (see Section 7) and subtracting from the P_{p} values.

   2) *In the office*—Calculate individual SPP losses (P_{x}) for a selected range of flow rates of interest.

d) Determine the slope of logarithmic SPP loss (u) and the SPP loss coefficient (K_x) in the parasitic pressure loss Equation (131). The value for slope (u) should be between 1.4 and 1.9.

1) *Manually*—Plot the parasitic pressure losses (P_x) vs flow rate (Q) on log-log paper and measure the slope (u) with a ruler. Calculate K_x for a known data set by rearranging Equation (131).

2) *Spreadsheet program*—Plot the sets of parasitic pressure loss (P_x) and flow rate (Q) in a graph. Fit the data points to a power function using the spreadsheet trend-line function. Extract the slope (u) and coefficient (K_x) from the curve fit.

e) Apply the optimization approach from Table 7. Equation numbers (132) to (137) are included in the cell with each formula.

Table 7—Hydraulic Optimization Equations

Criterion Limiting Factor	Maximum Impact Force		Maximum Hydraulic Power
	Hydraulic Power	Maximum Operating Surface Pressure	Maximum Operating Surface Pressure
Optimum bit pressure loss $P_{b\text{-}opt}$ lbf/in.^{2}	$P_{b\text{-}opt} = \left(\frac{u+1}{u+2}\right) P_{max}$ Equation (132)	$P_{b\text{-}opt} = \left(\frac{u}{u+2}\right) P_{max}$ Equation (134)	$P_{b\text{-}opt} = \left(\frac{u}{u+1}\right) P_{max}$ Equation (136)
Optimum flow rate Q_{opt} gal/min	$Q_{opt} = \left(\frac{P_{max}}{K_x\,(u+2)}\right)^{\frac{1}{u}}$ Equation (133)	$Q_{opt} = \left(\frac{2\,P_{max}}{K_x\,(u+2)}\right)^{\frac{1}{u}}$ Equation (135)	$Q_{opt} = \left(\frac{P_{max}}{K_x\,(u+1)}\right)^{\frac{1}{u}}$ Equation (137)

where

P_{max} is the maximum pump pressure, expressed in lbf/in.²

u is the slope of logarithmic system parasitic pressure loss, dimensionless.

K_x is the parasitic pressure loss coefficient, expressed in (lbf/in.²)/(gal/min)^u.

f) For maximum power at the drill bit nozzles, P_{max} (maximum P_p) shall be used, so the optimum flow rate shall be equal to or less than the critical flow rate, laminar to transitional, Q_{crit}.

g) For maximum hydraulic impact force, the optimum flow rate may be above, equal to, or less than Q_{crit} [1]. Q_{crit} should be the flow rate at the intersection of P_{max} and available hydraulic horsepower. Q_{crit},expressed in gallons per minute should be calculated using Equation (138).

$$Q_{crit} = \frac{1714\,HHP_{max}}{P_{max}} \tag{138}$$

where

$HHP_{\max}$ is the maximum pump hydraulic horsepower, expressed in horse power;

$P_{\max}$ is the maximum pump pressure, expressed in lbf/in.²

h) On the log–log diagram, see Figure 10, three regions can be identified when optimizing for maximum impact force.

1) *Region 1*—Limited by $P_{\max}$.

Q_{crit}, is the maximum flow rate for Region 1. For flow rates below Q_{crit}, the maximum hydraulic horsepower ($HHP_{\max}$) of the pumps cannot be reached because of the pump pressure limitation.

2) *Region 3*—Limited by $HHP_{\max}$.

Flow rates in Region 3 range from Q_{crit} to the maximum flow rate provided by the pumps. For flow rates larger than Q_{crit}, the maximum pump pressure cannot be reached because of the horsepower limitation.

3) *Region 2*—Intersection between Region 1 and Region 3.

It is coupled to Q_{crit} where both the maximum pump pressure and the maximum horsepower can be used as limiting criteria for the optimization.

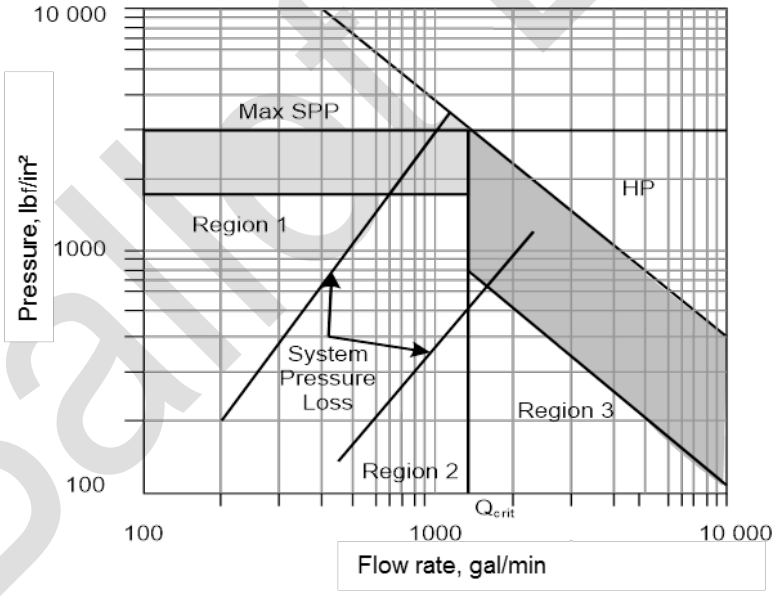

Key

Max SPP maximum system parasitic pressure

HP pump hydraulic horsepower

Figure 10—Optimizing Maximum Impact Force

i) Check whether the resulting optimum flow rate (Q_{opt}) is covered by the flow rate range used to determine the slope (u).

j) Determine the optimum TFA by rearranging the bit pressure drop equation using pressure loss across the bit optimum ($QP_{\text{b-opt}}$) using Equation (139).

$$TFA = \frac{Q}{C_{\text{d}}}\sqrt{\frac{\rho}{12{,}042 \times P_{\text{b-opt}}}} = 9.113 \times 10^{-3} \times \frac{Q}{C_{\text{d}}}\sqrt{\frac{\rho}{P_{\text{b-opt}}}} \tag{139}$$

where

Q is the flow rate, expressed in gallon per minute;

C_{d} is the jet nozzle discharge coefficient = 0.98;

ρ is the fluid relative density, dimensionless;

$P_{\text{b-opt}}$ is the optimum pressure loss through the bit, expressed in lbf/in.^{2}.

k) Choose the number of nozzles for the given situation and convert optimum TFA into individual nozzle sizes.

l) Calculate P_{p} based on the optimum flow rate Q_{opt} and using the resulting TFA. Adjust the flow rate if P_{p} exceeds P_{p}.

10.3 Reaming While Drilling with Pilot-bit Configuration

10.3.1 General

There are two distinct cases where the hole being drilled is opened to a larger diameter with the same drilling assembly. In these cases, it is necessary to optimize the flow distribution between the two drilling tools to maintain proper hydraulic balance.

10.3.2 Bicenter Bits

Specifications identify both a “pilot-section” diameter and a “reamer-section” diameter, i.e. the objective full hole diameter being drilled. The bit shall rotate concentrically around the pilot section in order to maintain the objective full hole diameter. If the pilot section were allowed to wash out (larger than the pilot diameter), the bit would not be able to drill to full hole diameter. To avoid this problem, the optimized flow distribution, from field experience, is 40 % flow on the pilot section, 60 % flow on the reamer wing. The ratio of the TFAs between the pilot and the reamer sections should be adjusted to this 40 % to 60 % flow ratio.

10.3.3 Underreamers/Ream-while-drilling (RWD) Tools

In most cases, the underreamer or RWD tools are run with a conventional drill bit leading the assembly. In this case, the flow distribution between the pilot and the reamer hole sections should follow the ratio of the areas of the hole diameters being drilled (flow-split ratio = [area of the bit]/[area of the RWD gauge]).

10.4 Bit-nozzle Selection

The bit TFA needs to be divided into individual nozzles following the hydraulics configuration of the bit.

The nozzles sizes for roller cone bits can be determined such that the flow underneath the bit is asymmetric. This is achieved by either blocking a nozzle or by using unequal nozzle diameters.

Modern PDC bits with bladed designs contain one or more nozzles per blade. A symmetrical nozzle arrangement is desirable for optimum cleaning. The available optimized TFA should be divided equally among the number of nozzles required. Following this rule can sacrifice the optimum TFA.

10.5 Pump-off Pressure/Force

Pump-off pressure and force are of interest when using PDC bits with shallow rib designs, impregnated bits and face-set natural diamond bits with shallow water courses. Due to the generally small flow path or junk slot area under the bit, the pump-off force pushing the bit up off-bottom can significantly reduce the effective weight-on-bit. The best practice should be to determine the hydraulic pump-off force (HPO) in a drill-off test or to estimate it using Equation (140).

$$HPO = \frac{0.942}{1000} \times P_{\mathrm{b}} \left(d_{\mathrm{b}} - 1.0 \right) \tag{140}$$

where

HPO is the negative weight on bit, expressed in 1000 lbf;

P_{b} Is the bit nozzle pressure loss, expressed in lbf/in.^{2};

d_{b} is the diameter of the bit, expressed in inches.

11 Rigsite Monitoring

11.1 Introduction

Most drilling hole problems occur when the downhole safe operating pressure limits are exceeded. These limits are defined by the pore, collapse, and fracture pressures. Additional hole problems can occur if the conditions are insufficient to remove the drilled cuttings from the hole. Poor cuttings removal (hole cleaning) often results in excessive reaming times, packing-off, and/or stuck pipe.

Careful monitoring of real-time annular pressure losses can reveal important information about hole cleaning, barite sag, and swab and surge pressures.

11.2 Annular Pressure-loss Measurement

11.2.1 Equivalent Circulating Density

Successful drilling requires the downhole fluid pressure to stay within a tight drilling fluid density window defined by the pressure limits for well control and wellbore integrity [11.1 to 11.6]. The lower pressure limit is either the pore pressure in the formation or the limit for avoiding wellbore collapse (Figure 11). If the drilling fluid pressure is less than the pore pressure, there is a risk of fluid movement from the formation into the wellbore. Fluids and/or gas can move into the well if formations are permeable, which can lead to well control issues. If the formation is impermeable then the trapped formation pressure can cause failure or caving of the rock into

the wellbore causing hole instability problems. If the drilling fluid pressure is higher than the fracture gradient, then loss of fluid into the formation can occur (lost circulation).

The total downhole annular pressure constitutes three components:

a) Static pressure due to the weight of the fluid column as function of its vertical height. This static density includes any entrained solids (such as cuttings) or gas. Commonly referred to as Equivalent Static Density (ESD), it is affected by downhole temperature and pressure.

b) Dynamic pressure caused by the movement of pipe or fluids in the annulus. These include pipe motion (swab, surge, and drill pipe rotation), inertial pressures from the drill string acceleration or deceleration while tripping, excess pressure to break drilling fluid gels, and the cumulative pressure required to move drilling fluids up the annulus. Equivalent dynamic density () is defined as the effective drilling fluid density at a given depth created by the total hydrostatic (including the cuttings pressure) and dynamic pressures (see Section 7).

c) Flow past and hydraulic restrictions, such as cuttings beds or swelling formations, changes in hole geometry, and influxes and effluxes of liquids, gases, and solids all contribute to the dynamic pressure. When the annulus becomes blocked due to excessive cuttings, cavings, or poor hole cleaning, the hole may pack-off, resulting in excessively high or low pressures below the restriction. There may also be occasions when the annulus is shut-in or restricted at surface such as Pressure Integrity Tests (PIT), well control incidents, or managed pressure drilling that can lead to higher or lower pressures than an open system.

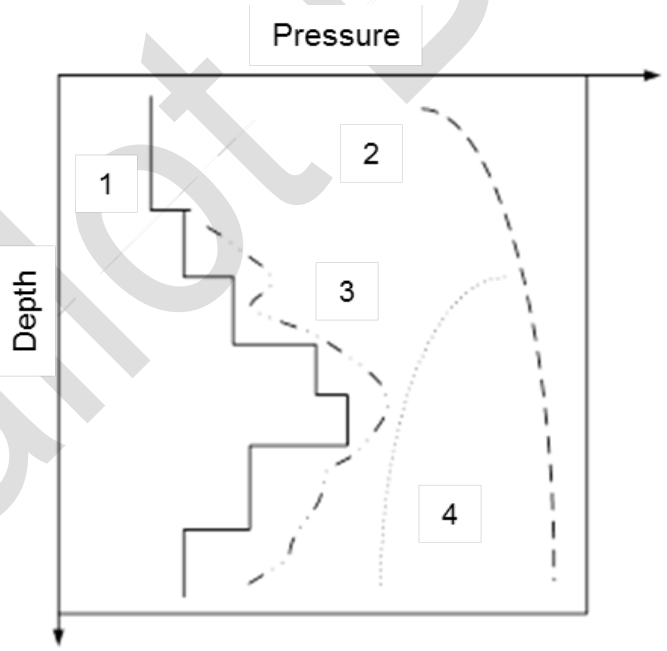

Key

1	Pore pressure	3	Annular pressure
2	Fracture gradient	4	Kick tolerance

Figure 11—Drilling Pressure Window

11.2.2 Pumps-off Measurements

Pressure tools are capable of continuous recording during times of no-flow with data pulsed to surface once flow is resumed. This enables real-time dynamic testing during pumps-off periods, such as during PIT, connections, or well-control incidents.

11.2.3 Data Formats

11.2.3.1 PWD data

There are three modes in which PWD data are recorded and displayed [11.1].

a) *Memory mode* (also known as recorded mode).

In this mode the downhole tool is continually recording data into the tool memory. These data can then be retrieved when the tool is brought back to surface. Recorded-mode data tend to be sampled at a higher frequency than real-time data and as such are richer in detail. Recording gauges are programmable and can store data at one (1) second interval, though typical rates are from 5 to 20 seconds. Some short time scale phenomena could be missed by an incorrect setting of the memory mode recording interval. For example, fast transients due to swab/surge pressures could be missed, or their peak pressure amplitudes distorted. However, faster acquisition rates and long intervals between trips can exceed physical data storage limits.

b) *Real-time mode*.

In this mode, the downhole pressure tool is interfaced with a downhole MWD system. This can be a drilling fluid-pulse, an electromagnetic system, or a hard-wired system to the surface, and the real-time data could be sent to surface every 30 seconds or so. With a drilling fluid-pulse MWD system, the data can only be sent to surface when the pump flow rate is above a certain threshold. Below this flow rate, no information can be sent to surface. There is no such limitation with electromagnetic or hard-wired systems.

c) *Pumps-off mode*.

In this mode, with drilling fluid-pulse MWD systems, recorded-mode data are processed in the downhole tool and a limited amount of information is sent to surface when pump circulation resumes. This mode is of use during connections or PIT. Either a continuous pumps-off recorded pressure or a limited set can be transmitted.

11.2.3.2 Data transmitted to surface

Typical information from the limited set that is processed and transmitted to surface includes:

a) maximum annular pressure (expressed in terms of ECD),

b) minimum annular pressure (expressed in terms of ECD),

c) average annular pressure during connections, and

d) static drilling fluid density, or equilibrated pressure (expressed as the ESD) if all transient fluid motion has ceased during the connection.

11.2.3 Drillers Logs

Typically, there are two distinct display modes for drilling logs—time-based and depth-based. Depth-based logs are more associated with wireline and formation evaluation measurements, where the characterization of the reservoir is important. For real-time drilling information and post-event interpretation of memory mode data, a time-based format is more appropriate.

Pressure data should be presented in the context of other drilling variables for useful data interpretation. For example, an annular pressure trace on its own tells nothing more than the minimum and maximum pressures that occurred during that time or depth interval. Other key measurements that provide contextual information may include:

a) pump flow rate,

b) standpipe pressure,

c) drill string rotation,

d) fluid temperatures in and out,

e) surface and downhole weight on bit,

f) surface and downhole torque,

g) block velocity (ROP),

h) drilling fluid properties (drilling fluid density in and out, rheology, and their temperature and pressure dependence),

i) total gas,

j) cuttings volume rate,

k) pit level, and

l) rig heave.

It is also important that measurements are made in the context of the previous drilling history in the region.

11.2.4 Time-based Log Format

Figure 12 shows a sample data set in a time-based log format, with the pressure-while-drilling measurement placed in the context of other downhole and surface measurements. It is important to note that for real-time applications, the scales for the various parameters should be chosen with care to maximize the visibility of data trends, particularly for the annular pressure (or ECD). For example, if the ESD is 12 lbm/gal (1440 kg/m^3), the ECD is 14 lbm/gal (1680 kg/m^3), and the expected swab/surge pressures are approximately equivalent to ±1 lbm/gal (±120 kg/m^3), then ECD could be plotted on a scale from 11 lbm/gal to 15 lbm/gal (1300 kg/m^3 to 1800 kg/m^3), so that the detailed pressure trace has a high sensitivity and drilling anomalies can be easily visualized.

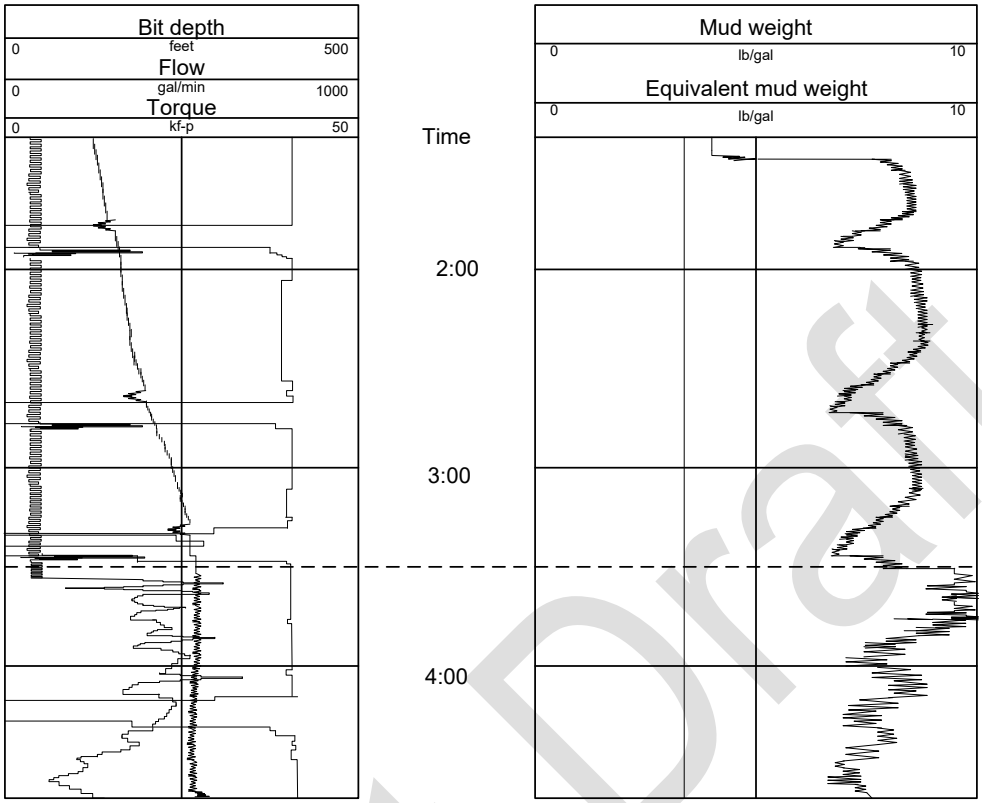

Figure 12—Typical Time-based Log Format

11.2.5 Sensor Calibration

Calibration of pressure sensors should be performed over a range of temperatures using a dead-weight tester. Calibrations can be verified both before and after use at the wellsite via hydraulics tests using a suitable hydraulic hand pump.

11.3 Validation of Hydraulics Models

11.3.1 Principle

The value of real-time downhole pressure measurement sensors lies in their ability to monitor pressures at the sensor location. These measurements can be used to validate predictive hydraulics models and also to refine those models by determining or tuning parameters that are unknown or poorly-defined [11.2]. Downhole pressure measurements can also be used to complement or overcome limitations of hydraulics models, particularly in allowing for the complex and transient distributions of cuttings that can occur along the annulus, the effects of which are difficult to model using conventional steady state models.

11.3.2 Rigsite Calibration

Hydrodynamic responses of pressure sensors are not always directly related to specific drilling parameters or practices. Field procedures should be developed that calibrate sensor response to drilling variables. This can help identify the contribution of control variables and processes on pressure response. For example, this can help identify the contribution of cutting buildup on ECD and help assess the effectiveness of hole cleaning.

For absolute validation of hydraulics models, it is critical to calibrate all rig sensors. This includes pressure gauges, flow meters, density meters, and viscometers. Where direct measurement flow meters are not used, it is important that the discharge characteristics and mechanical efficiencies of the pumps are determined under representative pressure conditions. It is also important that the dimensions of the drill pipe, tool joints and bit nozzles are accurately determined. For example, a 10 % error in nozzle diameter will lead to approximately 40 % error in pressure loss determination.

11.3.3 Drill Pipe Rotation

Another example demonstrates the measured effect of drill pipe rotation on hole cleaning. Figure 13 shows the ECD on the right-hand graph, rotary speed (left-hand trace on middle graph), and a rough approximation of produced cuttings seen at the surface (left-hand trace on the left-hand graph). While sliding, which commenced at approximately 15:00 timestamp, cuttings fall out of suspension, causing a gradual drop in the ECD and a sharp reduction in volume of cuttings at the surface.

At time approximate 19:20, pipe rotation resumes to around 100 r/min, resulting in an instantaneous increase in ECD. This instantaneous pressure increase is presumably related to removal of cuttings from cuttings beds and then being incorporated into the fluid flow stream causing a gradual increase in effective fluid density. This is followed by a sharp increase in the cuttings load at the surface at approximately at 20:35 timestamp as the excess cuttings are moved, and finally followed by a decrease in the ECD to a level similar to before the slide interval.

Once the cuttings are fully mobilized, a pressure maximum is reached, along with a corresponding increase in the volume of cuttings seen at surface after a delay. The pressure then drops back to normal with the corresponding decrease in cuttings seen at the surface.

It is important to recognize that some of the increase in ECD caused by drill pipe rotation can be related to the size of the cuttings bed. In the case of slide drilling, hole cleaning is less efficient, and cuttings tend to accumulate on the low side of the hole. Following long periods of slide drilling, it is recommended to circulate the hole clean while rotating the drill pipe at normal rotary drilling speed.

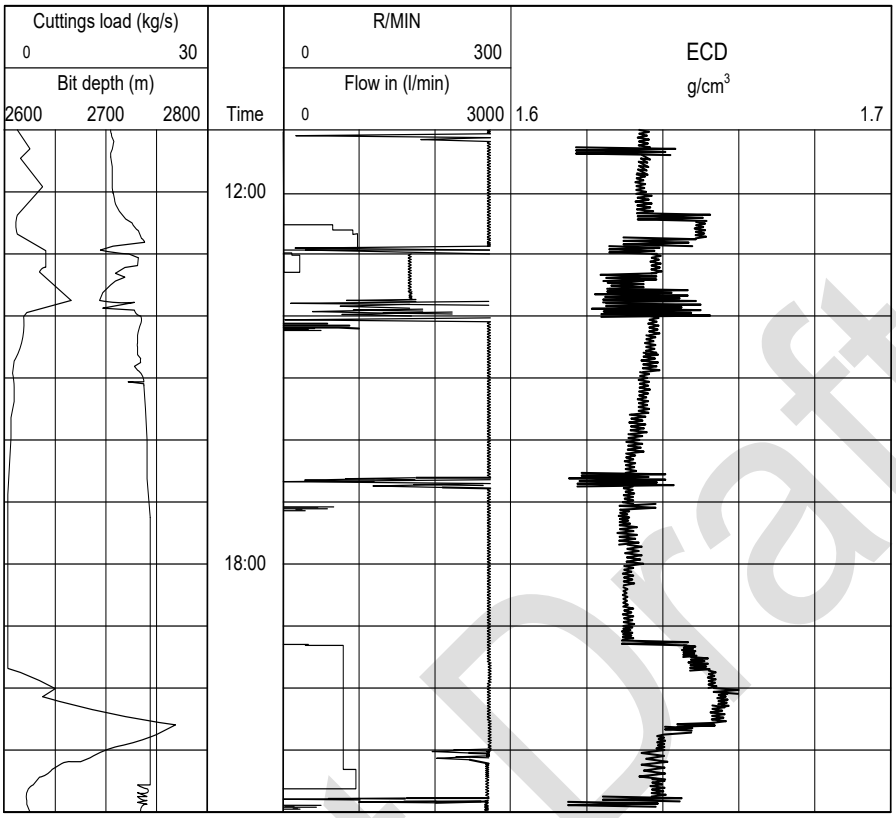

Figure 13—Cuttings Mobilization Example

11.4 Interpretation of Downhole Pressure Measurements

11.4.1 Principle

Downhole annular pressure interpretation is still an evolving technique which may be enhanced through machine learning and pattern recognition. All possible downhole events have probably been recorded but not properly identified due to complexity in operational sequences, while others may be enigmatic. Nonetheless, certain clearly identifiable and repeatable signatures can be used to help diagnose problems. Combining the information gleaned from downhole annular pressure logs with other drilling parameters creates an overall assessment. This global view helps decipher individual measurements used to detect drilling problems downhole.

11.4.2 Interpretation Guide

Table 8 below is an interpretation guide showing common events and their corresponding pressure signals. While not comprehensive, it can be used as a diagnostic reference when drilling parameters are tracked at the rigsite. ECD changes are shown along with confirmation indicators such as those observed via surface measurements.

Table 8—Downhole and Surface Pressure Measurement Interpretation Guide

Event or **Procedure**	***ECD* Change**	**Other Indications**	**Comments**
Drilling fluid gelation/pump startup	Sudden increase possible	Increase in pump pressure	Reduce surge pressures by staging into the well and start pipe rotation before slowly bringing pumps online
Cuttings pick-up	Increase then leveling as steady state reached	Cuttings at surface	Increase may be more pronounced with higher pipe rotation
Restricted annulus	Intermittent pressure increases or sudden spikes	— Standpipe pressure — Torque / rotary speed fluctuations — High over-pulls	Pack-off may "blow-through" before formation breakdown
Cuttings bed formation	Gradual increase	— Lower than expected volume of cuttings at surface — Increased torque and drag — Decreased *ROP*	If near plugging, may get surge pressure spikes
Plugging below sensor	Sudden increase as pack-off passes sensor — none if pack-off remains below sensor	— High over-pulls — "Steady" increase in standpipe pressure	Monitor both standpipe pressure and *ECD*
Gas migration	Increase in *ESD/ESD* when well is shut-in	Shut-in surface pressures increase linearly (approx.)	Take care if estimating gas migration rate
Running in hole	Increase—magnitude dependent on gap, rheological properties, speed, etc.	Monitor trip tank	Effect is enhanced if nozzles plugged
Pulling out of hole	Decrease—magnitude dependent on gap, rheological properties, speed, etc.	Monitor trip tank	Effect is enhanced if nozzles plugged
Making a connection	Decrease to static drilling fluid density	Pumps on/off indicator Pump flow rate lag	Watch for significant changes in static drilling fluid density
Barite sag	Decrease in static drilling fluid density or unexplained density fluctuations	High torque and over-pulls	While sliding periodically or rotating wiper trip to stir up deposited beds, use correct drilling fluid rheological properties
Gas influx	Decreases in typical size hole	Increases in pit level and differential pressure	Initial increase in pit gain may be masked
Liquid influx	Decreases if lighter than drilling fluid Increases if influx accompanied by solids	Evidence of flow at drilling mudline	Plan response if shallow water flow expected

Annex A
(informative)

Worked Example Parameters[1]

A.1 General

This annex provides basic data for an hypothetical well that is used in Annexes B through F to illustrate how equations contained within the document can be applied to hydraulics modeling.

A.2 Well Information

The following information includes key physical parameters of the hypothetical well.

a) Flow rate: Q = 420 gal/min.

b) Drill pipe: L = 21,490 ft; OD = 5 in.; ID = 4.276 in.

c) Drill collars: L = 200 ft; OD = 6 3/4 in.; ID = 3 in.

d) Marine riser: L = 3000 ft; OD = 20 in.; ID = 19 in.

e) Casing: L = 16,690 ft; OD = 9 5/8 in.; ID = 8.535 in.

f) Bit: d_b = 8.5 in.; Nozzles number and size: four 12/32 in.

g) Open hole: L = 2000 ft; d_h = 8 1/2 in.

A.3 Drilling Fluid Information

The following data summarizes key physical and chemical properties of the drilling fluid.

a) Surface density: ρ_s = 12.5 lbm/gal at 65 °F.

b) Fluid properties: Internal olefin synthetic-based fluid; oil content in whole fluid = 63 vol%.

c) Brine properties: 20 wt% $CaCl_2$; water content in whole fluid = 15 vol%.

d) Solids properties: Corrected solids concentration (suspended solids) = 21.1 vol%; ρ_{solids} = 3.615 g/cm^3.

A.4 Wellbore Temperature and Profile

The following information summarizes wellbore temperature and directional well profile.

a) Temperature conditions: T_0 = 65 °F; T_{fL} (static)= 41 °F, (dynamic) = 49 °F; ψ_s = 1.235 °F/100 ft.

[1] *The following examples are merely for illustration purposes only. They are not to be considered exclusive or exhaustive in nature. API makes no warranties, express or implied for reliance on or any omissions from the information contained in this document.*

b) Wellbore profile: tangent angle of 60°, see Figure A.1.

c) Wellbore profile schematic.

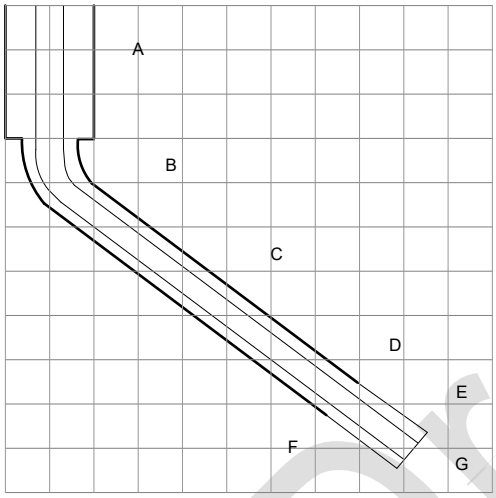

Key

A riser with 19 in. ID
B water depth = 3000 ft
C tangent angle = 60°
D 21,490 ft of 5-in. drill pipes (ID = 4.276 in.) and 200 ft of $6^{3}/_{4}$-in. drill collars (ID = 3.0 in.)
E 2000 ft of $8^{1}/_{2}$ in. open hole
F $9^{5}/_{8}$ in. casing @ 19,690 ft measured depth (MD) (11,595 ft TVD)
G $8^{1}/_{2}$ in. TD = 21,690 ft MD (12,595 ft TVD)

Figure A.1—Wellbore Profile Schematic

Annex B
(informative)

Downhole-properties Example[2]

B.1 General

This annex uses well, and selected drilling fluid information provided in Annex A to model downhole drilling fluid properties.

B.2 Downhole Density Modeling

Table B.1 contains the six hydraulic (geometric) sections of the hypothetical well. Static and dynamic drilling fluid temperatures added in the last two columns for each section are calculated using equations provided in 6.2. Table B.2 further subdivides the well into 500-ft, true-vertical increments and fills in static and dynamic fluid temperature information. Equations and procedures from 6.4 and 7.4 are used to compute the applied pressure and drilling fluid density under static and dynamic conditions for each cell.

Table B.1—Hydraulic Data by Section

	MD ft	**TVD** ft	**Casing/Hole Diameter** d_h in.	**Pipe OD** d_p in.	**Length** L ft	**Static Temperature** T_{bhs} °F	**Dynamic Temperature** T_{bhc} °F
Surf.	0	0	19.000	5.000	0	65.0	55
1	3000	3000	19.000	5.000	3000	41.0	49
2	3500	3500	8.535	5.000	500	47.2	51
3	11,600	7550	8.535	5.000	8100	97.2	84
4	19,690	11,595	8.535	5.000	8090	147.1	112
5	21,490	12,495	8.5	5.000	1800	158.3	117
6	21,690	12,595	8.5	6.750	200	159.5	117.5

[2] *The following examples are merely for illustration purposes only. They are not to be considered exclusive or exhaustive in nature. API makes no warranties, express or implied for reliance on or any omissions from the information contained in this document.*

Table B.2—Downhole Equivalent Density Calculations Under Static and Dynamic Conditions

MD ft	**TVD** ft	**Static Temperature** T_{bhs} °F	**Applied Static Pressure** P_a lbf/in.²	ESD_a Static Conditions lbm/gal	**Dynamic Temperature** T_{bhc} °F	**Applied Dynamic Pressure** P_{dca} lbf/in.²	***EDD*** *ECD* Dynamic Conditions lbm/gal
0	0	65	0	12.50	55	0	12.54
500	500	61	325	12.50	54	326	12.54
1000	1000	57	650	12.51	53	652	12.55
1500	1500	53	976	12.53	52	978	12.55
2000	2000	49	1303	12.54	51	1305	12.56
2500	2500	45	1631	12.56	50	1633	12.57
3000	3000	41	1959	12.57	49	1960	12.58
3500	3500	47	2288	12.58	51	2289	12.59
3690	3595	48	2350	12.59	52	2351	12.59
4690	4095	55	2679	12.59	54	2679	12.60
5690	4595	61	3008	12.60	57	3008	12.60
6690	5095	67	3336	12.60	63	3337	12.61
7690	5595	73	3664	12.61	68	3665	12.61
8690	6095	79	3992	12.61	72	3993	12.61
9690	6595	85	4320	12.61	76	4322	12.61
10,690	7095	92	4647	12.61	80	4650	12.62
11,600	7550	97	4945	12.61	84	4949	12.62
12,690	8095	104	5301	12.61	88	5306	12.62
13,690	8595	110	5628	12.61	92	5635	12.62
14,690	9095	116	5955	12.60	96	5963	12.62
15,690	9595	122	6282	12.60	100	6291	12.62
16,690	10,095	129	6608	12.60	104	6620	12.62
17,690	10,595	135	6934	12.60	107	6948	12.62
18,690	11,095	141	7260	12.60	109	7276	12.62
19,690	11,595	147	7586	12.59	112	7605	12.63
20,690	12,095	153	7912	12.59	115	7933	12.63
21,490	12,495	158	8172	12.59	117	8196	12.63
21,690	12,595	159	8237	12.59	117.5	8262	12.63

B.3 Modeling of Downhole Rheological Properties

B.3.1 General

Modeling drilling fluid rheological properties under downhole conditions requires measurements taken at the surface using low-temperature/low-pressure and HTHP viscometers as described in 5.1.3. Table B.3 provides representative fluid temperatures and pressures for each of the six hydraulic sections. These values were used as the test matrix in an HTHP viscometer, the results of which are given in Table B.4. Tables B.5, B.6, and B.7 include calculated rheological parameters using the H-B model (numerical and measurement methods) and Bingham plastic model described respectively in 5.2.3 and 5.2.5.

B.3.2 HTHP Viscometer Test Matrix

Table B.3—Test Matrix for HTHP Viscometer Data

Test #	Temperature °F	Pressure lbf/in.^{2}
1	61	975
2	69	2350
3	78	3970
4	94	6520
5	107	8120
6	114	8440

B.3.3 Results for Different Rheological Models

Table B.4—Example of HTHP Couette-type Viscometer Results

	Well Hydraulic Sections						
Viscometer Reading	**Surface**	**1**	**2**	**3**	**4**	**5**	**6**
R_{600}	63	80	102	105	117	119	124
R_{300}	38	48	63	65	70	74	79
R_{200}	28	35	47	48	51	55	60
R_{100}	18	23	30	30	33	36	39
R_6	8	9.2	10	11	12	13	14
R_3	7	8.2	9	10	11	12	13

NOTE Improved modeling accuracy can be achieved by also measuring the viscometer readings R_{60} and R_{30} at rotational speeds of 60 r/min and 30 r/min for more accurate determination of rheological model coefficients.

Table B.5—Herschel–Bulkley Parameters (Numerical Method)

Well Hydraulic Section								
Parameter	**Units**	**Surface**	**1**	**2**	**3**	**4**	**5**	**6**
n	—	0.845	0.840	0.765	0.77	0.831	0.768	0.726
k	lbf•s^n/100 ft^2	0.162	0.215	0.472	0.467	0.339	0.534	0.742
τ_y	lbf/100 ft^2	7.0	8.0	7.7	8.8	10.3	10.6	10.9

Table B.6—Herschel–Bulkley Parameters (Measurement Method)

Well Hydraulic Section								
Parameter	**Units**	**Surface**	**1**	**2**	**3**	**4**	**5**	**6**
n	—	0.833	0.84	0.773	0.778	0.835	0.778	0.741
k	lbf• s^n/100 ft^2	0.178	0.223	0.443	0.439	0.329	0.493	0.658
τ_y	lbf/100 ft^2	6.4	7.2	8.5	9.6	10.7	11.7	12.8

Table B.7—Bingham Plastic Parameters

Well Hydraulic Section								
Parameter	**Units**	**Surface**	**1**	**2**	**3**	**4**	**5**	**6**
η_{PV}	cP	25	32	39	40	47	45	45
Y_P	lbf/100 ft^2	13	16	24	25	23	29	34

Annex C
(informative)

Pressure-loss Example[3]

C.1 General

This annex illustrates how a spreadsheet can be used to integrate well parameters (provided in Annex A) and downhole fluid properties (provided in Annex B) into pressure-loss calculations in the drill string and annulus. Calculated annular ECD values also are included.

C.2 Input Parameters

The following hydraulics-related parameters represent additional information required to calculate pressure losses in the drill string and annulus of the hypothetical well.

a) Flow rate: Q = 420 gal/min.

b) Surface drilling fluid density: ρ_s = 12.5 lbm/gal.

c) Drill pipe eccentricity: e = 0 (concentric).

d) Surface connection pressure loss: Case 1, C_{sc}= 1 (see Table 5)

[3] *The following examples are merely for illustration purposes only. They are not to be considered exclusive or exhaustive in nature. API makes no warranties, express or implied for reliance on or any omissions from the information contained in this document.*

C.3 Pressure Loss in Drill String

Table C.1 presents the well and drilling fluid parameters used to calculate frictional pressure losses in the drill string for a flow rate of 420 gal/min. Equations for determining the friction factors are given in 7.4.

Table C.1—Spreadsheet Data of Pressure Loss in Drill String

												Drill String			
MD	**TVD**	**Hole/ Casing Diameter** d_h	**Pipe OD** d_p	**Pipe ID** d_i	**Drilling fluid density** ρ	**Hydro Pressure Complex Wells**	**Surface Conn.** P_{cs}	R_{600}	R_{300}	R_6	R_3	**Velocity** V_{ds}	**Fanning Friction Factor** f	**Pressure Loss**	
ft	ft	In.	In.	In.	lbm/gal	lbf/in²	lbf/in²	°	°	°	°	ft/min	-	Cell lbf/in.²	Sum lbf/in.²
0	0	19.000	5.000	4.276	12.54	**0**	**181**	80	48	9	8	563	0.00718		**0**
3000	3000	19.000	5.000	4.276	12.54	**1956**		80	48	9	8	563	0.00718	216	**216**
3500	3500	8.535	5.000	4.276	12.64	**2285**		102	63	10	9	563	0.00743	37	**253**
11,600	7550	8.535	5.000	4.276	12.64	**4947**		105	65	11	10	563	0.00750	612	**865**
19,690	11,595	8.535	5.000	4.276	12.64	**7606**		117	70	12	11	563	0.00793	647	**1512**
21,490	12,495	8.500	5.000	4.276	12.67	**8199**		119	74	13	12	563	0.00771	140	**1652**
21,690	12,595	8.500	6.750	3.000	12.69	**8265**		124	79	14	13	1144	0.00614	73	**1725**
						8265	**181**								**1725**
						P_{hd}	P_{sc}								P_{ds}

C.4 Pressure Loss in Annulus

Pressure-loss and ECD calculations for the sample well annulus at a flow rate of 420 gal/min are illustrated in Table C.2. Consistent with Table C.1, the data are presented for each hydraulic (geometric) section. The main objective of the calculations in this table is the range of ECD values shown in the last column on the right.

Table C.2—Spreadsheet Data of Pressure Loss in Annulus

												Annulus				
MD	**TVD**	**Hole/ Casing Diame-ter** d_h	**Pipe OD** d_p	**Pipe ID** d_i	**Drilling fluid density** ρ	**Hydro Pressure Complex Wells w/o cut**	**Surface Conn.**	R_{600}	R_{300}	R_6	R_3	**Velocity** V_a	**Fanning Friction Factor** f	**Pressure Loss**		ECD_a
ft	ft	In.	In.	In.	lbm/gal	lbf/in²	lbf/in²	°	°	°	°	ft/min	-	Cell lbf/in.²	Sum lbf/in.²	lbm/gal
0	0	19.000	5.000	4.276	12.54	**0**	**181**	80	48	9	8	31	0.30956		**0**	**12.54**
3000	3000	19.000	5.000	4.276	12.54	**1956**		80	48	9	8	31	0.30956	8	**8**	**12.59**
3500	3500	8.535	5.000	4.276	12.64	**2285**		102	63	10	9	215	0.01860	17	**25**	**12.69**
11,600	7550	8.535	5.000	4.276	12.64	**4947**		105	65	11	10	215	0.01952	282	**307**	**13.38**
19,690	11,595	8.535	5.000	4.276	12.64	**7606**		117	70	12	11	215	0.02027	292	**599**	**13.61**
21,490	12,495	8.500	5.000	4.276	12.67	**8199**		119	74	13	12	218	0.02225	74	**673**	**13.65**
21,690	12,595	8.500	6.750	3.000	12.69	**8265**		124	79	14	13	386	0.01557	36	**709**	**13.70**
						8265	**181**								**709**	
						P_{ha}	P_{sc}								P_a	

C.5 Pressure Loss vs Flow Rate

Use of a spreadsheet permits quick evaluation of circulating pressure losses at various flow rates. Table C.3 includes results for flow rates from 300 gal/min to 500 gal/min.

Table C.3—Data for Pressure Losses vs Flow Rate

Flow Rate gal/min	**Pressure Loss in Drill String** lbf/in.^{2}	**Pressure Loss in Annulus** lbf/in.^{2}
300	889	604
350	1259	648
400	1592	692
420	1725	709
450	1930	734
500	2289	775

Annex D
(informative)

Swab/Surge-pressures Example[4]

D.1 General

Included in this annex are swab and surge calculations during tripping using well data provided in Annex A. Closed-string and open-string cases for the hypothetical well are considered. Calculations should be done based on Equations provided in 8.4.

D.2 Input Parameters

The following data are required to calculate swab and surge pressures for the hypothetical well.

a) Operation: Tripping in hole.

b) Tripping speed: V_{ds} 60 ft/min.

c) Stand length: 93 ft.

d) Bit depth: 19,690 ft MD; 12,595 ft TVD.

e) Drilling fluid clinging factor: C_g 0.45.

D.3 Closed-string Case

Assuming the string is closed while tripping in, all fluid will be displaced in the annulus. The effects of acceleration and deceleration are ignored. With the bit close to TD @21,690 ft, the annulus consists of six sections as shown in Table D.1. For each section the effective velocity including the constant clinging factor of 0.45 and the pressure loss need to be calculated.

Table D.1—Closed-string Example

Hole ID in.	Pipe OD in.	Length ft	Eff. Velocity ft/min	Pressure Loss lbf/in.²	Inertial Surge Pressure lbf/in.²	Total Pressure Loss lbf/in.²
19.000	5.000	3000	31.5	5.9	4.2	10.1
8.535	5.000	500	58.4	5.5	4.9	10.4
8.535	5.000	8100	58.4	89.3	78.9	168.1
8.535	5.000	8090	58.4	89.2	78.8	167.9
8.500	5.000	1800	58.7	20.1	17.7	37.9
8.500	6.750	200	129.4	8.4	6.4	14.8

[4] *The following examples are merely for illustration purposes only. They are not to be considered exclusive or exhaustive in nature. API makes no warranties, express or implied for reliance on or any omissions from the information contained in this document.*

Total pressure loss is 409.2 lbf/in.^{2}. Together with the hydrostatic pressure at the casing shoe the pressure while tripping is 8673 lbf/in.^{2}. This calculates as EMW = 13.26 lbm/gal at a drilling fluid density of 12.54 lbm/gal at the surface.

D.4 Open-string Case

When the bit is open to flow, the flow split between the string and the annulus needs to be calculated such that the pressure loss is identical in both conduits. This requires iterative procedures.

The annular sections remain the same as before. Table D.2 demonstrates that the string has two different inside diameters and the bit TFA comes into play. Application of the iterative process required for the open-string case (described in 8.4) is illustrated in Table D.3.

Table D.2—Open-string Example

Segment	Annulus						Drill String					
L, ft	3000	500	8100	8090	1800	200	3000	500	8100	8090	1800	200
d_h, in.	19.000	8.535	8.535	8.535	8.500	8.500	19.000	8.535	8.535	8.535	8.500	8.500
d_p, in.	5.000	5.000	5.000	5.000	5.000	6.750	5.000	5.000	5.000	5.000	5.000	6.750
d_i, in.	4.276	4.276	4.276	4.276	4.276	3.000	4.276	4.276	4.276	4.276	4.276	3.000

Table D.3—Iterative Process for the Open-string Example

First Guess	**50% Flow in Annulus and 50% Flow in the String**											
Flow Split	0.5						0.5					
V_{eff}, ft/min	46.0	52.0	52.0	52.0	52.1	113.5	118.4	118.4	118.4	118.4	118.4	303.1
$P_{\text{ss,as}}$, lbf/in.²	7.2	6.3	101.7	101.5	22.9	11.7	32.6	5.4	88.1	88.0	19.6	6.0
Total Loss, lbf/in.²	251.2						239.7					
Delta, lbf/in.²	11.5											
Second Guess	**30% Flow in Annulus and 70% Flow in the String**											
Flow Split	0.3						0.7					
V_{eff}, ft/min	45.6	49.2	49.2	49.2	49.3	86.1	125.7	125.7	125.7	125.7	125.7	384.4
$P_{\text{ss,as}}$, lbf/in.²	7.2	6.2	100.3	100.2	22.6	10.6	33.4	5.6	90.2	90.1	20.0	10.3
Total Loss, lbf/in.²	247.2						249.6					
Delta, lbf/in.²	-2.5											
Final Guess	**33.2% Flow in Annulus and 66.8% Flow in the String**											
Flow Split	0.332						0.668					
V_{eff}, ft/min	45.7	49.7	49.7	49.7	49.7	90.5	124.5	124.5	124.5	124.5	124.5	371.4
$P_{\text{ss,as}}$, lbf/in.²	7.2	6.2	100.6	100.4	22.6	10.8	33.3	5.5	89.9	89.8	20.0	9.4
Total Loss, lbf/in.²	247.8						247.8					
Delta, lbf/in.²	0.0											

Total pressure loss is 247.8 lbf/in.^{2}. Together with the hydrostatic pressure at the casing shoe, the pressure while tripping is 8512 lbf/in.^{2}. This results in an EMW of 13.01 lbm/gal at a drilling fluid density of 12.54 lbm/gal at the surface.

Annex E
(informative)

Hole-cleaning Example[5]

E.1 General

This annex illustrates how hole-cleaning performance for the well described in Annex A can be quantified using different models.

E.2 Input Parameters

The following information is used to estimate hole-cleaning effectiveness using method 2 from 9.4.2 (for a marine riser and vertical casing) and charts provided in 9.5 for directional wells.

Rheological properties: η_{PV} = 25 cP; Y_{P} = 13 lbf/100 ft^2.

Drilling fluid density: ρ_{s} = 12.5 lbm/gal.

Drilling rate: ROP = 60 ft/h.

Flow rate: Q = 420 gal/min.

Tangent angle = 60°.

E.3 Hole Cleaning in Marine Riser (Model 2)

In riser section, at 420 gal/min, annular velocity (V_{a}) is 30.6 ft/min. Hole cleaning is evaluated through the CCI (see 9.4.2) calculated using Equation (121), (see 9.4.2.1).

$$CCI = \frac{\rho k_1 V_{\mathrm{a}}}{400{,}000} = 0.20 \tag{E.1}$$

where

k_1 = 206 cP; [Equation (122]

V_{a} = 30.6 ft/min.

The ideal CCI value for good hole cleaning is >1. In practice, the hole cleaning in the marine riser can be improved by additional flow rate from a riser booster pump together with increasing the Y_{P} of the drilling fluid. Increasing Y_{P} increases the k_1 factor and hence increases the value of CCI. Note that k_1 is defined in viscosity units in Equation (E.1).

[5] *The following examples are merely for illustration purposes only. They are not to be considered exclusive or exhaustive in nature. API makes no warranties, express or implied for reliance on or any omissions from the information contained in this document.*

E.4 Hole Cleaning in Vertical Casing (Model 2)

Below the marine riser, inside $9^5/_8$-in. casing at 420 gal/min annular velocity is 215 ft/min, CCI is calculated using Equation (E.2)

$$CCI = \frac{\rho k_1 V_a}{400{,}000} = 0.20 \tag{E.2}$$

where

k_1 = 206 cP; [see Equation (125)]

V_a = 215 ft/min.

The CCI value of 1.38 suggests adequate hole cleaning in the vertical casing below the marine riser.

E.5 Hole Cleaning in Directional Open-hole Section

The graphical procedure (see 9.5) is used to estimate hole-cleaning efficiency for the directional interval of the hypothetical well.

a) Enter the RF chart (Figure E.1) with the appropriate values of η_{PV} and Y_P values at 120 °F and atmospheric pressure. Read the value of the Rheology factor (RF=1.0).

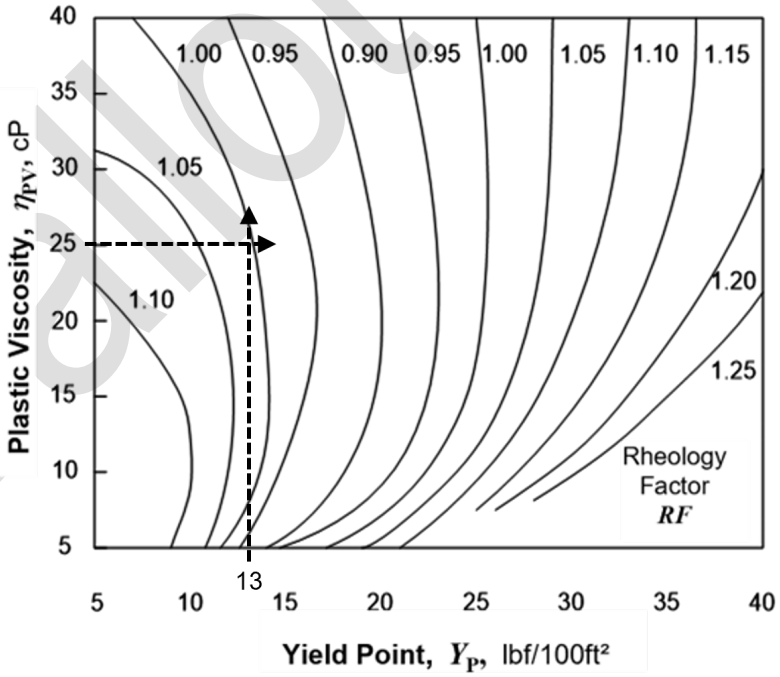

Figure E.1—Rheology Factor Chart for $8^1/_2$-in. Holes

b) Calculate the TI based on the drilling fluid flow rate and drilling fluid density given by Equation (E.3):

$$TI = \frac{Q\rho RF}{834.5} = 6.3 \qquad \text{(E.3)}$$

c) Enter the maximum ROP chart (Figure E.2). With the value of TI calculated at 6.3 and the maximum hole angle, read the maximum ROP (ROP ≥ 30 m/h [100 ft/h]) that can be sustained while still maintaining adequate hole cleaning.

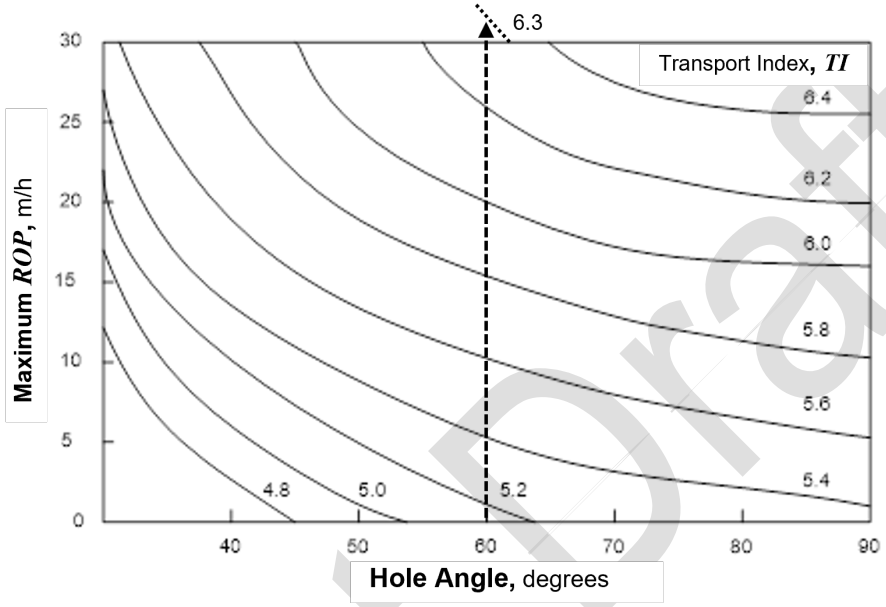

NOTE To convert Maximum ROP in ft/h, divide m/h by 0.3048.

Figure E.2—Hole-cleaning Chart for 8½-in. Holes

The drilling rate of 60 ft/h is below this maximum value (32 m/h = 102 ft/h); hence, hole cleaning should be adequate.

Annex F
(informative)

Hydraulics-optimization Example[6]

F.1 General

This annex presents example calculations to optimize bit hydraulics (see Section 10) using different criteria for the well data provided in Annex A.

F.2 Input Parameters

The rig is pumping 450 gal/min at a standpipe pressure of 5000 lbf/in.^{2} through four $^{12}/_{32}$-in. nozzles.

While drilling with four $^{12}/_{32}$-in. nozzles in an $8^{1}/_{2}$-in. PDC bit, a new 537 drill bit is programmed to drill the last 1000 ft of hole. The standpipe pressure is measured at several pump stroke rates while circulating bottoms-up before tripping out of the hole. The data are presented in Table F.1.

Table F.1—Rig Data for Flow Rate and Standpipe Pressure

Flow Rate gal/min	**Standpipe Pressure** lbf/in.^{2}
450	5000
422	4465
388	3852
342	3086
300	2451
287	2268

Pressure losses through the drill bit [see 7.5.1 Equation (100)] calculated using Equation (F.1) are presented in Table F.2:

$$P_{\mathrm{b}} = \frac{\rho_{\mathrm{b}} Q^2}{12{,}042\, C_{\mathrm{d}}^2\, TFA^2} \tag{F.1}$$

The TFA of four $^{12}/_{32}$-in. nozzles is 0.4418 in.^{2}, and drilling fluid density is 12.5 lbm/gal.

Pressure loss through the drill bit P_{b} is calculated for each flow rate and subtracted from the standpipe pressure. The results represent the SPP losses P_{x} through the system excluding the bit (see Table F.2).

[6] *The following examples are merely for illustration purposes only. They are not to be considered exclusive or exhaustive in nature. API makes no warranties, express or implied for reliance on or any omissions from the information contained in this document.*

Table F.2—Calculated System Parasitic Pressure Loss

Flow Rate Q galmin	Standpipe Pressure P_p lbf/in.²	Calculated	
		Bit Loss P_b lbf/in.²	Parasitic Loss P_x lbf/in.²
450	5000	1121	3879
422	4465	986	3479
388	3852	834	3018
342	3086	648	2438
300	2451	498	1953
287	2268	456	1812

The boundary condition imposed by the drilling fluid pumps is plotted on a log-log plot as pressure vs flow rate in Figure F.1. The drilling fluid pump is powered by a 2700 hp motor. Assuming an 85 % mechanical efficiency and a 90 % volumetric efficiency, 2066 hp can be delivered to circulate the drilling fluid. The maximum standpipe pressure is 5000 lbf/in.^{2}, so the flow rate (Q_{crit}) where the maximum pressure is delivered at the available horsepower is 706 gal/min. These lines also are shown in Figure F.1.

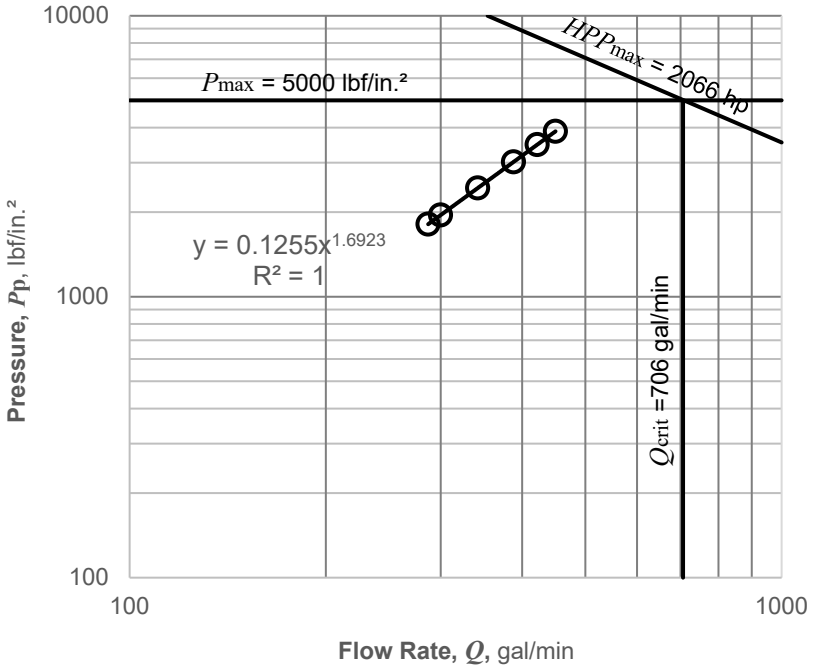

Figure F.1—Wellsite Nozzle Test

The slope of the P_x line is determined using a power curve fit in a spreadsheet. In this case, the slope u = 1.6923 and K_x = 0.1255. The limiting condition for this case is the maximum available pump pressure.

F.3 Optimization Methods

F.3.1 Maximum Hydraulic Impact Force Method

The optimum bit pressure loss for maximum hydraulic impact force is calculated using Equation (F.2):

$$P_{\text{b-opt}} = \left(\frac{u}{u+2}\right) P_{\max} = \frac{1.6923}{3.6923} \times 5000 = 2292 \text{ lbf / in.}^2 \quad \text{(F.2)}$$

The resulting parasitic pressure loss in the system, P_x, is 5000 – 2292 = 2708 lbf/in.^{2}. As shown in Figure F.2 on the graph, the intersection of the 2708 lbf/in.^{2} line and the parasitic pressure loss line indicates that the new optimum flow rate should be 364 gal/min as shown by the graph Figure F.2.

From the equation for pressure loss through bit nozzles, the TFA of 0.2499 in.^{2} can be created by two $^{13}/_{32}$-in. nozzles. They actually have an area of 0.2592 in.^{2}. A two-nozzle combination of a $^{12}/_{32}$-in. nozzle and a $^{13}/_{32}$-in. nozzle has a TFA of 0.2401 in.^{2}.

For maximum hydraulic impact force, the next bit is dressed with two nozzles, a $^{12}/_{32}$-in. and a $^{13}/_{32}$-in. nozzle. The new nozzle velocity is 486 ft/s, compared to the previous 327 ft/s. Maximum nozzle shear rate should be in the range of 124,457 s^{-1}, which could result in hole erosion. Shear rate should be less than 100,000 s^{-1} to decrease the possibility of erosion.

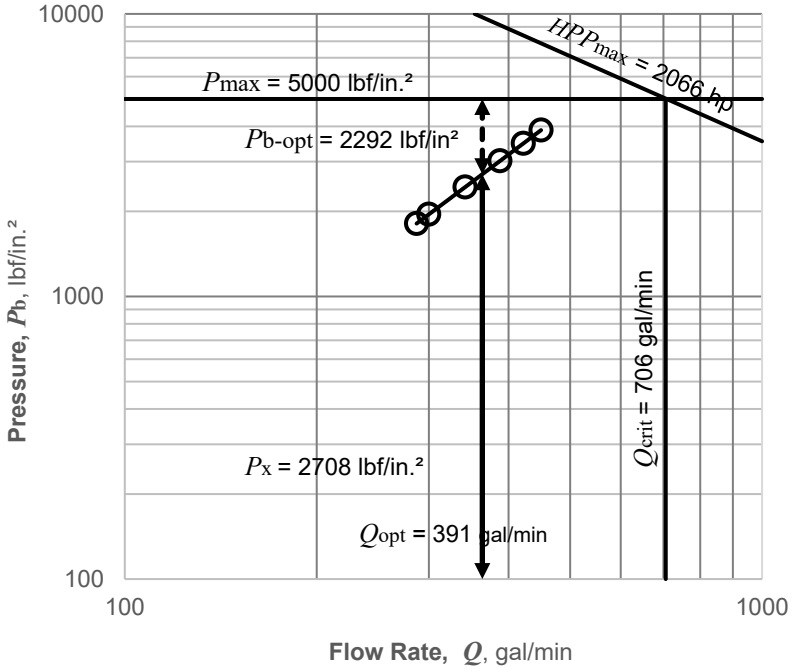

Figure F.2—On-site Nozzle Test for Maximum Hydraulic Impact Force

F.3.2 Maximum Hydraulic Power Method

If the preferred optimization criterion is to maximize hydraulic power at the drill bit, the optimum pressure loss across the nozzles ($P_{\text{b-opt}}$) can be calculated using Equation (F.3):

$$P_{\text{b-opt}} = \left(\frac{u}{u+1}\right) P_{\max} = \frac{1.7}{2.7} \times 5000 = 3143 \text{ lbf / in.}^2 \quad \text{(F.3)}$$

Pressure loss through the remainder of the circulating system is then 5000 lbf/in.^{2} – 3143 lbf/in.^{2} =1857 lbf/in.^{2}.

The circulating pressure loss through the system excluding the bit would intersect the optimum pressure at a value of 291 gal/min. The nozzles could then be selected to provide a pressure loss through the nozzles of 3143 lbf/in.^{2} at a flow rate of 291 gal/min as expressed by Equation (F.4):

$$P_{\text{b-opt}} = \frac{12.5 \times (291)^2}{12{,}042 \times (0.98)^2 \left(TFA\right)^2} = 3143 \text{ lbf / in.}^2 \quad \text{(F.4)}$$

From Equation (F.4), TFA can be calculated using Equation (F.5):

$$TFA = = \frac{291}{0.98} \times \sqrt{\frac{12.5}{12{,}042 \times 3143}} = 0.1707 \text{ in.}^2 \quad \text{(F.5)}$$

From the equation for converting nozzle size to TFA, the TFA of 0.1707 in.^{2} can be created by two nozzles, a $^{10}/_{32}$-in. and a $^{11}/_{32}$-in. nozzle. They actually have an area of 0.1695 in.^{2}.

For maximum hydraulic impact force, the next bit is dressed with two nozzles, a $^{10}/_{32}$-in. and a $^{11}/_{32}$-in. nozzle. The new nozzle velocity is 551 ft/s, compared to the previous 327 ft/s. Maximum nozzle shear rate should be in the range of 141,042 s^{-1}, which could result in hole erosion. Shear rate should be less than 100,000 s^{-1} to decrease the possibility of erosion.

F.4 Comparison of Optimization Methods

A comparison of the impact forces for the three cases (see Table F.3) indicates that the hydraulic impact forces should be 950 lbf, 1144 lbf, and 1037 lbf, in the order presented above. The impact force for the four-nozzle bit is 950 lbf. The Impact Force optimization procedure indicates a force of 1144 lbf would be applied to the bottom of the hole, while a force of 1037 lbf would be applied using the hydraulic power optimization procedure.

A comparison of hydraulic power losses through the nozzles for the three cases indicates that the hydraulic power is 294 hp, 527 hp, and 542 hp, in the order presented above. The hydraulic power for the four-nozzle bit is 294 hp. The Impact Force optimization procedure results in 527 hp being expended through the nozzles, while the hydraulic power optimization procedure results in 542 hp being applied through the nozzles.

Table F.3—Impact Force Methods Comparison

Standpipe Pressure lbf/in.^{2}	**Flow Rate** gal/min	**Nozzle Velocity** ft/s	**Impact Force** lbf	**Hydraulic Power @Bit** hp	**Nozzle Shear Rate** 10^6 s^{-1}	V_a **in Riser** ft/min
5000	450	327	950	294	0.84	33
5000	364	486	1144	527	1.24	26
5000	291	551	1037	542	1.41	21

Bibliography

Text Books

[1] A.T Bourgoyne, M. Chenevert, K.Milheim and F.S. Young, *Applied Drilling Engineering*, SPE Texbook Series Volume 2, SPE Richardson, Texas, July 2014.

[2] H.C.H. Darley, G.R. Gray, and R.Caenn *Composition and Properties of Oil Well Drilling Fluids,* Gulf Professional Publishing., Houston, Texas, Seventh Edition, 2017, pp. 151-254.

[3] P.L. Moore, *Drilling Practices Manual*, PennWell Books, Second Edition, 1986.

Rheological Models (Section 5)

[5.1] A.H.P Skelland, *Non-Newtonian Flow and Heat Transfer*, John Wiley & Sons, New York, 1967.

[5.2] G.W. Govier and K. Aziz, *The Flow of Complex Mixtures in Pipes*, Litton Education Publishing, New York, 1972.

[5.3] M. Zamora. and D. Power, *Making a case for AADE hydraulics and the unified rheological model*, AADE-02-DFWH-HO-13, AADE Technology Conference, Houston, Texas, April 2002.

[5.4] J.G Savins and W.F Roper, *A direct-indicating viscometer for drilling fluids*, API Drilling and Production Practices, API, 1954, pp. 7–22.

[5.5] API Recommended Practice 13D, *Rheology and Hydraulics of Oil-well Drilling Fluids*, 4th Edition, MAY 2003.

[5.6] T. Hemphill, A. Pileharvi and W. Campos, *Yield-power law model more accurately predicts drilling fluid rheology*, Oil & Gas Journal, August 23, 1993, pp. 45–50.

[5.7] W. Campos, G.S. Ribeiro and E.M. Brandão, *Exact determination of the three parameters of a Herschel-Bulkley Fluid*, XV Brazilian Congress of Mechanical Engineering, São Paulo, Brazil , November 1999.

[5.8] J.A. Klotz and W.E. Brigham, *To determine Herschel–Bulkley coefficients*, SPE 52527, Journal of Petroleum Technology, November 1998, pp. 80–81.

[5.9] T.MT. Yang and I.M. Krieger, "*Comparison of methods for calculating shear rates in coaxial Viscometers*", Journal of Rheology 22, August 1978, pp. 413-421.

Downhole Fluid Behavior (Section 6)

[6.1] I.M. Kutasov and A. Targhi, *Better deep-hole BHCT estimations possible* Oil & Gas Journal, May 25, 1987, pp.71.

[6.2] I.M. Kutasov, *Method corrects API borehole circulating-temperature correlations*, Oil & Gas Journal, July 15, 2002, pp. 47–51.

[6.3] R.F. Mitchell and S.Z. Miska, *Fundamentals of Drilling Engineering* , SPE Textbook Series Volume 12, Chapter 5 Drilling Hydraulics, SPR Richardson, Texas, January 2010.

[6.4] L.L. Hoberock, O.C. Thomas and H.V. Nickens, *Here's how compressibility and temperature affect bottom-hole mud pressure,* Oil & Gas Journal 80, March 22, 1982, pp.159-164.

[6.5] P. Isambourg, B. Anfinsen and C. Marken, *Volumetric behavior of drilling fluids at high pressure and high temperature*, SPE 36830, SPE European Petroleum Conference, Milan, Italy, October 1986, pp. 22–24.

[6.6] E. Peters, M. Chenevert and C. Zhang,. *A model for predicting the density of oil-based mudsat high pressures and temperatures*, SPE 18036, SPE Drilling Engineering, 5(02), June 1990, pp. 141–148.

[6.7] W. Foxenberg, M. Zamora, K.Slater and J. Trancoso , *Experimental study improves prediction of PVT behavior of completion brines*, SPE 170281, SPE Deepwater Drilling and Completion Conference, Galveston, Texas, September 2014.

[6.8] M. Zamora, F. Enriquez, S. Roy and M. Freeman, *Measuring PVT characteristics of base oils, brines, and drilling fluids under extreme temperatures and pressures*, AADE-12-FTCE-44, AADE Fluids Technology Conference and Exhibition, Houston, Texas, April 2012.

[6.9] M. Zamora, S. Roy, K. Slater and J. Troncoso, *Study on the volumetric behavior of base oils, brines, and drilling fluids under extreme temperatures and pressures*, SPE 160029, SPE Drilling and Completion 28(03), August 2013, pp. 278–288.

[6.10] M. Zamora, S. Roy and K. Slater, *Issues with the density and rheology of drilling fluids exposed to extreme temperatures and pressures*, OMAE2013-11428, ASME 32nd International Conference on Ocean, Offshore and Artic Engineering, Nantes, France, June 2013.

[6.11] R. Sorell, R. Jardiolin, P. Buckley, and J. Barrios, *Mathematical field model predicts downhole density changes in static drilling fluids*, SPE 11118, SPE Annual Technical Conference and Exhibition, New Orleans, Louisianan, September1982.

[6.12] M.R. Shaikh, B.S. Udaya and P.V. Suryanarayana, Thermodynamic Basis of Brine Density on Pressure, Temperature, and Chemical Composition in Ultrahigh Pressure/High Temperature Environments, SPE 199563, SPE Drilling and Completion 37(02), June 2022, pp 151-160.

[6.13] I.M. Kutasov, Determination of calcium chloride brine concentration required to provide pressure overbalance, , Journal of Petroleum Science and Engineering 58, August 2007, pp.133-137.

[6.14] C.S. Oakes, J.M. Simonson and R.J Bodnar, Apparent molar volumes of aqueous calcium chloride to 250 °C, 400 bars, and from molalities of 0.242 to 6.150, Journal of Solution Chemistry, Volume 24, September 1995, pp.897-916.

Pressure-loss Modeling (Section 7)

[7.1] W.W White, M. Zamora and C.F. Svoboda, *Downhole measurements of synthetic-based drilling fluid in offshore well quantify dynamic pressure and temperature distributions*, SPE Drilling & Completion, 12(03) September 1997, p. 149-157.

[7.2] M. Zamora, *Virtual rheology and hydraulics improve use of oil and synthetic-based drilling fluids*, Oil & Gas Journal, March 3, 1997, pp. 43–55.

[7.3] M. Zamora and D.L Lord, *Practical analysis of drilling mud flow in pipes and annuli,* SPE 4976, SPE Annual Technical Conference, Houston, Texas, October 1974.

[7.4] J.G. Savins, *Generalized Newtonian (pseudoplastic) flow in stationary pipes and annuli*, SPE 1151, Petroleum Transactions of AIME, Volume 213, 1958, pp. 325-332.

[7.5] M. Zamora and D. Power, *Making a case for AADE hydraulics and the unified rheological model*, AADE-02-DFWM-HO-13, AADE Technology Conference, Houston, Texas, April 2002.

[7.6] M. Haciislamoglu and U. Cartalos, Practical pressure loss predictions in realistic annular geometries, SPE 28304, SPE Annual Technical Conference and Exhibition, New Orleans, Louisiana, September 1994.

[7.7] R.C. McCann, M.S Quigley, M. Zamora and K.S. Slater, *Effects of high-speed rotation on pressure losses in narrow annuli,* SPE 26343. SPE Annual Technical Conference and Exhibition, Houston, Texas, October 1993.

[7.8] S.W. Churchill, *Friction factor equation spans all fluid-flow regimes*, Chemical Engineering 84, November 1977, pp. 91–92.

[7.9] *Yield Point software,* Smith International.

[7.10] Y-T. Jeong and S.N Shah, Analysis of tool joint effects for accurate friction pressure loss calculations, SPE 87182, IADC/SPE Drilling Conference, Dallas, Texas, March 2004.

[7.11] A. Sas-Jaworsky II and T.D Reed, *Predicting pressure losses in coiled tubing operations*, World Oil, September 1997, pp. 141–146.

[7.12] Y. Zhou and S.N. Shah, *New friction factor correlations for non-Newtonian fluid flow in coiled tubing,* SPE 77960, SPE Asia Pacific Oil and Gas Conference and Exhibition, Melbourne, Australia, October 2002.

[7.13] S.N. Shah and Y. Zhou, "*An experimental study of drag reduction of polymeric solutions in coiled tubing*", SPE Production & Facilities, 18(04) November 2003, pp. 280–287.

[7.14] ISO 5167-3:2003, Measurement of fluid flow by means of pressure differential devices inserted in circular cross-section conduits running full—Part 3: Nozzles and Venturi nozzles

[7.15] C. Baranthol, J. Alfenore, M.D. Cotterill and G. Guillaume-Poux, *Determination of hydrostatic pressure and dynamic ECD by computer models and field measurements on the directional HPHT well 22130C-13*, SPE 29430, SPE/IADC Drilling Conference, Amsterdam, Netherlands, February 1995.

[7.16] F.J. Schuh, "*Computer makes surge-pressure calculations useful*", Oil & Gas Journal, August 1964, pp. 96–104.

Swab/Surge Pressures (Section 8)

[8.1] J.E. Fontenot and R.K. Clark, *An improved method for calculating swab/surge and circulation pressures in a drilling well*, SPE Journal, October 1974, pp. 451–461.

[8.2] J.A. Burkhardt, *Wellbore Pressure Surges Produced by Pipe Movement,* SPE-1546, Journal of Petroleum Technology 13 (06), June 1961,) pp. 595-605.

[8.3] A.G. Brooks, *Swab and surge pressures in non-Newtonian fluids*, Unsolicited manuscript SPE10863, archived in SPE OnePetro, January 1982.

[8.4] G. Gjerstad, R.E. Time and K.S Bjorkevoll, *A Medium-Order Flow Model for Dynamic Pressure Surges in Tripping Operations*, SPE/IADC 163465, SPE/IADC Drilling Conference, Amsterdam, The Netherlands, March 2013

[8.5] R.L Rudolf and P.V.R. Suryanarayana, "Field validation of swab effects while tripping-in the hole on deep, high temperature wells", IADC/SPE 39395, IADC/SPE Drilling Conference Dallas, Texas, March 1998.

Hole Cleaning (Section 9)

[9.1] T.V. Aarrestad and H. Blikra, *Torque and Drag-Two Factors In Extended-Reach Drilling"* SPE 27491, 1994 IADC/SPE Drilling Conference Dallas, Texas, Journal of Petroleum Technology, September 1994 pp. 800-803.

[9.2] C. Lenamond, *A Graphical Hole Monitoring Technique to Improve Drilling in High-Angle and Inclined Deepwater Wells in Real-Time,* AADE-03-NTCE-24, AADE National Technology Conference, Houston, Texas, April 2003.

[9.3] H.U. Zeidler, *An experimental analysis of the transport of drilled particles*, SPE 3026, Transactions of the AIME, SPE Journal, February 1972, pp. 39–38.

[9.4] T.R. Sifferman et al., *Drilling-cutting transport in full-scale vertical annuli"* SPE 4514, Journal of Petroleum Technology, November 1974, pp. 1295–1302.

[9.5] K.J. Sample and A.T. Bourgoyne, *An experimental Evaluation of Correlation Used for Predicting Cutting Slip Velocity*, SPE 6645, SPE Annual Technical Conference and Exhibition, Denver, Colorado, October 1977.

[9.6] S.F. Chien, *Settling Velocity of Irregularly Shaped Particles*, SPE 26212, SPE Drilling and Completion, December 1994, pp. 281-289.

[9.7] R.E. Walker and T.M. Mayes, *Design of drilling fluids for carrying capacity*, Journal of Petroleum Technology, July 1975, pp. 893–900.

[9.8] L. Robinson and M. Morgan, *Effect of Hole Cleaning on Drilling Rate and Performance*, AADE-04-DF-HO-42, AADE Drilling Fluids Conference, Houston, Texas, April 2004.

[9.9] A.A. Gavignet and I.J. Sobey, *Model Aids Cuttings Transport Prediction*, Journal of Petroleum Technology, September 1989, pp. 916-921.

[9.10] T.I. Larsen, A.A Pilehvari and J.J. Azar, *Development of a New Cuttings-Transport Model for High-Angle Wellbores Including Horizontal Wells,* SPE 25872, SPE Annual Technical Conference and Exhibition, Denver, Colorado, April 1993.

[9.11] R.K. Clark and K.L. Bickham, *A Mechanistic Model for Cuttings Transport*,, SPE 28306, SPE Annual Technical Conference and Exhibition, New Orleans, Louisiana, September 1994.

[9.12] W. Campos, *Mechanistic Modeling of Cuttings Transport In Directional Wells,* PhD Dissertation, University of Tulsa, l995.

[9.13] A.A. Pilehvari, J.J. Azar and S.A. Shirazi, *State-of-the-Art Cuttings Transport in Horizontal Wellbores*, SPE 57716, SPE Drilling & Completion 14(03) September 1999, pp. 196-200.

[9.14] M. Duan et al., *Transport of Small Cuttings in Extended-Reach Drilling*, SPE 104192, SPE Drilling & Completion 23 (03), September 2008, pp. 258-265.

[9.15] F. Zhang, *Numerical Simulation and Experimental Study of Cuttings Transport in Intermediate Inclined Wells,* Ph.D. Dissertation, University of Tulsa, 2015.

[9.16] Y. Luo, P.A. Bern and B.D. Chambers, *Flow rate predictions for cleaning deviated wells*, SPE 23884, IADC/SPE 1992 Drilling Conference, New Orleans, Louisiana, February 1992.

[9.17] Y. Luo, P.A. Bern and B.D. Chambers, *Simple charts to determine hole cleaning requirements*, SPE 27486, IADC/SPE 1994 Drilling Conference, Dallas, Texas, February 1994.

Hydraulics Optimization (Section 10)

[10.1] L.H. Robinson and M.S Ramsey, *Onsite continuous hydraulic optimization (OCHO),* AADE 01-NC-HO-30, AADE National Drilling Conference, Houston, Texas, March 2001.

[10.2] B.V. Randall, *Optimum hydraulics in the oil patch*, Petroleum Engineering, September 1975, pp. 36–52.

[10.3] L.H. Robinson, *On-site nozzle selection increases drilling performance*, Petroleum Engineering International, December 1981, pp. 7–82.

[10.4] L.H. Robinson, *Optimizing bit hydraulics increases penetration rates*, World Oil, July 1982, pp. 167–179.

[10.5] M.S. Ramsey, *Are you drilling optimized or spinning your wheels?,* AADE 01-NC-HO-31, AADE National Drilling Conference, Houston, Texas, March 200.

Rigsite Monitoring (Section 11)

[11.1] M. Hutchinson and I. Rezmer-Cooper*, Using downhole annular pressure measurements to anticipate drilling problems*, SPE 49114, SPE Annual Technical Conference and Exhibition, New Orleans, Louisiana, September 1998.

[11.2] M. Zamora et al., *Major advancements in true real-time hydraulics"*, SPE 62960, SPE Annual Technical Conference and Exhibition, Dallas, Texas, October 2000.

[10.3] S.Roy and M. Zamora, "*Advancements in true real-time wellsite hydraulics*," AADE Technical Conference, Houston, Texas, February 2000.

[10.4] C. Ward and R. Clark, "*Anatomy of a ballooning borehole using PWD"*, Workshop on Overpressures in Petroleum Exploration, Pau, France, April 1998.

[10.5] C. Ward and E. Andreassen, "*Pressure-while-drilling data improve reservoir drilling performance",* SPE Drilling & Completions 13(01) March 1998, pp. 19–24.

[11.6] C.R. Mallary et al., "*Using pressure-while-drilling measurements to solve extended-reach drilling problems on Alaska's North Slope*," SPE 54592, SPE Western Regional Meeting, Anchorage, Alaska, May 1999.